METHODS FOR TESTING THE EFFECT OF HYDRAULIC GRADIENT ON THE POLYMER ELUTION OF POLYMER GCLs

By

WILLIAM REYBROCK

A Thesis submitted in partial fulfillment of the requirements for the degree of

MASTER OF SCIENCE

(Geological Engineering)

at the

UNIVERSITY OF WISCONSIN-MADISON

May 2017

METHODS FOR TESTING THE EFFECT OF HYDRAULIC GRADIENT ON THE POLYMER ELUTION OF POLYMER GCLs

Approved by:

_____

William J. LIKOS, PhD

ABSTRACT

Geosynthetic Clay Liners (GCLs) were developed in the 1980's as an alternative landfill liner or cover material. GCLs are primarily comprised of a layer of processed sodium bentonite (Na-B), generally 7-10 mm thick, sandwiched between two geosynthetic fabrics or membranes. The layer of bentonite is held in place with some combination of adhesive, needle punching, or stitch-bonding.

Because of the susceptibility of Na-Bentonite GCLs to chemical incompatibility (e.g., increases in hydraulic conductivity) with aggressive (e.g., high ionic strength) permeant solutions, there has been a demand for chemically resistant GCLs, such as those composed of a dry blend of polymer and bentonite. The mechanism for decreased hydraulic conductivity (K) in these GCLs is hypothesized to be physical clogging of the intergranular pore space with polymer hydrogel. Subsequent increases in K are hypothesized to partially result from elution of polymer from the pore space, which may be exacerbated from seepage forces associated with permeation at high hydraulic gradient.

ASTM D5084 recommends using a hydraulic gradient less than 30 for materials with K values less than $1*10^{-7}$ m/s, while laboratory hydraulic conductivity testing procedures generally have much higher hydraulic gradients. Higher gradients are used because of the extremely long test durations associated with low hydraulic conductivity values of GCLs. The effect of hydraulic gradient on conventional Na-B GCLs has been studied extensively and shown to have a negligible effect on K values for gradients as high as 2500. As dry blended polymer GCLs (DB GCLs) continue to gain popularity, it is important to understand the effect that hydraulic gradient can have on the hydraulic

conductivity and polymer elution of these GCLs, in order to ensure that laboratory compatibility testing is applicable to field compatibility. The primary objective of this study is to determine if high hydraulic gradient and flow rate have an effect on polymer elution and hydraulic conductivity of DB polymer GCLs.

Three GCL types were used in this study, one Na-B GCL, Bentomat, and two DB GCLs, Resistex and Resistex Plus. GCLs were permeated with one of five permeant liquids: DI water, 50 mM $CaCl_2$, and three synthetic Coal Combustion Product (CCP) leachates. The three CCP leachates were selected from an Electric Power Research Institute (EPRI) database representing CCP disposal facilities in the United States and include flue gas desulfurization residual (Typical FGD), high ionic strength leachate (High Strength), and trona ash leachate (Trona).

A constant flow pump method was developed in accordance with ASTM D5084 and D6766 to afford precise control of flow rate and corresponding hydraulic gradient. A total of four constant flow pump tests were performed with the following materials: Test 1; Bentomat GCL permeated with DI water, Test 2; Bentomat GCL permeated with 50mM $CaCl_2$, Test 3; Resistex Plus GCL permeated with 50 mM $CaCl_2$, and Test 4; a replicate Resistex Plus GCL permeated with 50 mM $CaCl_2$. A total of four falling head tests following ASTM D6766 and D5084 were performed with the following materials: Test 5; Resistex Plus GCL permeated with High Strength leachate, Test 6; Resistex Plus GCL permeated with Trona leachate, Test 7; Resistex GCL permeated with Trona leachate, and Test 8; Resistex Plus GCL permeated with Typical FGD leachate.

Test 1 and Test 2 gave hydraulic conductivity values of $3.8*10^{-11}$ m/s and $1.3*10^{-7}$ m/s, respectively. Test durations and K values for Tests 1 and 2 are comparable to those

found in literature using the falling head test method. Test 3 showed unusually low K values from 0 – 8.5 PVF, and achieved chemical equilibrium at ~35 PVF at K = $2.1*10^{-7}$ m/s. Incremental flow rate changes from 20 to 40, 40 to 80, and 80 to 120 ml/hr were tested at ~40, ~50, and ~60 PVF, respectively. A negligible amount of change was observed in K and Total Organic Carbon (TOC) concentrations after each increase in flow rate. Test 4 is still in progress at ~1.5 PVF, and is performing similarly to test 3.

Tests 5 – 8 were all running for ~1000 days at an average hydraulic gradient of 190, showed low hydraulic conductivity values (< $1.0*10^{-11}$ m/s), and showed relatively consistent hydraulic conductivity values for at least 600-1000 days. For test 5 and test 6, the average hydraulic gradient was doubled and cell pressure was increased in order to keep average effective stress nearly constant. A slight increase in effective stress (i.e. from 20 kPa to 26.5 kPa) was implemented to prevent low minimum effective stresses, because ASTM D5084 recommends keeping effective stresses > 7 kPa or else risk separation of the membrane from the rest of the specimen. After the hydraulic gradient increase, both tests showed a hydraulic conductivity increase of more than 3 orders of magnitude within 1-2 days, from $8.0*10^{-12}$ to $8.6*10^{-9}$ m/s for test 5 and from $3.8*10^{-12}$ to $4.8*10^{-9}$ for test 6. The change was accompanied by a spike in TOC followed by a decrease in test 6, but only a decrease in TOC for test 5. For test 7 and test 8, the gradient was increased incrementally to give average values of 190, 233, 276, 319, 380, and 470. Slight increases in effective stress (i.e. from 20 to 21.4, 22.9, 24.4, 26.5, and 29.5 kPa respectively) were implemented. Each test was allowed to permeate for approximately 1 week at each interval to allow for any alterations to occur. Test 7 and test 8 showed constant hydraulic conductivity values at each hydraulic gradient interval.

Tests 1 and 2 showed that a constant flow pump can be used to find K values of Na-B GCLs equivalent to those found using the falling head method in a comparable amount of time. Tests 3 and 4 showed that there is an extended period of time where the constant flow method causes the K values of DB GCLs to be significantly lower than those measurements found using the falling head method. The precise mechanism for this observation isn't fully understood at this time. Nevertheless, this is a significant disadvantage as it could take months to years longer for a constant flow pump test to reach chemical equilibrium. Test 3 also showed that when K is high, an increase in hydraulic gradient causes no change in polymer elution or hydraulic conductivity.

Tests 5 and 6 showed that an immediate increase in hydraulic gradient from 190 to 380 can cause the hydraulic conductivity of DB GCLs to increase by greater than 3 orders of magnitude in as little as 1 to 2 days. The increase in hydraulic conductivity will likely be accompanied by a short surge of polymer elution followed by very low elution. Tests 7 and 8 showed that by incrementally increasing the hydraulic gradient from 190, 233, 276, 319, 380, and 470, and allowing one week for any change to occur at each gradient, the hydraulic conductivity can remain constant. There appears to be some mechanism during an incremental increase rather than an immediate increase that allows the hydraulic conductivity to remain low at gradients as high as 500. The precise mechanism for this observation is unknown at this time.

ACKNOWLEDGEMENTS

I would like to take this opportunity to thank everyone who has contributed to the completion of this study. Foremost, I would like to express my gratitude to my advisor Professor William J. Likos for his encouragement, feedback, and advice. I would also like to express my thanks towards Professor Craig H. Benson for participating in weekly research meetings and sharing his knowledge and advice. In addition, I would like to show thanks to all the above and Professor Matthew Ginder-Vogel for serving as my committee members and sharing their knowledge and experience with me.

Special thanks to Xiaodong Wang for his patience and commitment to helping whenever I needed. I would like to show appreciation toward Jiannan Chen and Kuo Tian for their mentoring during my undergraduate research and continued help as I began my graduate research.

I owe a great deal of thanks to former and current graduate students who have offered personal academic assistance and advice including Weijuan Geng, Hulya Salihoglu, Idil Akin, Adam McDaniel, and Alex Michaud, and to all of the GLE students for their friendship. I would also like to show thanks to my undergraduate research assistant Dan Graf, for his countless hours of assistance.

I would like to thank my parents, Steve and Therese Reybrock, and my sisters, Jenny, Lizzy, and Emily, for loving and supporting me during my years of studies. I would also like to thank my girlfriend, Hannah Maas, for her endless support.

Financial support of this research work was provided by Colloid Environmental Technologies Co. (CETCO). This support is gratefully acknowledged.

Table of Contents

ABSTRACT ii

ACKNOWLEDGEMENTS vi

1 INTRODUCTION 1

2 BACKGROUND 3

2.1 Landfill Liners – CCLs 3

2.2 Geosynthetic Clay Liners – GCLs 3

2.3 Bentonite 4

2.4 Methods for Measuring Hydraulic Conductivity 6

2.5 Factors That Can Influence Hydraulic Conductivity 10

2.5.1 Hydraulic Gradient 10

2.5.2 Microorganisms 11

2.5.3 Consolidation 12

2.5.4 Effective Stress 13

2.5.5 Void Ratio and Specimen Thickness 13

2.5.6 Permeant Effect on Hydraulic Conductivity 14

2.6 Polymer Clay Interactions 15

2.6.1 PAM 15

2.6.2 Types of Bonds with Clay Particles 15

2.7 Polymer GCLs 17

2.7.1 Modified GCLs and Mechanisms for Decreased K 17

2.7.2 CETCO DB GCLs: Mechanism of Decreased K and Polymer Elution 17

3 MATERIALS 20

3.1 Three GCL Types: Bentomat, Resistex, and Resistex Plus 20

3.2 Permeant Liquids 20

4 METHODS 21

4.1 Falling Head Hydraulic Conductivity Testing 21

4.2 Constant Flow Hydraulic Conductivity Testing 21

4.3 Termination Criteria 23

4.4 Chemical Analysis of Effluent 23

4.5 Soluble Cations, Bound Cations, and CEC 24

4.6 Total Organic Carbon (TOC) Analysis of Effluent 24

4.7 Loss on Ignition (LOI) Analysis of GCL Material 24

5 RESULTS 25

5.1 Bentomat Permeation Using Flow Pump 25

5.1.1 Bentomat Permeated with DI Water 25

5.1.2 Bentomat Permeated with 50 mM $CaCl_2$ 26

5.2 Resistex Plus Permeation Using Flow Pump 26

5.2.1 Resistex Plus Permeated with 50 mM $CaCl_2$ 26

5.3 Falling Head Results 27

5.3.1 Resistex Plus GCL Permeated with High Strength Leachate 27

5.3.2 Resistex Plus GCL Permeated with Trona Leachate 28

5.3.3 Resistex GCL Permeated with Trona Leachate 28

5.3.4 Resistex Plus GCL Permeated with Typical FGD Leachate 29

6 DISCUSSION 30

6.1 Bentomat Permeation Using Flow Pump 30

6.1.1 Bentomat Permeated with DI Water 30

6.1.2 Bentomat Permeated with 50 mM $CaCl_2$ 30

6.2 Resistex Plus Permeation Using Flow Pump 31

6.2.1 Resistex Plus Permeated with 50mM $CaCl_2$ 31

6.2.2 Replicate Resistex Plus Permeated with 50mM $CaCl_2$ 32

6.2.3 Comparison of Falling Head and Constant Flow Pump Results for Resistex Plus Permeated with 50mM $CaCl_2$ 32

6.3 Falling Head Tests 34

6.3.1 Resistex Plus GCL Permeated with High Strength Leachate 35

6.3.2 Resistex Plus GCL Permeated with Trona Leachate 36

6.3.3 Resistex GCL Permeated with Trona Leachate 37

6.3.4 Resistex Plus GCL permeated with Typical FGD Leachate 38

7 CONCLUSIONS 40

8 TABLES 42

9 FIGURES 44

10 REFERENCES 82

List of Tables

Table 8.1: Physical and chemical properties of 3 GCL types (Salihoglu, 2015) . 42

Table 8.2: Bentonite Mineralogy of 3 GCL Types (Salihoglu, 2015) 42

Table 8.3: Concentrations of major ionic species, pH, ionic strength, and RMD for all leachates used; modified from (Salihoglu, 2015) 43

List of Figures

Figure 9.1: Conceptual model of two main types of bond between PAM and exchangeable cations in the interlayer of montmorillonite (a) ion-dipole interaction or coordination and (b) Hydrogen bonding of amide groups with water molecules in the hydration shells of exchangeable cations (from Deng et al. 2006). 44

Figure 9.2: Conceptual model of clogging mechanism of hydrogel in DB Polymer GCL (a) hydrogel formation with bound water and (b) hydrogel clogs intergranular flow path and yields to low hydraulic conductivity when bentonite loses swell (from Tian et al. 2016). 45

Figure 9.3: SEM image of a freeze-dried DB polymer GCL permeated with DI water. The image shows hydrogel clogging the intergranular pore space (from Tian et al. 2016). 46

Figure 9.4: Total Organic Carbon (TOC) versus cumulative outflow for Resistex GCLs for several different leachate types (from Salihoglu, 2015). 47

Figure 9.5: Hydrogel that had clogged the outflow plate on a Resistex Plus GCL during the early stages of permeation with Trona leachate 48

Figure 9.6: (a) hydraulic conductivity of a GCL increases with PVF for Resistex and Resistex Plus GCL permeated with CCP leachate and (b) TOC concentration is highest during beginning stage of flow and decreases with time. As polymer elution occurs, the hydraulic conductivity increases (from Chen, 2015). 49

Figure 9.7: Hydraulic conductivity of Resistex and Resistex Plus GCLs permeated with a CCP leachate increases as the cumulative polymer percent eluted increases (from Chen, 2015). 50

Figure 9.8: Conceptual model of polymer elution causing increased hydraulic conductivity in DB Polymer GCL (a) hydrogel clogs intergranular flow path and yields low hydraulic conductivity with restricted bentonite swell (b) hydrogel can elute out and cause hydraulic conductivity to increase (from Tian et al. 2016)..... 51

Figure 9.9: Granule size distributions of each GCL obtained by dry sieving of bentonite and bentonite-polymer dry mixtures (from Salihoglu, 2015). 52

Figure 9.10: Digital microscope camera view of GCLs: a) Bentomat b) Resistex and c) Resistex plus GCL (from Salihoglu, 2015). 53

Figure 9.11: Photograph with main components of constant flow pump apparatus 54

Figure 9.12: Differential Head Results for 10 mL of Constant Flow of DI Water through Bentomat GCL at 0.2 mL/hr. Data points were recorded electronically every 10 minutes..... 55

Figure 9.13: Differential and Inflow Head Results for 10 mL of Constant Flow of DI Water through Bentomat GCL at 0.2 mL/hr. Data points were recorded electronically every 10 minutes. 55

Figure 9.14: Bentomat GCL is permeated with DI water using a constant flow pump. Discharge per unit area (Q/A) is plotted versus the equilibrium hydraulic gradients achieved after 10 mL of flow. Darcy's Law gives a hydraulic conductivity of $3.8 * 10^{-11}$ m/s. 56

Figure 9.15: Hydraulic conductivity, EC_{out}/EC_{in} ratio, $Ca^{2+}{}_{out}/Ca^{2+}{}_{in}$ ratio, and Na^{+} concentrations plotted with PVF for constant flow of Bentomat GCL permeated with 50 mM $CaCl_2$. 57

Figure 9.16: Hydraulic conductivity, polymer flushes, flow rate, hydraulic gradient, Ca^{2+out}/Ca^{2+in}, and Na^{+} concentrations plotted with PVF for constant flow testing of Resistex Plus GCL permeated with 50 mM $CaCl_2$..... 58

Figure 9.17: Hydraulic conductivity, flow rate, hydraulic gradient, and TOC plotted with PVF for constant flow testing of Resistex Plus GCL permeated with 50 mM CaCl2 59

Figure 9.18 : Rhodamine dye tracer test for Resistex Plus GCL permeated with 50 mM $CaCl_2$. Pink areas indicate areas of concentrated flow. 60

Figure 9.19: Polymer content distribution for Resistex Plus GCL permeated with 50 mM $CaCl_2$. Lowest polymer content exists in areas of concentrated flow. 60

Figure 9.20 : Hydraulic conductivity, polymer flushes, flow rate, and hydraulic gradient plotted with PVF for replicate constant flow testing of Resistex Plus GCL permeated with 50 mM $CaCl_2$..... 61

Figure 9.21 : Hydraulic conductivity and hydraulic gradient plotted with PVF for Resistex Plus GCL permeated with High Strength leachate for 992 days..... 62

Figure 9.22 : Hydraulic conductivity and hydraulic gradient plotted with PVF for Resistex Plus GCL permeated with High Strength leachate before and after average gradient increase..... 62

Figure 9.23 : Hydraulic conductivity and major cation concentration ratios plotted with PVF for Resistex Plus GCL permeated with High Strength leachate before and after average gradient increase..... 63

Figure 9.24 : Hydraulic conductivity, hydraulic gradient, and TOC plotted with PVF for Resistex Plus GCL permeated with High Strength leachate. A noticeable decrease in polymer content is observed after the increase in hydraulic gradient. 64

Figure 9.25: Measured hydraulic conductivity and hydraulic gradient results plotted with PVF of Resistex Plus GCL permeated with High Strength leachate, along with measured and possible TOC measurements. Possible incremental results give a potential explanation for the lack of measured TOC surge accompanying the increase in hydraulic conductivity. 65

Figure 9.26: Rhodamine dye tracer test for Resistex Plus GCL permeated with High Strength Leachate. Pink areas indicate areas of concentrated flow..... 66

Figure 9.27: Polymer content distribution for Resistex Plus GCL: permeated with High Strength leachate. Polymer content is spatially homogeneous. 66

Figure 9.28: Hydraulic conductivity and hydraulic gradient plotted with PVF for Resistex Plus GCL permeated with Trona leachate for 997 days 67

Figure 9.29: Hydraulic conductivity and hydraulic gradient plotted with PVF for Resistex Plus GCL permeated with Trona leachate before and after average gradient increase..... 67

Figure 9.30: Hydraulic conductivity, hydraulic gradient, and TOC plotted with PVF before and after gradient increase of Resistex Plus GCL permeated with Trona leachate. 68

Figure 9.31: Rhodamine dye tracer test for Resistex Plus GCL permeated with Trona Leachate. Pink areas shows areas of concentrated flow. 69

Figure 9.32: Polymer content distribution for Resistex Plus GCL permeated with Trona leachate. Polymer content is slightly lower in areas of concentrated flow. 69

Figure 9.33: Hydraulic conductivity and hydraulic gradient plotted with PVF for Resistex GCL permeated with Trona leachate for 1016 days. 70

Figure 9.34: Hydraulic conductivity and hydraulic gradient plotted with PVF after incremental increases to hydraulic gradient for Resistex GCL permeated with Trona leachate..... 70

Figure 9.35: Hydraulic conductivity, hydraulic gradient, and TOC plotted with PVF of Resistex GCL permeated with Trona leachate. 71

Figure 9.36: Hydraulic conductivity, hydraulic gradient, and TOC plotted with PVF of Resistex GCL permeated with Trona leachate. 72

Figure 9.37: Hydraulic conductivity and hydraulic gradient plotted with PVF for Resistex Plus GCL permeated with Typical FGD leachate for 1016 days. 73

Figure 9.38: Hydraulic conductivity and hydraulic gradient plotted with PVF after incremental increases to hydraulic gradient for Resistex Plus GCL permeated with Typical FGD..... 73

Figure 9.39: Hydraulic conductivity, hydraulic gradient, and TOC plotted with PVF of Resistex Plus GCL permeated with Typical FGD leachate. 74

Figure 9.40: Hydraulic conductivity, hydraulic gradient, and TOC plotted with PVF of Resistex Plus GCL permeated with Typical FGD leachate. 75

Figure 9.41: Outflow effective stress, overall GCL effective stress, maximum inflow effective stress, average inflow effective stress, minimum inflow effective stress, and lowest recommended effective stress (ASTM D5084) for hydraulic gradient increases in 4 falling head tests after changes in hydraulic gradients. 76

Figure 9.42: Hydraulic conductivity and hydraulic gradient plotted with PVF for both Resistex Plus GCLs permeated with 50 mM $CaCl_2$. 77

Figure 9.43: Hydraulic conductivity values plotted with PVF for constant flow method and falling head methods of varying average hydraulic gradients for Resistex Plus GCLs permeated with 50 mM $CaCl_2$. 78

Figure 9.44: Hydraulic conductivity values plotted with PVF for constant flow method and falling head methods of varying average hydraulic gradients for 0-15 PVF for Resistex Plus GCLs permeated with 50 mM $CaCl_2$. 78

Figure 9.45: Cumulative inflow minus cumulative outflow plotted with PVF for falling head tests for Resistex Plus GCLs permeated with 50 mM $CaCl_2$ provided by Geng (2017). Only the first 8 PVF are plotted, because this is the range where the large difference in hydraulic conductivity values is seen. All of these results show a decrease

in pore space volume ranging from 15 mL to 60 mL, excluding the permeameter where hydraulic gradient equals 120. This was likely due to a leak in the inflow plate. The ‘no change’ line represents the constant flow test method, where inflow is equal to the outflow. 79

Figure 9.46: The inflow and outflow pressures measured using the constant flow method for Resistex Plus GCL permeated with 50 mM $CaCl_2$ from 0 – 8.5 PVF. Both the inflow and outflow pressures show a build-up of pressure from 0 – 3 PVF, followed by a slow decrease of pressure from 3 – 8.5 PVF. 80

Figure 9.47: (a) Before cation exchange occurs, the Na-Bentonite will have negatively charged montmorillonite particles, with water and sodium ions occupying the interlamellar space giving it a large DDL thickness. Calcium ions and water will be occupying the intergranular pore space. (b) After cation exchange occurs, calcium ions will be occupying the interlamellar space. The stronger charges of the calcium ions will have a stronger pull on the negatively charge montmorillonite particles, which will cause the DDL thickness to decrease and cause a higher portion of water molecules to enter the intergranular space..... 81

METHODS FOR TESTING THE EFFECT OF HYDRAULIC GRADIENT ON THE POLYMER ELUTION OF POLYMER GCLs

1 INTRODUCTION

Geosynthetic Clay Liners (GCLs) were developed in the 1980's as an alternative landfill liner material (EPA, 2001). GCLs are primarily comprised of a layer of processed sodium bentonite (Na-B), generally 7-10 mm thick, sandwiched between two geosynthetic fabrics or membranes. The layer of bentonite is held in place with some combination of adhesive, needle punching, or stitch-bonding.

Because of the susceptibility of Na-Bentonite GCLs to chemical incompatibility (e.g., increases in hydraulic conductivity) with aggressive (e.g., high ionic strength) permeant solutions, there has been a demand for chemically resistant GCLs, such as those composed of a dry blend of polymer and bentonite. The mechanism for decreased hydraulic conductivity (K) in these GCLs is hypothesized to be physical clogging of the intergranular pore space with polymer hydrogel. Subsequent increases in K are hypothesized to partially result from elution of polymer from the pore space, which may be exacerbated from seepage forces associated with permeation at high hydraulic gradient.

ASTM D5084 recommends using a hydraulic gradient less than 30 for materials with K values less than $1*10^{-7}$ m/s, while laboratory hydraulic conductivity testing procedures generally have much higher hydraulic gradients. Higher gradients are used because of the extremely long test durations associated with low hydraulic conductivity values of GCLs. The effect of hydraulic gradient on conventional Na-B GCLs has been

studied extensively and shown to have a negligible effect on K values for gradients as high as 2500 (Rad et al., 1994). In order to understand the accuracy of hydraulic conductivity testing for a wider range of GCLs, it is advised to study this same relationship for dry blended polymer GCLs (DB GCLs). The main purpose of this study is to determine if hydraulic gradient and corresponding flow rate have an effect on the amount of polymer elution and related hydraulic conductivity values of DB GCLs.

2 BACKGROUND

2.1 Landfill Liners – CCLs

When large amounts of waste are present at a site such as a landfill, leachates are produced from water that has percolated through the solids and leached out some of the waste constituents. Since 1988, there have been specific design standards implemented in the United States in order to minimize the effect that this leachate has on surrounding environments. These standards describe the proper way to construct a compacted clay liner (CCL), which is considered a traditional landfill liner. A CCL is viable because of the low hydraulic conductivity values of clay. Installing a CCL can be quite rigorous because of the regulations enforced to ensure a high quality barrier system (Gordon et al., 1990). A model developed by Wong (1977) and further evaluated by Kmet et al. (1981), showed that even a perfectly uniform CCL with a thickness less than 0.6 m would cause unacceptable increases in permeation. This model also showed that permeation is kept low at thicknesses of 1.2 to 1.8 m (Wong, 1977; Kmet et al., 1981). Thinner CCLs constructed in the past have been known to have been extremely laterally heterogeneous, thus providing a weak barrier in certain areas of the liner. As a result, the EPA recommends a CCL thickness of 1.5 m to be constructed in lifts of 15.24 cm or less, which provides a factor of safety for construction quality (Gordon et al., 1990).

2.2 Geosynthetic Clay Liners – GCLs

Geosynthetic Clay Liners (GCLs) were developed in the 1980's as an alternative landfill liner material (EPA, 2001). GCLs are comprised of a thin layer of processed bentonite, generally 7 – 10 mm thick, sandwiched between two geosynthetic fabrics or

membranes. The layer of bentonite is held in place with some combination of adhesive, needle punching, or stitch-bonding.

GCLs gained popularity in the 1990's, and the product's usage continues to grow because it has several advantages over CCLs. The low thickness of GCLs relative to CCLs allows for minimal shipping costs and significant savings in the volume of landfill. In addition, GCLs can perform better with regards to differential settlement than CCLs. Perhaps the most distinct advantage of GCLs is the easy installation compared to CCLs, however it is important to note that there are significant quality assurance measures for both GCLs and CCLs. For most scenarios, the cost of GCLs tend to be quite low compared to CCLs (Bouzza, 2002).

2.3 Bentonite

The term bentonite is a loosely used term referring to a clay that is composed of primarily montmorillonite, which is a member of the smectite group of minerals (Grim & Guven, 1978). There are many properties unique to smectite minerals, including a very large specific surface area (SSA), a very large cation exchange capacity (CEC), and the characteristic of fluid swelling/hydration between interparticle surfaces (Odom, 1984).

Clay particles have a plate-like structure, meaning the surface area of an average particle is several orders of magnitude larger than its thickness. This high SSA allows for physicochemical interactions to dominate the properties of clay. Isomorphous substitution causes clay particles to have a net negative charge (Mitchell & Soga, 2005). Soluble cations are attracted to the mineral surface, and move into the interlamellar surface between particles in order to establish neutrality. These cations are concentrated at the

particle surface and diffuse at a distance. The preference for exchange is dictated by the lyotropic series ($Fe^{3+} > Al^{3+} > Cu^{2+} > Ba^{2+} > Ca^{2+} > Mg^{2+} > Cs^{+} > Rb^{+} > NH_4^{+} = K^{+} > Na^{+} > Li^{+)}$ which trends from high valence and small ionic size to low valence and large ionic size (Norrish, 1954). CEC is a quantification of the total amount of cations that can be exchanged in units of meq (Mitchell & Soga, 2005).

When gravimetric water contents are less than about 100%, the water molecules are subject to crystalline swelling, which is also known as Type I Swelling. This is a process by which one, two, three, or four layers of H_2O molecules are sequentially intercalated into the interlamellar space between individual clay particles.

When gravimetric water contents are greater than about 100%, a different mode of hydration occurs. On the boundary of every clay particle is a double diffuse layer (DDL), which is comprised of the surface charge of the clay particle and the distributed charge of ions in the adjacent pore fluid phase. The Gouy-Chapman theory of a DDL shows that cationic and anionic charge densities will decay exponentially with distance. It also indicates a higher concentration of cations compared to anions, which is a result of the negatively charged clay particles preferentially adsorbing cations.

Any increase in gravimetric water content above about 100% occurs via osmotic swelling. This type of swelling occurs as a result of the concentration gradient between the high ionic concentrations of the interlamellar space and the lower ionic concentrations of the bulk pore fluid. The interlamellar space acts as an osmotic membrane, which causes the lower ionic strength bulk pore fluid to force its way into the interlamellar space, causing osmotic swelling.

A change in the thickness of the DDL will cause a change in the amount of osmotic swelling in a smectite. The Gouy-Chapman theory considers the effect of several factors on the thickness of a DDL. For the purpose of this paper, there are two main factors that will be taken into account. The first factor is ion valence; high valency results in a compressed DDL, while low valency results in a thick DDL. The second factor is the concentration of the bulk pore fluid; a higher concentration results in a compressed DDL, while a lower concentration will result in a thick DDL (Bouazza & Bowders, 2010). On a macroscopic scale, a compressed DDL results in a flocculated fabric, while a thick DDL will result in a dispersed soil fabric. The effect of this characteristic on hydraulic conductivity will be discussed in later chapters (Mitchell & Soga, 2005).

2.4 Methods for Measuring Hydraulic Conductivity

There are currently three ASTM Standards that are used to conduct laboratory hydraulic conductivity testing procedures. ASTM D5084 gives standard test methods for the measurement of hydraulic conductivity of saturated porous materials using a flexible wall permeameter. Given in the standard are: Method A) constant head; Method B) falling head, constant tailwater elevation; Method C) falling head, rising tailwater elevation; Method D) constant rate of flow; Method E) constant volume – constant head (by mercury); and Method F) constant volume – falling head (by mercury), rising tailwater elevation.

ASTM D6766 gives standard test methods for evaluation of hydraulic properties of geosynthetic clay liners permeated with potentially incompatible aqueous solutions. This standard is similar to D5084, with slightly different termination criteria that are designed to ensure that aqueous solutions will be compatible in longer term scenarios. Methods A,

B, C, and D found in D6766 are equivalent to methods of the same name used in ASTM D5084.

ASTM D5887 gives standard test methods for the measurement of index flux through saturated geosynthetic clay liner specimens using a flexible wall permeameter. Unlike D6766 and D5084, which give direct hydraulic conductivity measurements to a permeant, D5887 is designed to give a flux measurement with deionized water. The main purpose of D5887 is to maintain manufacturer quality control. D6766, D5084, and D5887 have been used in varying degrees to test the permeability and/or hydraulic conductivity of GCLs.

Estornell and Daniel (1992) designed a bench scale hydraulic conductivity test able to measure the hydraulic conductivity of a 1.2 by 2.4 m rectangular specimen of GCL. Bentomat and Claymax GCLs were tested and hydraulic conductivity results were compared to those measured using flexible wall permeameters following ASTM D5084. While the Claymax hydraulic conductivity results matched well between the two methods, there were some discrepancies in the Bentomat results, and the cause for this was not determined (Estornell & Daniel, 1992).

A fixed-wall constant flow method was developed by Fernandez (1989), and further studied by Fernandez and Quigley (1991). The apparatus used a computer controlled steel syringe to maintain a constant flow of various permeants into samples of clay. The apparatus successfully measured vertical stress, vertical consolidation, and hydraulic conductivity values (Fernandez & Quigley, 1991). This constant flow method was similar to those described in Method D of ASTM D5084 and D6766.

Rad et al. (1994) was able to successfully measure the hydraulic conductivities of a Claymax GCL with benzene, styrene, ethanol, unleaded gasoline, gasohol, diesel fuel, jet fuel, and a municipal solid waste (MSW) leachate by using flexible wall permeameters. The apparatus used a falling head method and followed ASTM D5084, while several modifications were made to ensure that a GCL could be successfully substituted in place of a CCL (Rad et al., 1994).

Petrov et al. (1997B) was able to successfully measure hydraulic conductivities of a Na-B GCL using 3 methods: 1) the fixed-wall, constant flow method mentioned previously and developed by Fernandez (1989), 2) a constant head, double-ring permeameter, and 3) a falling head, flexible wall permeameter similar to those described in ASTM D5084. The fixed-wall, constant flow method can be advantageous because it is able to directly measure the thickness of the GCL while directly applying vertical pressure. In addition, the constant flow method gives a very precise control of flow, which can be used for a variety of other analyses. The constant head, double-ring permeameter method can be advantageous because the inner and outer effluents are separated from each other, making sidewall leakage easy to detect. The flexible wall permeameter can be advantageous because it has the lowest probability of sidewall leakage. The hydraulic conductivity values, which were found using DI (deionized water), 0.6 N NaCl, and 2.0 N NaCl, were found to be reasonably similar for all 3 methods (Petrov et al., 1997B).

Daniel et al. (1996) performed a “round-robin” compilation of 18 lab results, each with three tests that used GRI Method GCL-2, which is similar to ASTM D5084, but with slightly different termination criteria. The results of the study showed that all 18 labs, each with three tests, produced K results within one order of magnitude (Daniel et al., 1997).

Wang and Benson (1999) measured the hydraulic conductivity of a Na-B GCL using 2 versions of a constant volume method. Using GRI Method GCL-2, the falling-head constant-volume (FHCV) and the constant-head constant-volume (CHCV) methods were developed, tested, and the results were compared to those found using open system tests. FHCV was performed using ASTM D5087 Method E as guidance. CHCV was developed by the authors, and was later incorporated into ASTM D5087 as Method F. Although the designs of both constant volume methods are more complex than open system designs, it was determined that results can be found much faster using both FHCV and CHCV (Wang & Benson, 1999).

The majority of hydraulic conductivity tests on GCLs use the falling head method because it is less complex than the alternatives. The flexible wall permeameter has also become common because of its ability to minimize sidewall leakage. As a result, the majority of hydraulic conductivity testing performed in the last 20 years have used Methods B or C in ASTM D5084 and/or ASTM D6877.

ASTM D5084 Method B was used by Jo et al. (2001) to measure the hydraulic conductivity of nonprehydrated Na-Bentonite GCLs to single-species salt solutions with a range of effective stresses and pH values (Jo et al., 2001).

Shan and Lai (2002) used ASTM D5887 to measure the flux of Bentomat and Claymax GCLs to tap water, acidic water, seawater, MSW leachate, and gasoline (Shan & Lai, 2002).

A combination of ASTM D5084 and ASTM D6766 was used by Kolstad et al. (2004) to measure the hydraulic conductivity of nonprehydrated Na-B GCLs permeated

with multispecies inorganic solutions, Jo et al. (2005) to measure the long term hydraulic conductivity of Bentomat GCLs to tailings impoundment solutions, Katsumi et al. (2007) to measure the hydraulic conductivity of nonprehydrated Bentofix GCLs with inorganic chemical solutions and waste leachates, Shackelford et al. (2009) to measure the hydraulic conductivity of Bentomat GCLs to tailings impoundment solutions for zinc and copper mines, Bradshaw et al. (2013) to measure the hydraulic conductivity of Na-B GCLs after subgrade hydration, Scalia et. al (2014) to measure the long term hydraulic conductivity of Bentonite Polymer Composite (BPC) GCLs permeated with aggressive inorganic solutions, and Bradshaw and Benson (2014) to measure the hydraulic conductivity of Na-B GCLs permeated with MSW leachate (Kolstad et al., 2004; Jo et al., 2005; Katsumi, et al., 2007; Shackelford et al., 2010; Bradshaw et al., 2013; Scalia IV et al., 2014; and Bradshaw & Benson, 2014).

2.5 Factors That Can Influence Hydraulic Conductivity

2.5.1 Hydraulic Gradient

ASTM D5084 recommends using a maximum hydraulic gradient of 10 for 10^{-7} m/s < K < 10^{-8} m/s, 20 for 10^{-8} m/s < K < 10^{-9} m/s, and 30 for K < 10^{-9} m/s. In lab tests, hydraulic gradients as high as 150 – 200 are commonly used because of timing and budget constraints. Therefore, when running hydraulic conductivity tests, it is important to understand any potential alterations caused by high hydraulic gradients. Dunn and Mitchell (1984) tested the effect of hydraulic gradient on two clays, a predominantly kaolinite clay and a predominantly bentonite clay. The tests started with a hydraulic gradient of 20 and increased in increments to 200. The hydraulic conductivity of both soils decreased and was irreversible. The cause of this decrease was attributed to migration

of the finer particles clogging the pore spaces. Several other mechanisms were studied and it was concluded that none were playing a significant part in hydraulic conductivity values in these particular experiments. Finer particle migration out of the clay sample could have caused increased K values. However, this mechanism is easy to detect as eroded particles are often visible in effluent solution. It was also noted that microorganism growth could have contributed to a decrease in hydraulic conductivity (Dunn & Mitchell, 1984). It was shown using a Claymax GCL that hydraulic gradients can be as high as 2500 without major effects on the hydraulic conductivity measurements (Rad et al., 1994).

2.5.2 Microorganisms

Bacteria and the metabolic products that they excrete within soil pores can decrease the hydraulic conductivity of silty clay loams (Frankenberger, 1979). This effect is positively correlated with the amount of organic material within the soil. Frankenberger (1979) noted that bacterial numbers were lower in soils that were dried. It is believed that bacterial growth within GCLs are minimal as they are quite dry before permeation, with water contents around 3 – 5 %.

Jo et al. (2001) permeated three Na-B GCLs with 5 mM $CaCl_2$ for greater than 2 years and several hundred PVF. One of the three tests used a biocide designed to eliminate microbial growth while inducing negligible physicochemical effects that could alter the hydraulic conductivity of the GCLs. The results for all three tests were very similar. It was concluded that the biological activity was minimal and likely had a negligible effect on the hydraulic conductivity measurements (Jo et al., 2001).

2.5.3 Consolidation

While running hydraulic conductivity tests on fine-grained materials, there is a chance of consolidation occurring and altering hydraulic conductivity values. Fox (1996) examined the effect that seepage-induced consolidation would have on the hydraulic conductivity of clay materials. They found that an increase in hydraulic gradient is accompanied by a seepage induced consolidation and a decrease in K. Subsequently, they found that this effect is most significant in highly compressible materials, and negligible in less compressible materials (Fox, 1996).

The effect of consolidation of a GCL has been compared to that of a compacted clay prepared in a Proctor mold. Seepage-induced consolidation is controlled by the difference in effective stresses between the inflow and outflow surfaces of the specimen. Shackelford et al. (2000) provides an example of a hydraulic conductivity test where the average effective stress caused by backpressure and permeation remain constant. The minimum and maximum effective stresses in this case will be controlled only by the applied hydraulic gradient. Using the maximum hydraulic gradient of 30 recommended by ASTM D5084 and a Proctor mold with a length of 116 mm, a difference of 34 kPa between the inflow and outflow was calculated. In order to get a 34 kPa difference in head between the inflow and outflow using a GCL with a thickness of 9 mm, a hydraulic gradient of 380 would have to be applied (Shackelford et al., 2000).

Petrov (1995) was able to show during a Na-B GCL hydraulic conductivity test that incremental increases in hydraulic gradient and resulting increases in flow rate and seepage-induced stresses can cause a small amount of seepage-induced consolidation. However, this did not cause a significant change in hydraulic conductivity (Petrov, 1995).

2.5.4 Effective Stress

An increase in confining stress and corresponding effective stress can cause the hydraulic conductivity of a GCL to decrease. Na-B GCLs were shown to decrease in hydraulic conductivity by half an order of magnitude or more during incremental increases in effective stress from 14 kPa to 140 kPa (Shackelford et al., 2000).

For single-species salt solutions over a 20 – 500 kPa effective stress range, the decrease in hydraulic conductivity caused by an increase in effective stress was shown to decrease as the concentration of permeant increases (Jo et al., 2001).

Chen (2015) performed a comprehensive study of the effect of effective stress on hydraulic conductivity using three different GCL types and five different CCP leachates. Hydraulic conductivity testing was performed with effective stresses of 20, 100, 250, and 450 kPa. It was determined that effective stress is inversely correlated with hydraulic conductivity. In some instances, K decreased by up to 3 orders of magnitude when the effective stress was increased from 20 to 250 kPa (Chen, 2015).

2.5.5 Void Ratio and Specimen Thickness

Petrov et al. (1997A) and Petrov and Rowe (1997) demonstrated a linear relationship between Na-B GCL specimen thickness and the logarithm of Na-B GCL hydraulic conductivity. The relationship and scatter within it depended on the specific GCL type and the permeant and hydrating liquid. Both studies showed a linear relationship between Na-B GCL void ratio and the logarithm of Na-B GCL hydraulic conductivity. The void ratio to hydraulic conductivity relationship was shown to have lower R^2 values and therefore less scatter. This relationship exists because fine-grained materials with lower

void ratios have less flow space available and therefore will have lower hydraulic conductivity values (Petrov et al., 1997A; Petrov & Rowe, 1997).

2.5.6 Permeant Effect on Hydraulic Conductivity

For conventional Na-B GCLs, the hydraulic conductivity is largely controlled by the thickness of the DDL. Generally, the greater the thickness of the DDL, the lower K values will be. This has been confirmed in many ASTM D5890 free swell tests and hydraulic conductivity tests (Jo et al., 2001; Shan & Lai, 2002; Kolstad et al., 2004; Jo et al., 2005; Katsumi et al., 2007; Bradshaw & Benson, 2014; Scalia IV et al., 2014; and Chen, 2015).

Kolstad (2000) performed hydraulic conductivity tests on Na-B GCLs with multi-species salt solutions consisting of various concentrations of LiCl, NaCl, $CaCl_2$, and $MgCl_2$, with ionic strengths ranging 0.05 M to 0.5 M and relative abundance of monovalent and multivalent cations (RMD) values ranging from 0 to 1.39. It was shown that K is directly related to ionic strength and inversely related to RMD (Kolstad, 2000). Jo et al. (2001) performed hydraulic conductivity tests on Na-B GCLs with single-species salt solutions consisting of various concentrations of NaCl, KCl, LiCL, $MgCl_2$, $ZnCl_2$, $CuCl_2$, and $LaCl_3$. At a constant salt solution concentration, hydraulic conductivity increased with increasing valence. This effect was most noticeable for the less extreme salt concentrations between 0.025 M and 0.1 M. Hydraulic conductivity also increased as concentration increased for all tested salt solutions (Jo et al., 2001).

2.6 Polymer Clay Interactions

2.6.1 PAM

Polyacrylamide (PAM), is a polymerized version of the monomer acrylamide. It has been used for clarification of drinking water, flocculants for wastewater treatment, oil recovery, biomedical applications, agriculture, and soil conditioning – including GCL modification (Caulfield et al., 2002).

2.6.2 Types of Bonds with Clay Particles

Adsorption of polymer molecules on external surfaces of clay particles is the most common interaction between clays and polymers on the molecular scale. Intercalation of polymer molecules between montmorillonite unit layers requires more energy, and is more difficult to achieve (Lagaly et al., 2006).

Soluble, nonionic, flexible, linear polymers are adsorbed on clay surfaces due to an entropy driven process. In solution, the polymers are generally coiled. During adsorption, the polymers are uncoiled and spread out at the clay particle surface. This process causes water molecules to be desorbed from the clay particle surface (Theng, 1982). The adsorption of soluble nonionic PAM to the interlayer of montmorillonite particles has been shown to be the result of two interactions. The first is an ion-dipole interaction between exchangeable cations of the clay and the carbonyl oxygen atoms of the polymer's amide groups. The second interaction is hydrogen bonding between the polymer's amide groups and clay's water molecules in the hydration shells of the exchangeable cations. Both interactions are conceptualized in Figure 9.1 (Deng et al., 2006).

It is believed that soluble anionic PAM bonds with bentonite by similar mechanisms as nonionic PAM (Liu, 2007). The negatively charged bentonite would be expected to repel anionic PAM; however, this is not the case. Gungor and Karaoglan (2001) were able to prove using calcium montmorillonite that anionic PAM can be adsorbed at the bentonite particle surface, but is not intercalated (Gunger & Karaoglan, 2001). Because of the electrostatic repulsion between negatively charged clay particles and anionic PAM, it is believed that the polymer remains suspended in the DDL. This is the result of interactions between anionic polymer chains and cations present in the DDL. Because of this, anionic PAM shows less adsorption and intercalation than cationic and nonionic PAM (Theng, 2012).

Similar to anionic PAM, it is believed that soluble cationic PAM bonds with bentonite by mechanisms similar to nonionic PAM (Liu, 2007). Because of the positive charge associated with cationic PAM, the primary driving force is the cation exchange capacity of the bentonite. Cations associated with the montmorillonite particles are replaced with the positive charges on the cationic polymers (Schenning, 2004). The bond formed between cationic polymers and montmorillonite has the potential to be strong, such that the polymer will collapse or adsorb onto the clay particle. The higher the charge of the polymer and/or clay, the more likely this phenomenon is to occur (Breen, 1999). This strong polymer-clay interaction can decrease the rate of cation exchange, the result of which would be expected to decrease K. This polymer-clay interaction can also cause flocculation, which is a process that increases hydraulic conductivity. The flocculation appears to have a dominant effect, as cationic polymer composites have been associated with poor hydraulic conductivity performance (McRory & Ashmawy, 2005).

2.7 Polymer GCLs

2.7.1 Modified GCLs and Mechanisms for Decreased K

Because of the susceptibility of Na-B GCLs to chemical incompatibility, there has been a demand for chemically resistant GCLs. Trauger and Darlington (2000) developed bentonite polymer alloy (BPA), the first alteration to conventional Na-B GCLs, which consists of anionic polymers intercalated within the montmorillonite particles. This was proven to reduce the hydraulic conductivity for certain solutions by several orders of magnitude (Trauger & Darlington, 2000).

Scalia IV (2012) provides a detailed background summary of amended bentonite materials used for barrier applications. The goal of achieving bentonite compatibility has been achieved with varying degrees of success through intercalation of organic molecules within montmorillonite layers, locking monovalent cations onto the exchange complex with a polymeric molecule, and adding superabsorbent polymers (Scalia IV, 2012).

2.7.2 CETCO DB GCLs: Mechanism of Decreased K and Polymer Elution

The properties of the polymer used in CETCO's Resistex and Resistex Plus GCLs are proprietary. However, it is believed that they include some variation of insoluble PAM, with the majority being nonionic and anionic (Geng, 2017). The polymers used in CETCO's polymer GCLs are considered hydrogels, which are PAM monomers that form a 3D network structure. The dry blending of bentonite and polymers causes both materials to be phase-separated, meaning a negligible amount of intercalation of polymer and bentonite particles. The mechanism for reduced K has been hypothesized to be mainly the result of PAM hydrogel blocking or clogging flow paths in the intergranular pore space (Tian et al., 2016). A conceptual model of hydrogel formation with bound water and

clogging of intergranular flow path, resulting in low hydraulic conductivity for DB GCLs even for conditions of reduced swell of the bentonite in shown in Figure 9.2. A scanning electron microscope (SEM) image of PAM hydrogel clogging the intergranular pore space in a freeze-dried DB GCL permeated with DI water is shown in Figure 9.3.

Free swell tests have shown that PAM is a more important factor than bentonite in controlling the pore properties of DB GCLs (Scalia IV, 2012; Chen, 2015; Tian, 2015; Salihoglu, 2015). During GCL permeation with high strength leachates, as cation exchange and subsequent collapse of the DDL occurs within the bentonite, the intergranular pore space of bentonite during permeation is filled with the PAM hydrogel, keeping hydraulic conductivity values lower than conventional Na-B GCLs. Tian et al. (2016) provided evidence that higher ionic strength pore fluid inhibits hydrogel formation. This provides an explanation for the increases in hydraulic conductivity observed when using high ionic strength leachates (Tian et al., 2016).

Depending on the amount of polymer loading and ionic strength of the leachate, there will be a certain amount of polymer elution. The total organic carbon content (TOC) concentrations (a measure of polymer content within the effluent) as a function of cumulative outflow for Resistex GCLs permeated with several different leachate types is shown in Figure 9.4 (Salihoglu, 2015). TOC is highest at the early stages of flow, and decreases towards some steady state elution concentration. A Resistex Plus GCL in the early stages of permeation with Trona leachate, where hydrogel had formed a clog in the outflow plate within the permeameter is pictured in Figure 9.5. Polymer elution has been shown to be positively correlated to increases in hydraulic conductivity by Chen (2015). The relationship between hydraulic conductivity, TOC concentration in the effluent, and

pore volumes of flow (PVF) for Resistex and Resistex Plus GCLs permeated with a CCP leachate is shown in Figure 9.6. The relationship between hydraulic conductivity of Resistex and Resistex Plus GCLs permeated with a CCP leachate with respect to the cumulative polymer percent eluted is shown in Figure 9.7. Tian et al. (2016) proposed that elution is caused by hydrogel being pushed out of the intergranular space, and an increase in hydraulic conductivity is caused by flow preferentially occurring where hydrogel had once limited flow. This process is conceptualized in Figure 9.8. For dry mix polymer GCLs, the amount of polymer elution increases as the ionic strength increases (Tian, 2015; Salihoglu, 2015) The main purpose of this study is to determine if hydraulic gradient and corresponding flow rate have an effect on the amount of polymer elution and related hydraulic conductivity values.

3 MATERIALS

3.1 Three GCL Types: Bentomat, Resistex, and Resistex Plus

Three GCL types used in this study were provided by CETCO, including one conventional Na-B GCL (Bentomat) and two DB GCLs (Resistex and Resistex Plus). All 3 GCLs contain a needle-punched layer of Na-B or DB sandwiched between a woven geotextile and nonwoven geotextile. Both DB GCLs were manufactured using a dry blend of polymer and granular bentonite. Physical and chemical properties of all 3 GCLs can be found in Table 8.1. Mineral constituents of all 3 GCLs can be found in Table 8.2.

3.2 Permeant Liquids

GCLs were permeated with one of five permeant liquids: DI water, 50 mM $CaCl_2$, and three synthetic Coal Combustion Product (CCP) leachates. The three CCP leachates were selected from an Electric Power Research Institute (EPRI) database representing CCP disposal facilities in the United States and include flue gas desulfurization residual (Typical FGD), high ionic strength leachate (High Strength), and trona ash leachate (Trona) (Salihoglu, 2015). The concentrations of constituents, pH, ionic strength, and RMD for each of these leachates are summarized in Table 8.3.

4 METHODS

4.1 Falling Head Hydraulic Conductivity Testing

Falling head hydraulic conductivity tests were performed using both DB GCLs (Resistex and Resistex Plus) and flexible wall permeameters following ASTM D5084 Method B and ASTM D6766 Method B (falling head-water, constant tail-water method). Average hydraulic gradients ranging from 190 – 470 were used.

Prior to initiation of flow, GCL specimens were hydrated with a permeant for 48 hours at an average cell pressure of 27 kPa. During hydration, the influent valve was left open while the effluent valve was closed to prevent outflow. Permeation was initiated at an effective stress of 20 kPa. This follows Scenario 2 – Hydrated-Saturated with Test Liquid (Worst Case) from ASTM D6766. Average hydraulic gradients of 190, 233, 276, 319, 380, and 470 were used with average effective stresses of 20, 21.4, 22.9, 24.4, 26.5, and 29.5 kPa, respectively.

Each permeameter has two influent lines, two effluent lines, and a connection to a cell pressure line. One influent and one effluent line are closed during flow, and are used when needed for polymer flushing. The inflow is connected to a burette, while the effluent is collected in bottles for analysis.

4.2 Constant Flow Hydraulic Conductivity Testing

Constant flow hydraulic conductivity tests were run with Bentomat and Resistex Plus GCLs using flexible wall permeameters following ASTM D5084 Method D and ASTM D6766 Method D. A wide range of flow rates and hydraulic gradients were used in this study.

Prior to initiation of flow, GCL specimens were hydrated with the permeant for 48 hours at an average cell pressure of 27 kPa. During hydration, the influent valve was left open while the effluent valve was closed to prevent outflow. Permeation was initiated at an average effective stress ranging from 13.4 to 20.0 kPa. This follows Scenario 2 – Hydrated-Saturated with Test Liquid (Worst Case) from ASTM D6766.

The flexible wall permeameters used in the constant flow method were set up in exactly the same way as tests using the falling head method. There are two influent lines, two effluent lines, and a connection to a cell pressure line. One influent and one effluent line are closed, and are generally used during polymer flushing. Both the influent and effluent lines are connect to a KDS 120 Legacy Dual Syringe, Single Cycle Push-Pull Syringe Pump. The influent line is connected to the push portion of the pump, while the effluent line is connected to the pull portion of the pump (Figure 9.11). This effectively forces the volume of inflow to equal the volume of outflow during testing. A differential pressure transducer is connected to the inflow and outflow lines in order to measure the flow-induced head loss. A one-way pressure transducer is connected to the inflow line in order to calculate the effective stress of the sample by considering the inflow pressure and the measured differential pressure. There is a two-way valve connecting the inflow and outflow that is used to zero out the differential transducer prior to testing. After the influent syringe has been emptied into the permeameter and the effluent syringe has been filled, the effluent is then pushed into a bottle for analysis, while the influent is recharged with fresh permeant using a bottle connected to the influent syringe. A photograph of the constant flow setup with captions can be found in Figure 9.11.

4.3 Termination Criteria

According to ASTM D6766, hydraulic equilibrium is defined as when steady hydraulic conductivity has been maintained for three consecutive measurements with no significant upward or downward trend. The volumetric outflow to inflow ratio should be within 1±0.25 (i.e., 25%).

According to the same standard, chemical equilibrium is defined as when the ratio of effluent to influent pH (pH_{out}/pH_{in}), electrical conductivity (EC_{out}/EC_{in}), and cation (Ca^{2+}, Mg^{2+}, Na^{+}, K^{+}) concentrations are within 1.0±0.1 (i.e., 10%). Equilibrium hydraulic conductivity values were reported by taking the average of the last three consecutive readings at steady state. Reaching chemical equilibrium proved to be difficult for many of the tests with very low K, and exceptions were made on a test-to-test basis. Individual judgments on termination criteria can be found in the results sections of this document.

4.4 Chemical Analysis of Effluent

Electrical Conductivity (EC) values of each sample were measured using an EC meter. The pH values of each sample were measured using a pH meter. There were four major cations measured: Ca^{2+}, Mg^{2+}, Na^{+}, and K^{+}. Before analysis, samples were diluted 10 – 25 times and digested in nitric acid until pH levels were under 2. Calibration standards were prepared using stock solutions preserved with nitric acid at pH < 2. Samples were analyzed using a Varian MPX inductively coupled plasma atomic emission spectroscopy (ICP-AES) in accordance with method 6010B defined by the U.S. Environmental Protection Agency (EPA).

4.5 Soluble Cations, Bound Cations, and CEC

Soluble cations, bound cations, and cation exchange capacity (CEC) were determined using ASTM D7503.

4.6 Total Organic Carbon (TOC) Analysis of Effluent

Total organic carbon (TOC) concentrations of effluent samples were analyzed using a Shimadzu TOC analyzer in accordance with ASTM D4839-03.

4.7 Loss on Ignition (LOI) Analysis of GCL Material

Loss on Ignition (LOI) percentages were determined in accordance with ASTM D7348.

5 RESULTS

5.1 Bentomat Permeation Using Flow Pump

5.1.1 Bentomat Permeated with DI Water

Bentomat GCL was placed in the permeameter and hooked up to the constant flow pump apparatus. The first permeant liquid used was DI water. Each syringe was filled with 10 mL of liquid, and the syringe pump pushed the liquid through the permeameter containing the GCL, as shown on Figure 9.11. Before initiation of flow of each 10 mL syringe, the differential pressure transducer was zeroed out by opening the 2-way ball valve (Figure 9.11). As flow occurred, an equilibrium differential head was achieved. After 10 mL of flow, the flow was terminated and differential head began to decrease quickly towards zero. This can be seen in Figure 9.12, which is a plot of differential head results recorded at 10 minute increments at a flow rate of 0.2 mL/hr. Inflow head results generally started at a nonzero positive value, and increased as flow occurred. Values nearing equilibrium were usually reached, however it was unpredictable compared to the differential head results. This can be seen in Figure 9.13, where differential and inflow head results recorded at 10 minute increments at a flow rate of 0.2 mL/hr are shown. In total, four flow rates: 0.1, 0.2, -0.1, and -0.2 mL/hr were used, and each run had its own equilibrium head value. By dividing this by the thickness of the GCL, an equilibrium hydraulic gradient was found. All four of these values are plotted in Figure 9.14, where discharge per unit area (Q/A) is plotted over the equilibrium hydraulic gradients measured. Average effective stresses ranging from 19.8 to 22.4 kPa were used. Using Darcy's Law, the slope of the line gives a hydraulic conductivity of $3.8*10^{-11}$ m/s, with an R^2 value of 0.986.

5.1.2 Bentomat Permeated with 50 mM $CaCl_2$

Bentomat GCL was once again placed in the permeameter and hooked up to the constant flow pump apparatus. This time, the permeant liquid was 50mM $CaCl_2$. High flow rates were used because of the corresponding high hydraulic conductivity values. Unidirectional flow was used, and each 10 mL syringe of flow had its own differential equilibrium head value used to find a hydraulic conductivity value. The average effective stress used during permeation was 13.4 kPa. Ca^{2+} and Na^{+} concentrations were measured in the effluent solution in order to check for chemical equilibrium. After 38 PVF, the permeameter was detached from the flow pump and attached to a falling head apparatus. Additional hydraulic conductivity values were obtained using the falling head method until 67 PVF. Hydraulic conductivity, $EC_{out}/EC_{in,}$ $Ca^{2+}{}_{out}/Ca^{2+}{}_{in}$, and Na^{+} concentrations plotted with PVF are shown in Figure 9.15.

5.2 Resistex Plus Permeation Using Flow Pump

5.2.1 Resistex Plus Permeated with 50 mM $CaCl_2$

Resistex Plus GCL was placed in a permeameter and hooked up to the constant flow pump apparatus. A 10 mL syringe was used and constant flow was strategically implemented in an attempt to keep hydraulic gradient constant. The average effective stress used during permeation was 13.4 kPa. Polymer flushes were carried out by forcing flow through the top and bottom plates in order to ensure excess polymer wasn't causing blockage and excess pressure build-up in the permeameter. After chemical equilibrium was established, constant flow was increased in increments. Figure 9.16 shows hydraulic conductivity, polymer flushes, flow rate, hydraulic gradient, $Ca^{2+}{}_{out}/Ca^{2+}{}_{in}$, and Na^{+} concentrations plotted against PVF. Polymer content of effluent was measured in TOC

units of mg/L, and the results are shown in Figure 9.17 along with flow rate and hydraulic gradient.

Immediately before disassembly, rhodamine tracer dye was used to observe the distribution of flow through the GCL. Areas dyed pink show the location of highest flow in Figure 9.18. The GCL was then tested for polymer content using the LOI method. The distribution of polymer content within the GCL is shown in Figure 9.19.

Replicate testing was performed with the same GCL and permeant liquid, this time with a 1.0 mL syringe. This was used in order to have better control of the hydraulic gradient. Hydraulic conductivity, given flow rate, and hydraulic gradient results are shown in Figure 9.20.

5.3 Falling Head Results

A continuation of the same test results published in Hulya Salihoglu's "Behavior of Polymer-Modified Bentonites with Aggressive Leachates (2015)," 19 falling head tests have been maintained for the purpose of monitoring their long-term behavior. All tests have been maintained for 2.5 – 3.0 years with an average hydraulic gradient of 190. Four tests were modified and studied for the purpose of this research.

5.3.1 Resistex Plus GCL Permeated with High Strength Leachate

On May 30, 2014, permeation began on a Resistex Plus GCL with High Strength Leachate. An average hydraulic gradient of 190 was used until February 15, 2017, for a total of 992 days. Hydraulic conductivity and hydraulic gradient results for this period can be found on Figure 9.21. On February 15, 2017, the average hydraulic gradient was doubled and cell pressure was increased giving a slight increase in effective stress (i.e.

from 20 kPa to 26.5 kPa). The hydraulic conductivity and hydraulic gradient results measured before and after the gradient change can be found on Figure 9.22. Major cation ratio concentrations during this entire permeation process can be found on Figure 9.23. Immediately before disassembly, rhodamine tracer dye was used to observe the distribution of flow through the GCL. Areas dyed pink show the location of highest flow in Figure 9.26. The GCL was then tested for polymer content using LOI (Figure 9.27).

5.3.2 Resistex Plus GCL Permeated with Trona Leachate

On May 25, 2014, permeation began on a Resistex Plus GCL with Trona leachate. An average hydraulic gradient of 190 was used until February 15, 2017, for a total of 997 days. Hydraulic conductivity and hydraulic gradient results for this period can be found on Figure 9.28. On February 15, 2017, the average hydraulic gradient was doubled and cell pressure was increased giving a slight increase in effective stress (i.e. from 20 kPa to 26.5 kPa). The hydraulic conductivity and hydraulic gradient results before and after the gradient change can be found on Figure 9.29. Immediately before disassembly, rhodamine tracer dye was used to observe the distribution of flow through the GCL. Areas dyed pink show the location of highest flow in Figure 9.31. The GCL was then tested for polymer content using LOI (Figure 9.32).

5.3.3 Resistex GCL Permeated with Trona Leachate

On June 4, 2015, permeation began on a Resistex GCL with Trona leachate. An average hydraulic gradient of 190 was used until March 16, 2017, for a total of 1016 days. Hydraulic conductivity and hydraulic gradient results for this period can be found on Figure 9.33. On March 16, 2017, the average hydraulic gradient was increased incrementally giving average gradients of 190, 233, 276, 319, 380, and 470 and cell

pressure was increased giving slight increases in effective stress (i.e. from 20 to 21.4, 22.9, 24.4, 26.5, and 29.5 kPa respectively). The hydraulic conductivity and hydraulic gradient results before and after the gradient increases can be found on Figure 9.34, and TOC concentration can be found in Figure 9.35, with a zoomed in version found on Figure 9.36.

5.3.4 Resistex Plus GCL Permeated with Typical FGD Leachate

On June 4, 2015, permeation began on a Resistex Plus GCL with Typical FGD leachate. An average hydraulic gradient of 190 was used until March 16, 2017, for a total of 1016 days. Hydraulic conductivity and hydraulic gradient results for this period can be found on Figure 9.37. On March 16, 2017, the average hydraulic gradient was increased incrementally giving average gradients of 190, 233, 276, 319, 380, and 470 and cell pressure was increased giving slight increases in effective stress (i.e. from 20 to 21.4, 22.9, 24.4, 26.5, and 29.5 kPa respectively). The hydraulic conductivity and hydraulic gradient results before and after the gradient increases can be found on Figure 9.38, and TOC concentration can be found in Figure 9.39, with a zoomed in version found on Figure 9.40.

6 DISCUSSION

6.1 Bentomat Permeation Using Flow Pump

6.1.1 Bentomat Permeated with DI Water

The tests giving the four data points in Figure 9.14 used effective stresses ranging from 19.8 to 22.4 kPa. The hydraulic conductivity of $3.8*10^{-11}$ m/s from Figure 9.14 is comparable to the hydraulic conductivity of $4.4*10^{-11}$ (m/s) found using the same GCL type and permeant liquid and an effective stress of 20 kPa (Chen, 2015). The results were also found in a relatively short time of less than 2 weeks. However, it is noted that the strategy of plotting discharge per unit area (Q/A) over the equilibrium hydraulic gradients and finding the slope equaling the hydraulic conductivity will not work if the hydraulic conductivity is changing over PVF, which is true for most GCLs and permeants where cation exchange will occur.

6.1.2 Bentomat Permeated with 50 mM $CaCl_2$

Because significant cation exchange was expected for this permeant, the method described in the previous section of using positive and negative flow rates to find K was not used. Rather, unidirectional flow was implemented and hydraulic conductivity was plotted as changing with PVF in Figure 9.15. This test showed that the constant flow method can be used to achieve chemical equilibrium very quickly for Na-B GCLs permeated with high concentration leachates. It is noted that this would take the same amount of time to occur as the falling head method. As is shown in Figure 9.15, by switching the permeameter directly from constant flow to falling head, it was proven that comparable hydraulic conductivity values can be achieved using both methods.

6.2 Resistex Plus Permeation Using Flow Pump

6.2.1 Resistex Plus Permeated with 50mM $CaCl_2$

The goal of this portion of testing was to answer the question: after chemical equilibrium is reached, will an increase in hydraulic gradient affect the polymer elution and hydraulic conductivity of a Resistex Plus GCL? It was desirable to reach chemical equilibrium before increasing flow rate in order to isolate the hydraulic gradient as the potential mechanism for increased polymer elution. It was also desirable to strategically change the flow rate in order to keep a constant hydraulic gradient until it was time to test its effect. However, as can be seen in

Figure 9.16, the hydraulic gradient for the first 5 PVF was very high. This proved difficult to control because of the unexpectedly low hydraulic conductivity values giving high hydraulic gradients, despite using the lowest allowable flow rate. In addition, hydraulic conductivity increased so significantly after ~20 PVF that it proved difficult to maintain a reasonably high gradient for 20-40 PVF.

Nevertheless, chemical equilibrium was achieved and incremental flow rate changes from 20 to 40, 40 to 80, and 80 to 120 ml/hr were tested at ~40, ~50, and ~60 PVF, respectively. The relationship between hydraulic conductivity, flow rate, hydraulic gradient, and TOC concentration can be found in Figure 9.17. For Resistex Plus permeated with 50 mM $CaCl_2$, there is no evidence that an increase in flow rate and gradient is causing a change in hydraulic conductivity or polymer elution after chemical equilibrium has been achieved. However, it was noted that because the hydraulic conductivity is so high, perhaps at the points of given flow rate change (e.g. ~40, 50, and 60 PVF), there was no more elutable polymer within the flow pattern of the GCL. Dye

testing and polymer content testing using LOI given in Figure 9.18 and Figure 9.19 show significant preferential flow and low polymer content in the region of high flow. It is preferable to run a similar type of gradient test on a GCL reaching chemical equilibrium with a significantly lower hydraulic conductivity values.

6.2.2 Replicate Resistex Plus Permeated with 50mM $CaCl_2$

Replicate testing is in progress using a 1.0 mL syringe in order to have a lower minimum flow rate. This was used in order to prevent the high hydraulic gradient values seen in the first 5 PVF in Figure 9.16. A side-by-side comparison of hydraulic conductivity results between the two tests can be found in Figure 9.42. This shows that the results are repeatable, and the gradient difference appears to be having a slight but likely negligible effect on the hydraulic conductivity results.

6.2.3 Comparison of Falling Head and Constant Flow Pump Results for Resistex Plus Permeated with 50mM $CaCl_2$

Falling head results are provided by Geng (2017) using identical GCL and permeant liquids. Average hydraulic gradients of 40, 50, 80, 90, 120, 130, and 150 are provided with a comparison to both constant flow pump results in Figure 9.43. Falling head results have average effective stresses ranging from 16.6 to 20.0 kPa, while constant flow pump results have an average effective stress of 13.4 kPa. A closer look at the first 15 PVF is provided in Figure 9.44. On average, constant flow pump hydraulic conductivity results are 2 orders of magnitude smaller for 0-8.5 PVF. These results are confirmed by the replicate test.

The exact reasoning for this large difference in hydraulic conductivity isn't known with full confidence. However, this section will serve as a preliminary explanation of why

this difference in hydraulic conductivity values is occurring. The constant flow method has an equal amount of inflow and outflow, while the falling head method doesn't follow the same constraint. By subtracting the cumulative outflow from the cumulative inflow of the falling head results, a rough change in the pore space volume can be calculated. Cumulative inflow minus cumulative outflow plotted with PVF is shown in Figure 9.45 for all tests provide by Geng (2017). Only the first 8 PVF are plotted, because this is the range where the large difference in hydraulic conductivity values is seen. All of these results show a decrease in pore space volume ranging from 15 mL to 60 mL, excluding the permeameter where hydraulic gradient equals 120. This anomaly was likely due to a leak in the inflow plate.

The decrease in pore space volume is consistent with the cation exchange process described in Figure 9.47. Before cation exchange occurs, the Na-Bentonite will have negatively charged montmorillonite particles, with water and sodium ions occupying the interlamellar space giving it a large DDL thickness. Calcium ions and water will be occupying the intergranular pore space, as long as $CaCl_2$ is used as the permeating liquid. This pre-cation exchange scenario is described in Figure 9.47a. After cation exchange occurs, calcium ions will be occupying the interlamellar space. The stronger charges of the calcium ions will have a stronger pull on the negatively charged montmorillonite particles, which will cause the DDL thickness to decrease and cause a higher portion of water molecules to enter the intergranular space. This post-cation exchange scenario is described in Figure 9.47b.

The constant flow method doesn't allow the outflow to be greater than the inflow, as is seen in the falling head method. Because of this, a build-up of pressure within the

GCL as cation exchange causes a higher portion of water molecules to enter the intergranular pore space. The falling head method allows this pressure to dissipate quickly; however, in the constant flow method, this process would be expected to take a longer amount of time because the outflow isn't allowed to be greater than the inflow. The inflow and outflow pressures measured using the constant flow method from 0 – 8.5 PVF are shown in Figure 9.46. Both the inflow and outflow pressure show a build-up of pressure from 0 – 3 PVF, followed by a slow decrease of pressure from 3 – 8.5 PVF. This author hypothesizes that the inability of the constant flow method to quickly dissipate excess pore water is what caused the hydraulic conductivity values to remain low from 0 – 8.5 PVF. It is also hypothesized that large scale polymer elution and preferential flow caused the hydraulic conductivity of the constant flow method to increase to the same range as the falling head method. This increase in hydraulic conductivity can be seen in Figure 9.43 and Figure 9.44 from approximately 9 – 12 PVF.

6.3 Falling Head Tests

The effect of hydraulic gradient on hydraulic conductivity was tested on 4 GCLs. One of them, Resistex Plus GCL permeated with High Strength leachate, was tested for chemical equilibrium via major cation ratios, Ca^{2+}, Mg^{+}, and K^{+}. As shown in Figure 9.23, the test was nearly in chemical equilibrium before any hydraulic gradient changes were made. Ideally, all GCLs would be in chemical equilibrium before gradient alterations would be made. This is desirable in order to isolate hydraulic gradient as a mechanism for change rather than cation exchange. All 4 GCLs tested had been running for 16 – 23 PVF, 992 – 1016 days with constant hydraulic conductivity results for 600 – 1000 days. Because of this, it was assumed that all 4 tests were nearly in chemical equilibrium before

any hydraulic gradient changes were made, and that any cation exchange occurring would have a negligible effect on the measurements made.

6.3.1 Resistex Plus GCL Permeated with High Strength Leachate

The hydraulic conductivity results given in Figure 9.21 show that the hydraulic conductivity has remained quite constant for nearly the entirety of the 992 days and 23 PVF that the test was running. After the average hydraulic gradient was increased from 190 to 380, the hydraulic conductivity increased by 3 orders of magnitude, from $8.0*10^{-12}$ to $8.6*10^{-9}$, within a few days. This is seen in Figure 9.22. The slight increase in effective stress accompanying the change in gradient (i.e. from 20 kPa to 26.5 kPa) was implemented to prevent low minimum effective stresses, because ASTM D5084 recommends keeping effective stresses > 7 kPa or else risk separation of the membrane from the rest of the specimen. Maximum, minimum, and average effective stresses at the inflow, outflow, and middle margins of the GCL are shown in Figure 9.41.

It was hypothesized that an increase in hydraulic gradient would cause an increase in polymer elution, which in turn would cause an increase in preferential flow and subsequent hydraulic conductivity. The hydraulic conductivity, hydraulic gradient, and TOC results for this test are shown in Figure 9.24. It can be seen that there is actually a significant decrease in TOC content after the increase in gradient was implemented. It is possible that a very small amount of polymer elution is needed for preferential flow to develop. In addition, as soon as preferential flow develops, there is no longer as much polymer blocking the flow, so elution will significantly decrease. The first TOC concentration measurement performed after the increase in hydraulic gradient was taken on a 60 mL sample of effluent. Figure 9.25 gives a representation of what TOC

concentrations in the effluent might have looked like had measurements been taken every 5 mL, rather than all at once. An increase in elution followed by a significant decrease is shown in Figure 9.25. Given the TOC concentration of the first sample, it is possible for the first 5 mL to have had a very high TOC measurement, which would fit the original hypothesis, but then it was diluted by the following 55 mL of flow. This possibility is consistent with the results seen in the next section, 6.3.2. The dye testing and polymer contents from LOI results in Figure 9.26 and Figure 9.27 show that the majority of flow occurred in the upper right corner, but the polymer content remained spatially homogeneous. This provides evidence that the mechanism shown is occurring for a large area of GCL, rather than being isolated to a small portion. It also provides evidence that sidewall leakage was not occurring.

6.3.2 Resistex Plus GCL Permeated with Trona Leachate

Hydraulic conductivity results for the GCL before any changes were made to the hydraulic gradient are shown in Figure 9.28. From approximately 4 – 7 PVF, there were some large increases in hydraulic conductivity. This was believed to be a result of sidewall leakage. As a result, the permeameter was taken apart and put back together with a new flexible membrane. After that, the hydraulic conductivity has remained quite constant from 10 – 20 PVF, which occurred over 600 days. After the average hydraulic gradient was increased from 190 to 380, the hydraulic conductivity increased by 3 orders of magnitude, from $3.8*10^{-12}$ to $4.8*10^{-9}$, within a few days. This is seen in Figure 9.29. The slight increase in effective stress accompanying the change in gradient (i.e. from 20 kPa to 26.5 kPa) was implemented to prevent low minimum effective stresses, because ASTM D5084 recommends keeping effective stresses > 7 kPa or else risk separation of the membrane

from the rest of the specimen. Maximum, minimum, and average effective stresses at the inflow, outflow, and middle margins of the GCL are shown in Figure 9.41.

It was hypothesized that an increase in hydraulic gradient would cause an increase in polymer elution, which in turn would cause an increase in preferential flow and subsequent hydraulic conductivity. Hydraulic conductivity, hydraulic gradient, and TOC results are shown in Figure 9.30. It can be seen that there is significant increase in TOC in the first measurement after the increase was implemented, followed by a significant decrease in TOC in the subsequent sample measurements. The increase in TOC fits the original hypothesis that an increase in polymer elution is causing the increase in hydraulic conductivity. The subsequent decrease in TOC is explained in that there is no longer any polymer blocking the flow, so elution will significantly decrease. The dye testing and LOI results shown in Figure 9.31 and Figure 9.32 show that the majority of flow occurred in the upper left corner, and the polymer content was slightly lower in the area of concentrated flow. This provides evidence that the mechanism described is occurring for a large area of GCL, rather than being limited to a small portion. It also provides evidence that sidewall leakage was not occurring.

6.3.3 Resistex GCL Permeated with Trona Leachate

Hydraulic conductivity results for the GCL before any changes were made to the hydraulic gradient are shown in Figure 9.33. From approximately 5 – 8 PVF, there was a large increase in hydraulic conductivity. This was believed to be a leak which was fixed after which the hydraulic conductivity returned to a low value. After that, the hydraulic conductivity remained quite constant from 8 – 18 PVF, which occurred over 800 days. After incremental gradient increases giving average gradients of 190, 233, 276, 319, 380,

and 470, there was little to no change in hydraulic conductivity values. This is seen in Figure 9.34. The slight increases in effective stress (i.e. from 20 to 21.4, 22.9, 24.4, 26.5, and 29.5 kPa respectively) were considered to have a negligible effect on hydraulic conductivity and TOC values. Maximum, minimum, and average effective stresses at the inflow, outflow, and middle margins of the GCL are shown in Figure 9.41.

It was hypothesized that an increase in hydraulic gradient would cause an increase in polymer elution, which in turn would cause an increase in preferential flow and subsequent hydraulic conductivity. Hydraulic conductivity, hydraulic gradient, and TOC results are found in Figure 9.35. It can be seen that there is no significant change in TOC measurements during the hydraulic gradient increases. A zoomed in version of hydraulic conductivity, hydraulic gradient, and TOC results are found in Figure 9.36. It can be seen that the hypothesis for this was incorrect. Based off the first 2 tests described in 6.3.1 and 6.3.2, it was expected that there would be a significant increase in hydraulic conductivity at some gradient less than 380. This was not the case. There appears to be some mechanism during an incremental increase rather than an immediate increase that allows the hydraulic conductivity to remain low.

6.3.4 Resistex Plus GCL permeated with Typical FGD Leachate

Hydraulic conductivity results for the GCL before any changes were made to the hydraulic gradient are shown in Figure 9.37. The hydraulic conductivity has remained quite constant for the majority of the test, which has been over 1000 days. After incremental gradient increases were applied, giving average gradients of 190, 233, 276, 319, 380, and 470, there was little to no change in hydraulic conductivity values. This is seen in Figure 9.38. The slight increases in effective stress (i.e. from 20 to 21.4, 22.9,

24.4, 26.5, and 29.5 kPa respectively) were considered to have a negligible effect on hydraulic conductivity and TOC values. Maximum, minimum, and average effective stresses at the inflow, outflow, and middle margins of the GCL are shown in Figure 9.41.

It was hypothesized that an increase in hydraulic gradient would cause an increase in polymer elution, which in turn would cause an increase in preferential flow and subsequent hydraulic conductivity. Hydraulic conductivity, hydraulic gradient, and TOC results are shown in Figure 9.39. It can be seen that there is a small increase in polymer elution, but the increase is accompanied by no change in hydraulic conductivity values. A zoomed in version of hydraulic conductivity, hydraulic gradient, and TOC results are shown in Figure 9.40. It can be seen that the hypothesis for this was incorrect. Based off the first 2 tests in 6.3.1 and 6.3.2, it was expected that there would be a significant increase in hydraulic conductivity at some gradient less than 380. This was not the case. There appears to be some mechanism during an incremental increase rather than an immediate increase that allows the hydraulic conductivity to remain low.

7 CONCLUSIONS

A constant flow pump was developed and tested on both Na-B and DB GCLs permeated with DI water and different concentrations of $CaCl_2$. Hydraulic conductivity values equivalent to those in the literature using falling head test methods were measured using Na-B GCLs permeated with DI water and 50 mM $CaCl_2$, and DB GCLs permeated with 50 mM $CaCl_2$. The following conclusions were drawn from these testing results.

1. Precise hydraulic conductivity measurements with multiple flow rates can be measured for tests where low amounts of hydraulic conductivity changes over time are expected (i.e. Na-B GCL permeated with DI water).
2. Measurements equivalent to those found in falling head tests can be found in a comparable amount of time using Na-B GCLs.
3. There is an extended period of time where the constant flow method causes the hydraulic conductivity measurements of DB GCLs to be significantly lower than those measurements found using the falling head method. This is a significant disadvantage as it could take months to years longer for a constant flow pump test to reach chemical equilibrium.
4. When hydraulic conductivity values are very high, an increase in hydraulic gradient causes no extra polymer to be eluted out of DB GCLs.

Four falling head permeameter tests with DB GCLs that had been running for ~1000 days at low hydraulic conductivity values ($< 1.0*10^{-11}$ with either Trona, Typical FGD, or High Strength leachate at an average hydraulic gradient of 190 were manipulated by either doubling the gradient from 190 to 380, or incrementally increasing the gradient from 190, 233, 276, 319, 380, and 470. Minor increases in effective stress (i.e. from 20 to

21.4, 22.9, 24.4, 26.5, and 29.5 kPa respectively) were implemented to prevent low minimum effective stresses, because ASTM D5084 recommends keeping effective stresses > 7 kPa or else risk separation of the membrane from the rest of the specimen. The following conclusions were drawn from these testing results.

1. An immediate increase in hydraulic gradient from 190 to 380 can cause the hydraulic conductivity of DB GCLs to increase by greater than 3 orders of magnitude in as little as 1 to 2 days. The increase in hydraulic conductivity will likely be accompanied by a short surge of polymer elution followed by very low elution.
2. By incrementally increasing the hydraulic gradient from 190, 233, 276, 319, 380, and 470, and allowing one week for any change to occur at each gradient, the hydraulic conductivity can remain constant.
3. There appears to be some mechanism during an incremental increase rather than an immediate increase that allows the hydraulic conductivity to remain low at gradients as high as 500. The precise mechanism for this is unknown at this time.
4. This stability of the hydraulic conductivity of DB GCLs for tests with incremental increases in hydraulic gradient shows great promise for expedited hydraulic conductivity testing of DB GCLs.

8 TABLES

Table 8.1: Physical and chemical properties of 3 GCL types (Salihoglu, 2015)

Property		Bentomat	Resistex	Resistex Plus	Method
Initial Water Content (%)		4.84	3.22	4.42	ASTM D 2216
Swell Index to DI water (mL/2 g)		29.5	27.5	27.0	ASTM D 5890-11
Loss on Ignition (%)		1.92 ± 0.10	3.70±1.80	6.17± 1.93	Scalia (2012)
Initial Thickness (mm)		7.3 - 8.2	7.2 - 8.8	7.1 - 8.3	-
Bentonite mass per unit area (kg/m^2)		3.6	3.6	3.6	-
Cation Exchange Capacity (cmol+/kg)		84.0	79.1	85.5	ASTM D 7503-10
Bound Cations ($cmol^+/kg$)	Na	28.7	40.4	18.0	
	K	2.94	1.1	0.5	
	Ca	23.6	20.7	10.3	
	Mg	11.1	9.9	5.3	

Table 8.2: Bentonite Mineralogy of 3 GCL Types (Salihoglu, 2015)

Mineral Constituent	Chemical Formula	Relative Abundance (%)		
		Bentomat	Resistex	Resistex Plus
Quartz	SiO_2	9	7	8
Cristobalite	SiO_2	-	5	2
Albite feldspar	$NaAlSi_3O_8$	-	2	7
Augite	$Ca(Fe, Mg)Si_2O_6$	1	1	-
Plagioclase Feldspar-Oligoclase	$(Na_{0.82}Ca_{0.18})AlSi_3O_8$	3	-	-
K-Feldspar-Orthoclase	$KAlSi_3O_8$	Trace	1	trace
Calcite	$CaCO_3$	1	-	-
Gypsum	$CaSO_4 . 2H_2O$	trace	1	1
Clinoptilolite	$(Na,K,Ca)6(Si,Al)_{36}O_{72} . 20H_2O$	2	2	2
Kaolinite	$Al_2Si_2O_5(OH)_4$	trace	-	trace
Illite/Mica	$KAl_2(Si_3AlO_{10})(OH)_2$	1	1	1
Montmorillonite	$(Na,Ca)_{0.3}(Al,Mg)_2Si_4O_{10}(OH)_2 . xH_2O$	84	80	79

Table 8.3: Concentrations of major ionic species, pH, ionic strength, and RMD for all leachates used; modified from (Salihoglu, 2015)

Cation or Anion	50 mM $CaCl_2$	High Strength	Typical FGD	Trona
Ca (mg/L)	2003.9	512	542	500
Na (mg/L)	-	2500	968	14800
Mg (mg/L)	-	140	73.1	150
K (mg/L)	-	22.2	49.9	200
Cl (mg/L)	3545.3	1720	784	-
SO_4 (mg/L)	-	4720	2620	33000
pH	7.6±0.3	8.0±0.5	8.0±0.5	11.0±0.5
Ionic Strength (mM)	150	177	96.8	755
RMD ($M^{1/2}$)	0	1.00	0.39	4.4

9 FIGURES

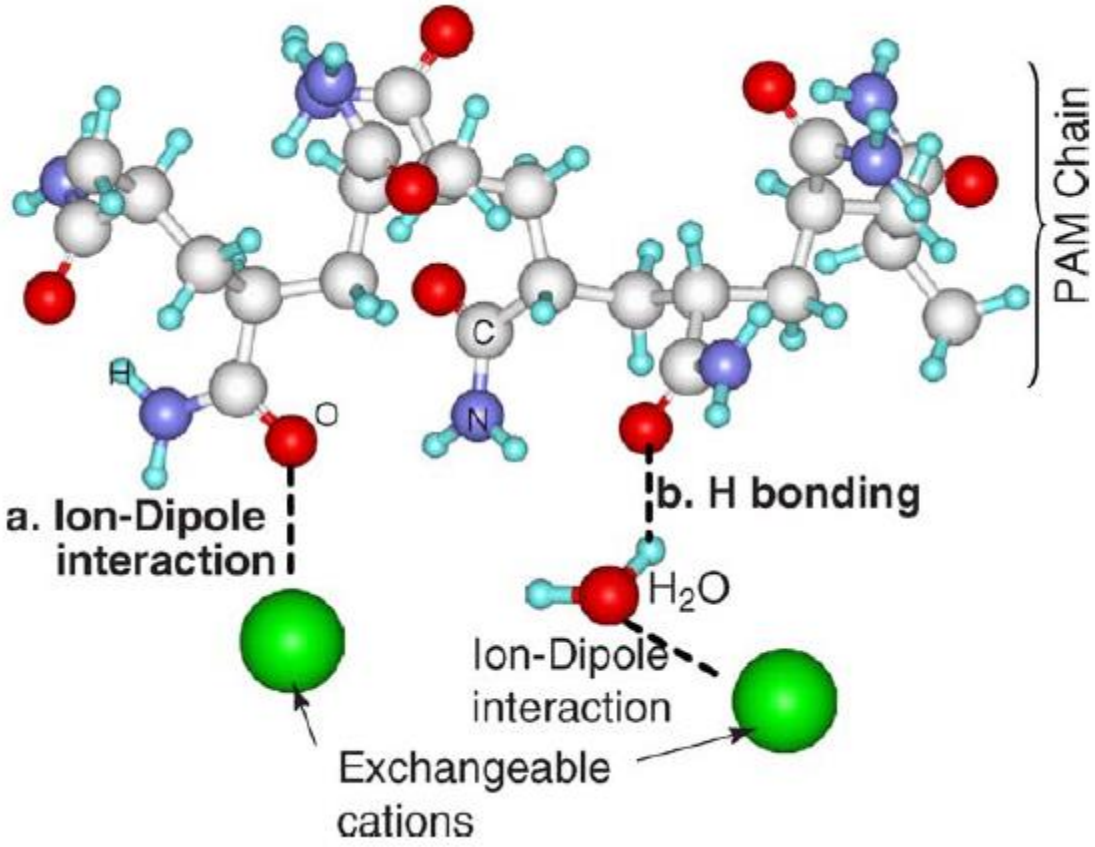

Figure 9.1: Conceptual model of two main types of bond between PAM and exchangeable cations in the interlayer of montmorillonite (a) ion-dipole interaction or coordination and (b) Hydrogen bonding of amide groups with water molecules in the hydration shells of exchangeable cations (from Deng et al. 2006).

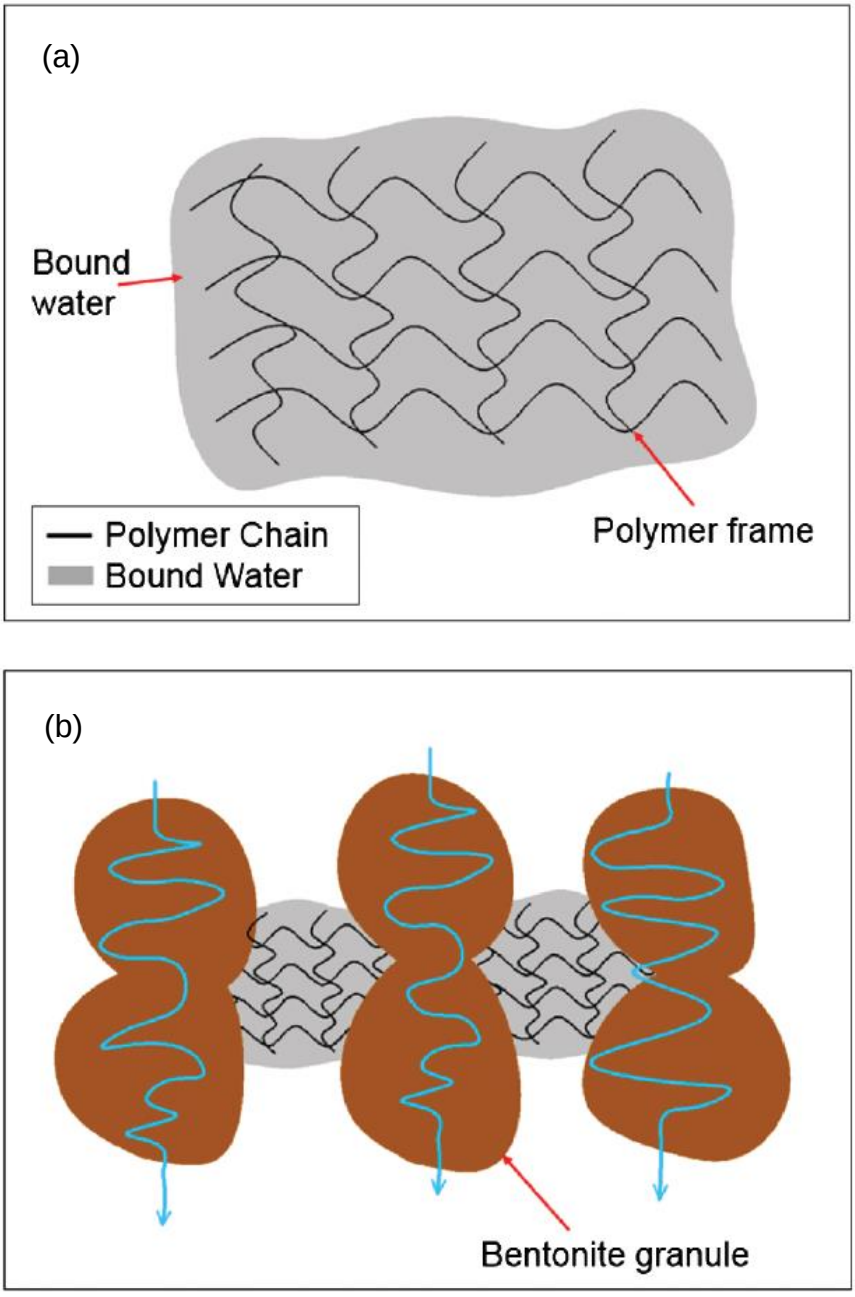

Figure 9.2: Conceptual model of clogging mechanism of hydrogel in DB Polymer GCL (a) hydrogel formation with bound water and (b) hydrogel clogs intergranular flow path and yields to low hydraulic conductivity when bentonite loses swell (from Tian et al. 2016).

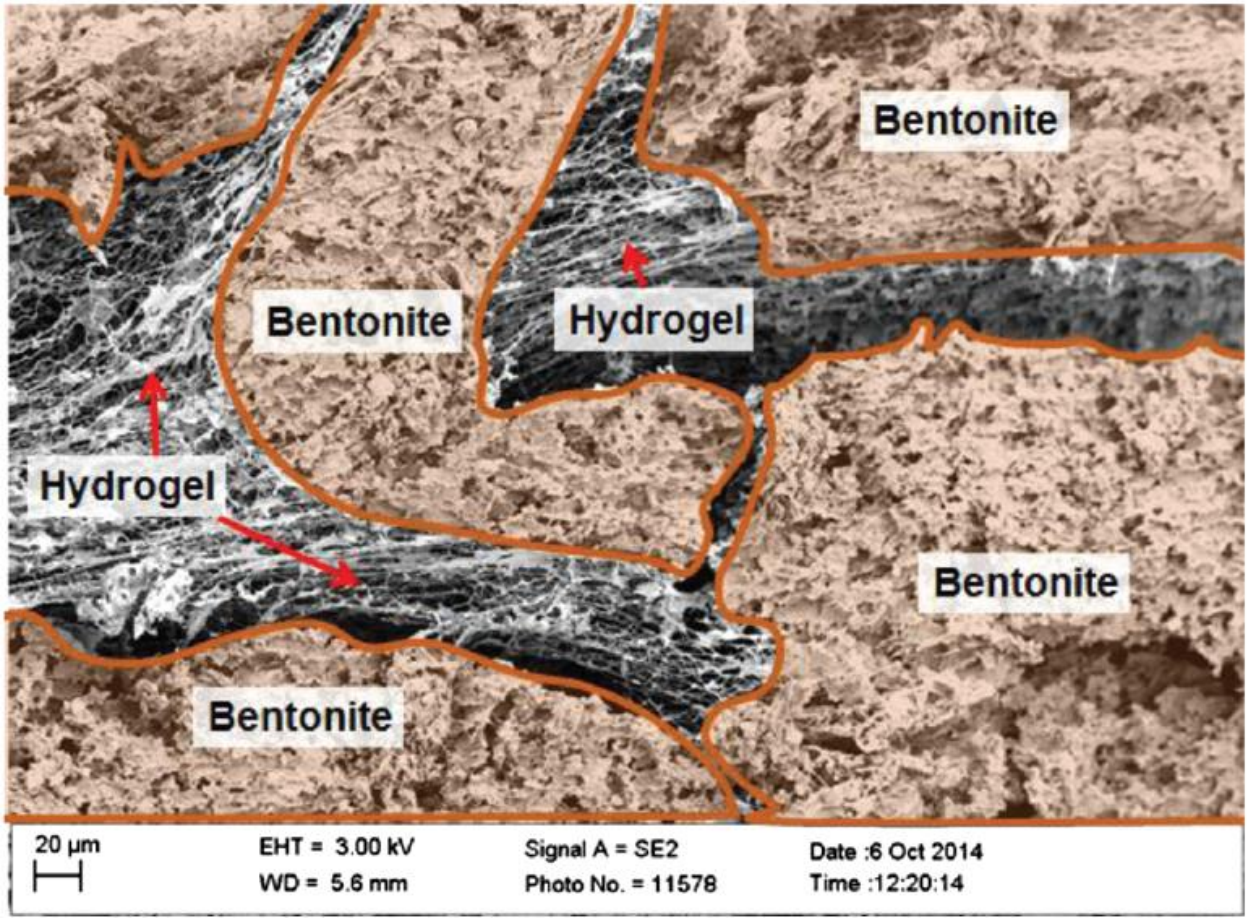

Figure 9.3: SEM image of a freeze-dried DB polymer GCL permeated with DI water. The image shows hydrogel clogging the intergranular pore space (from Tian et al. 2016).

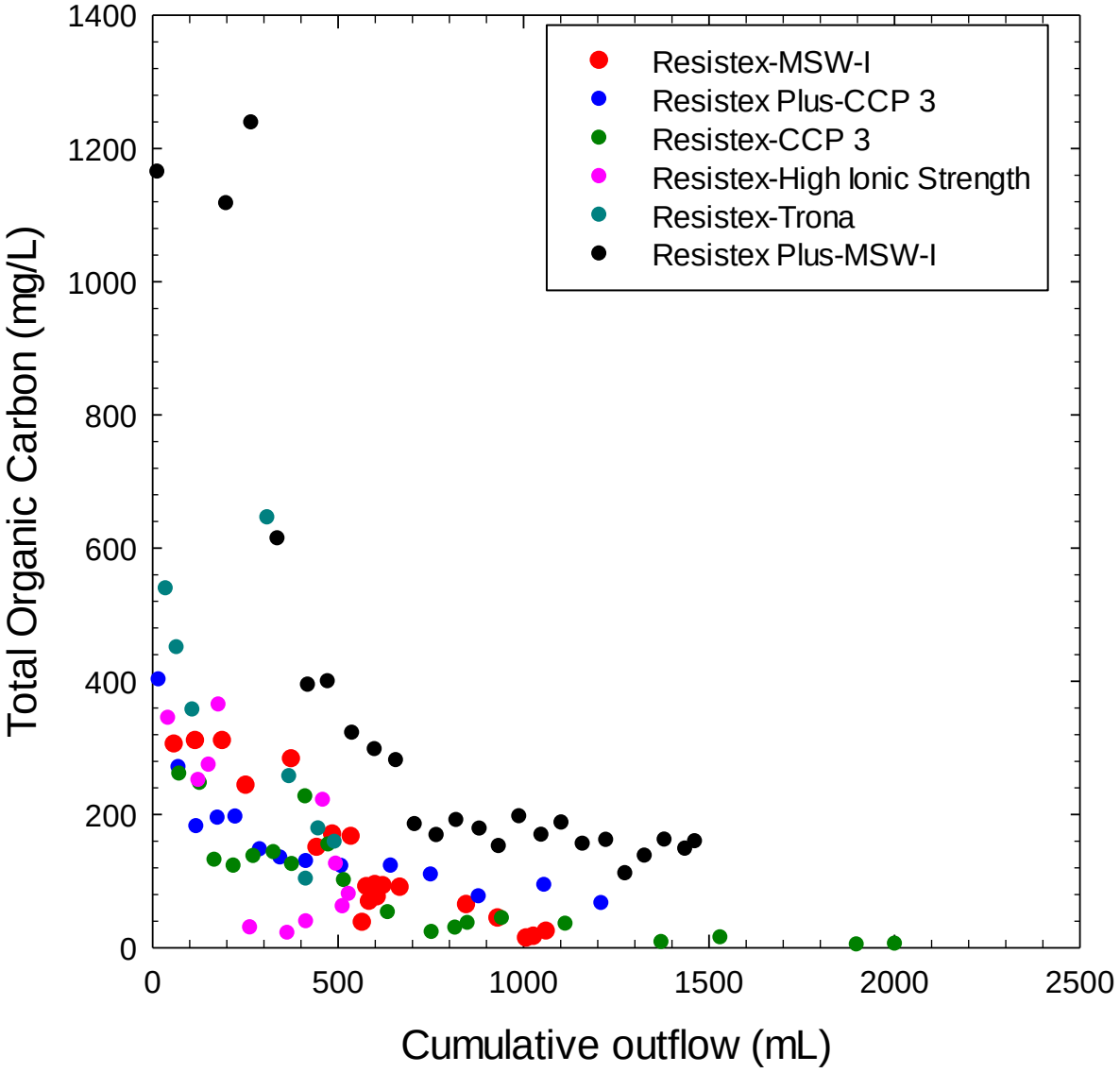

Figure 9.4: Total Organic Carbon (TOC) versus cumulative outflow for Resistex GCLs for several different leachate types (from Salihoglu, 2015).

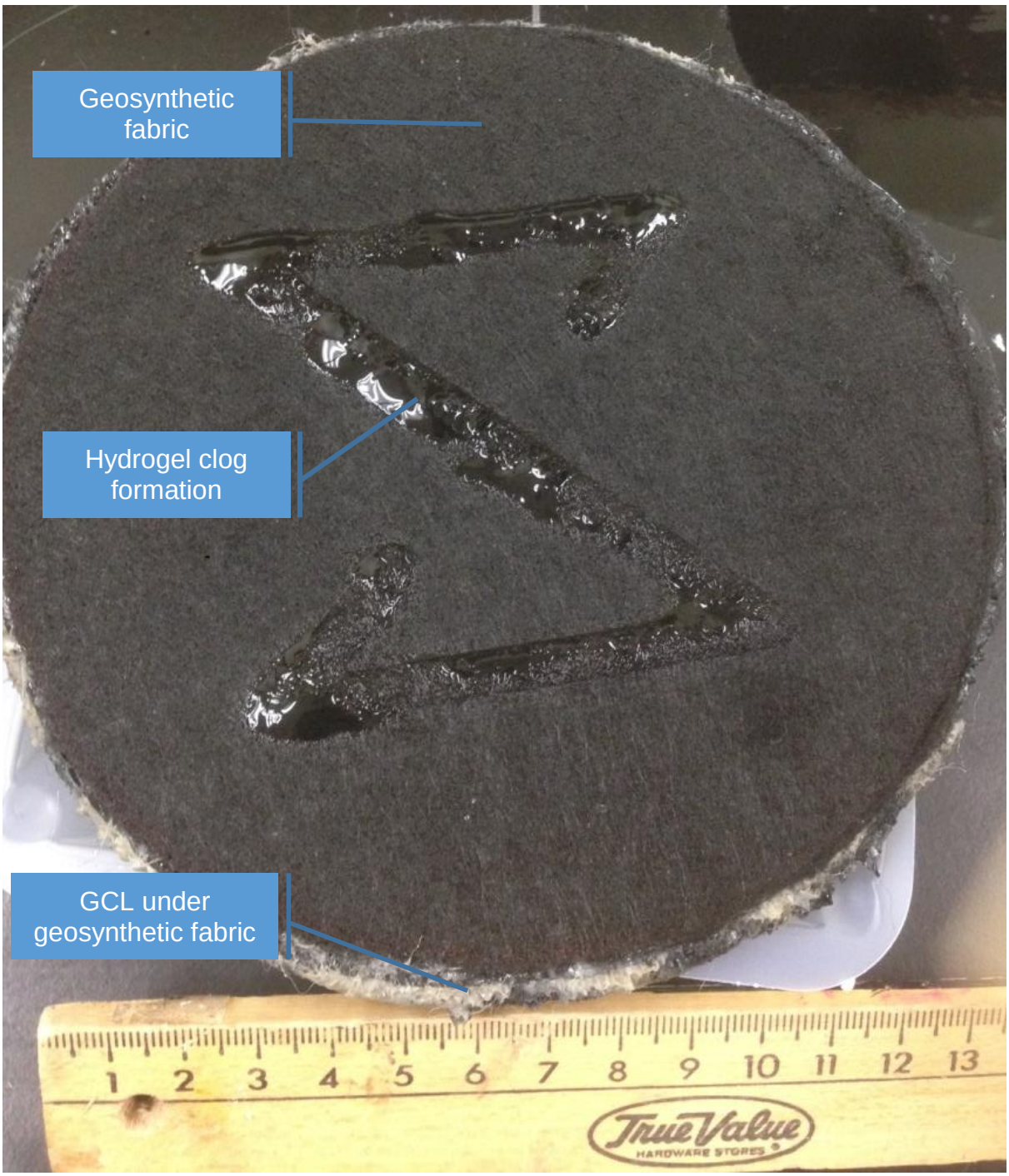

Figure 9.5: Hydrogel that had clogged the outflow plate on a Resistex Plus GCL during the early stages of permeation with Trona leachate

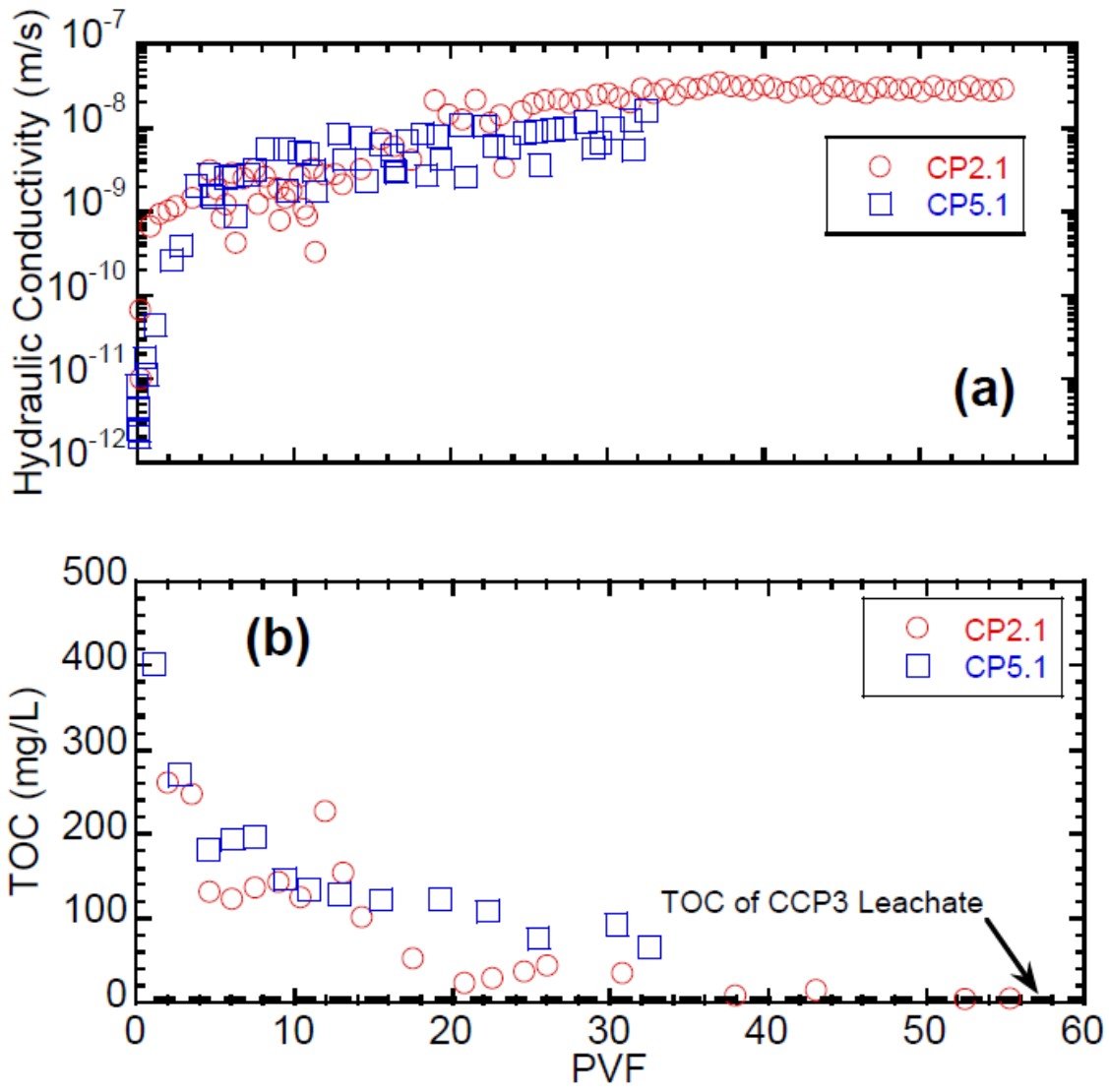

Figure 9.6: (a) hydraulic conductivity of a GCL increases with PVF for Resistex and Resistex Plus GCL permeated with CCP leachate and (b) TOC concentration is highest during beginning stage of flow and decreases with time. As polymer elution occurs, the hydraulic conductivity increases (from Chen, 2015).

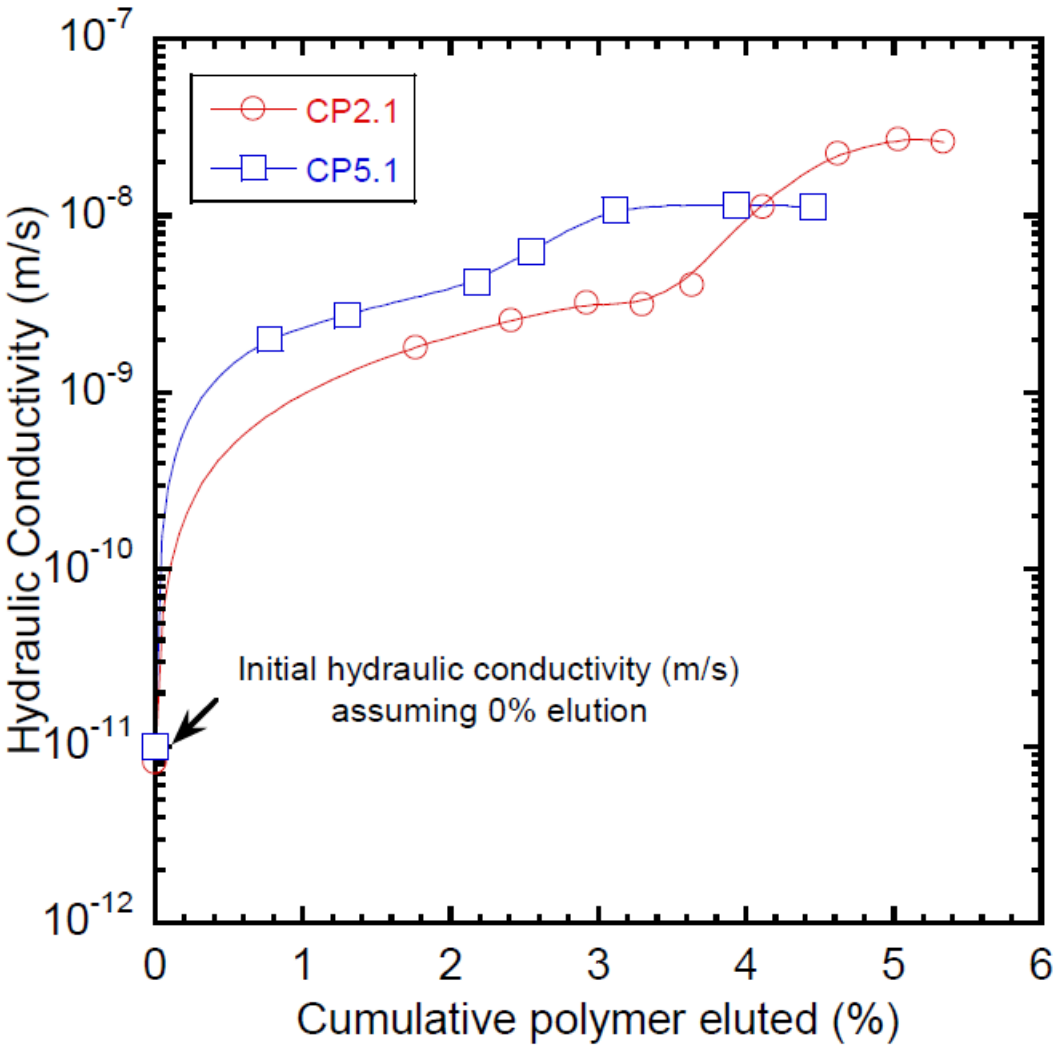

Figure 9.7: Hydraulic conductivity of Resistex and Resistex Plus GCLs permeated with a CCP leachate increases as the cumulative polymer percent eluted increases (from Chen, 2015).

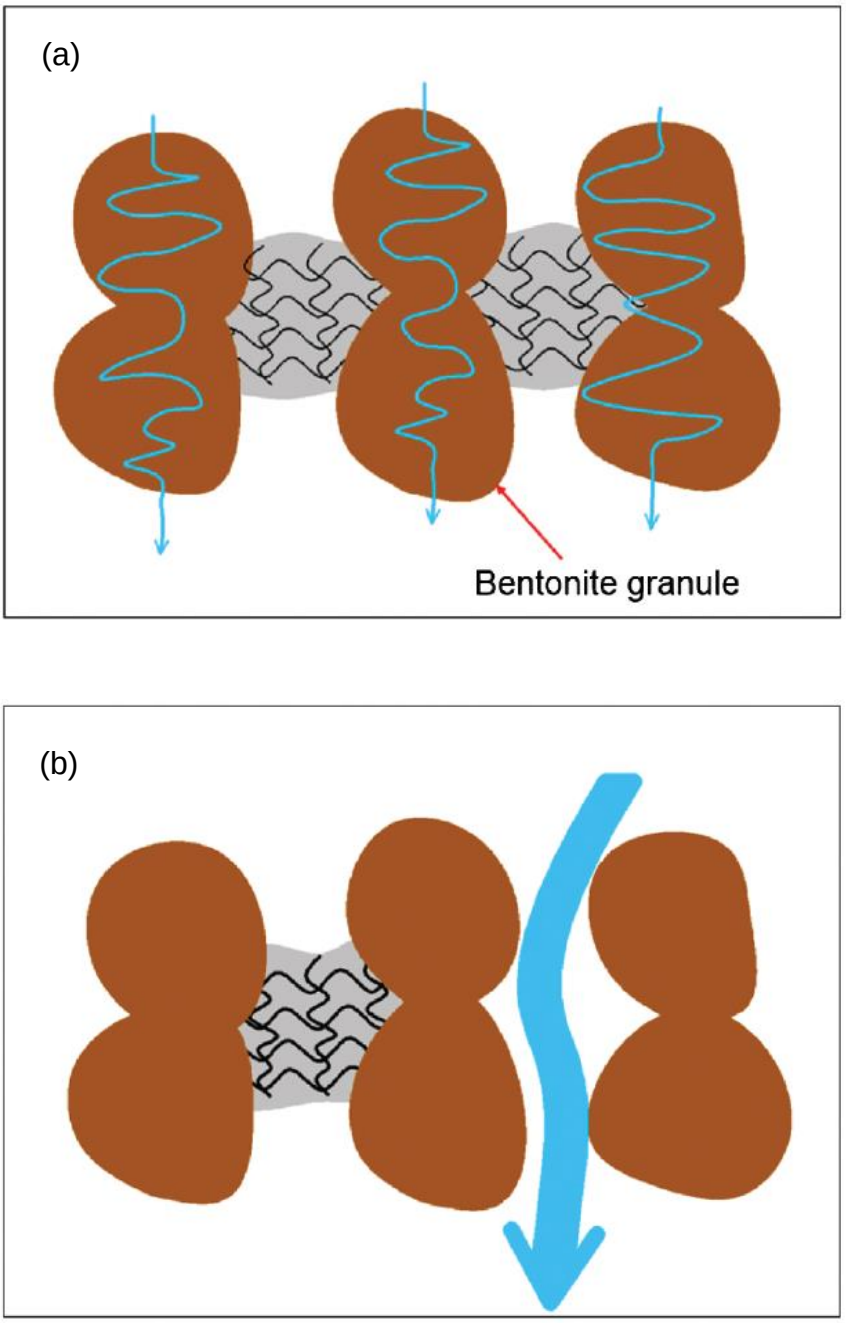

Figure 9.8: Conceptual model of polymer elution causing increased hydraulic conductivity in DB Polymer GCL (a) hydrogel clogs intergranular flow path and yields low hydraulic conductivity with restricted bentonite swell (b) hydrogel can elute out and cause hydraulic conductivity to increase (from Tian et al. 2016)

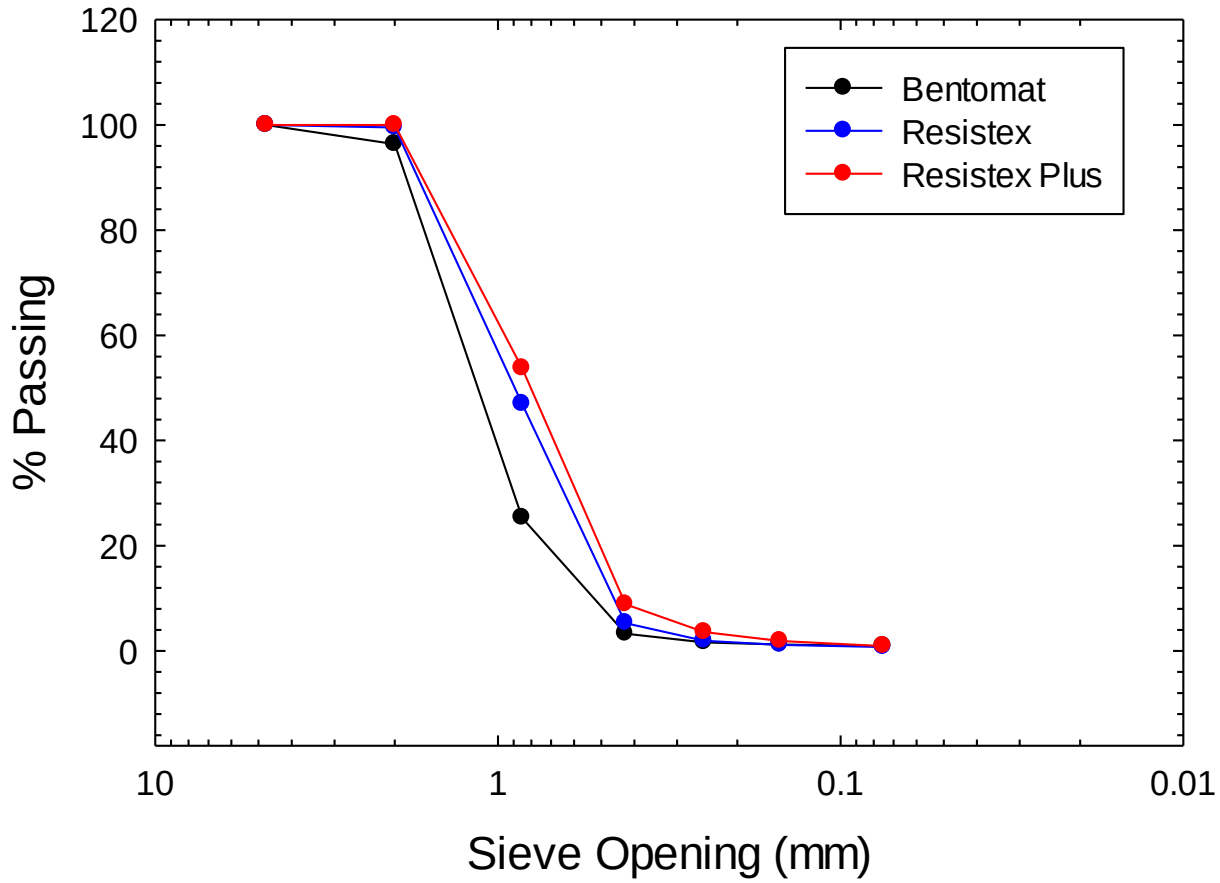

Figure 9.9: Granule size distributions of each GCL obtained by dry sieving of bentonite and bentonite-polymer dry mixtures (from Salihoglu, 2015).

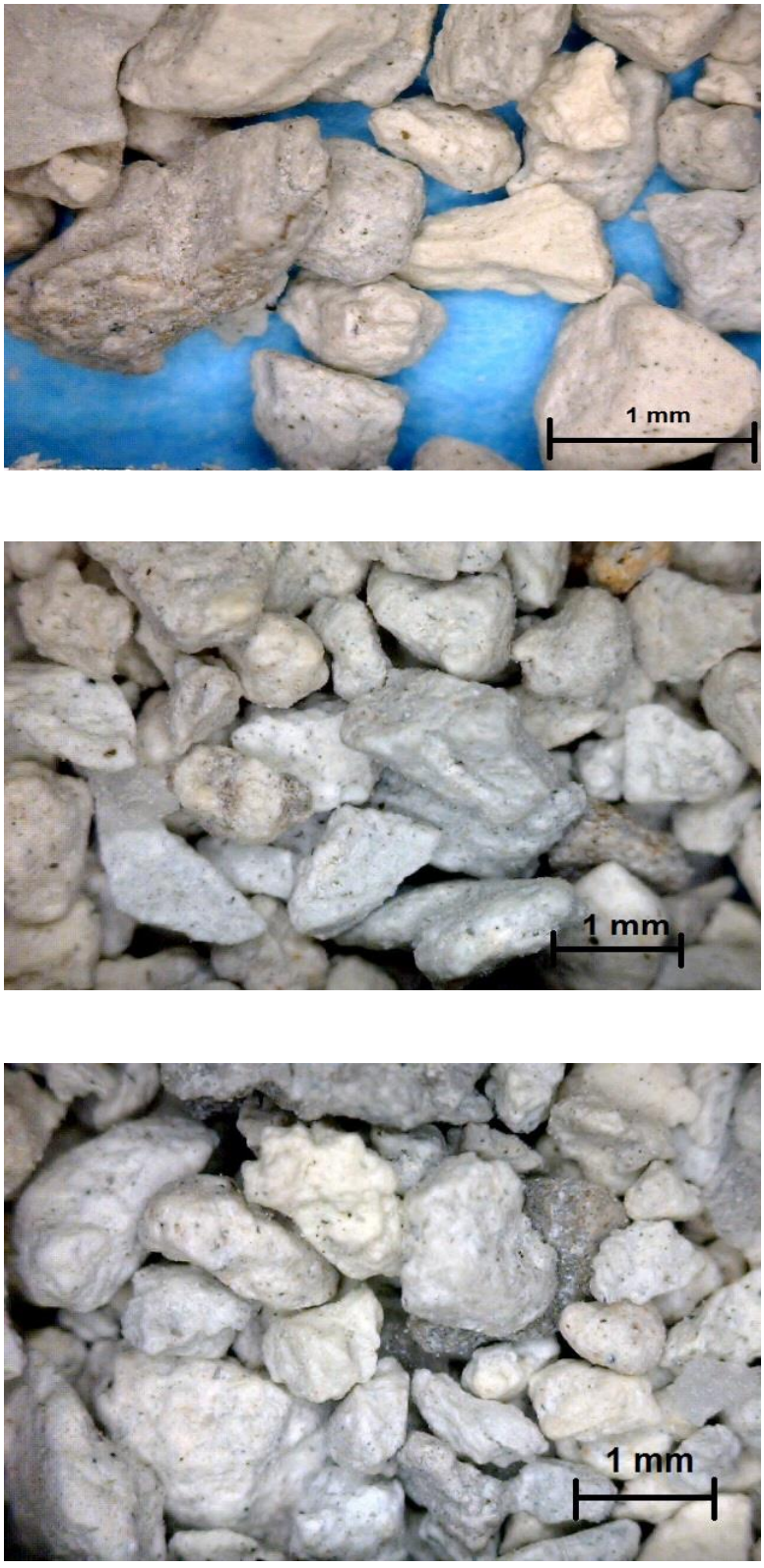

Figure 9.10: Digital microscope camera view of GCLs: a) Bentomat b) Resistex and c) Resistex plus GCL (from Salihoglu, 2015).

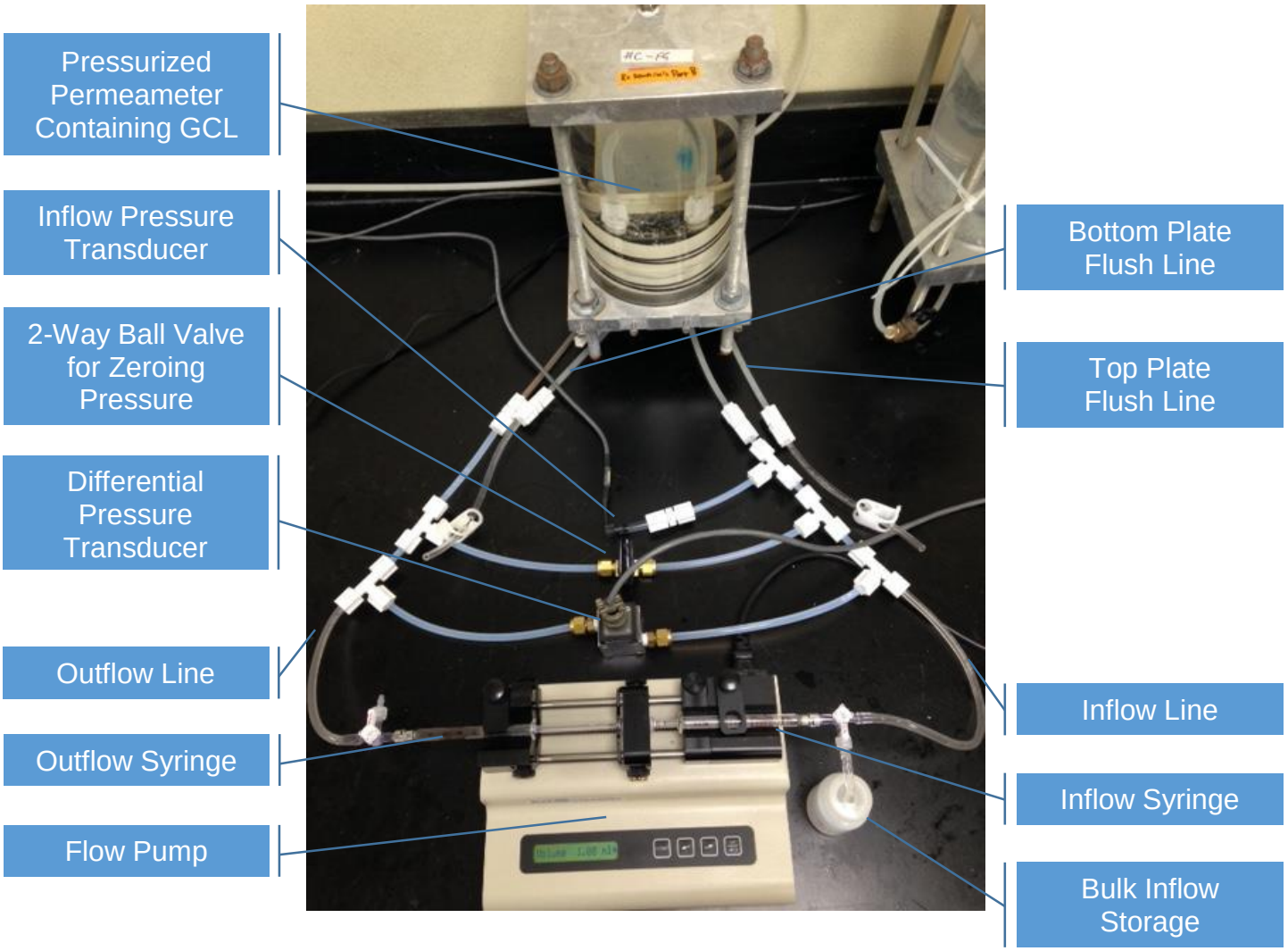

Figure 9.11: Photograph with main components of constant flow pump apparatus

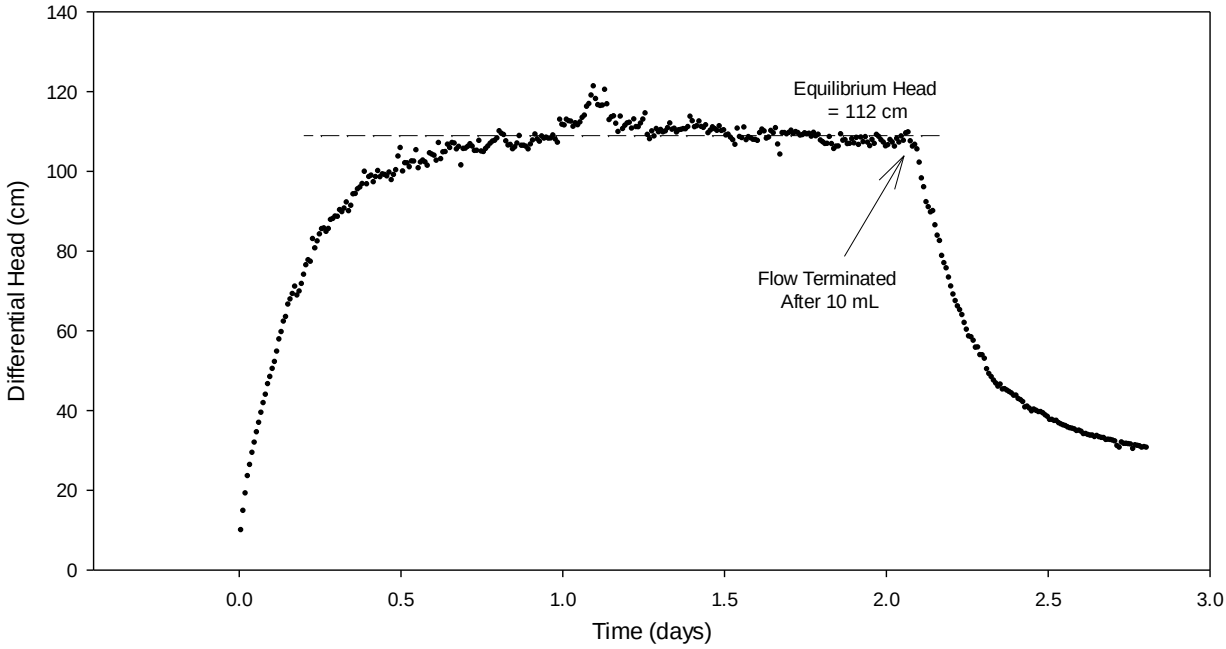

Figure 9.12: Differential Head Results for 10 mL of Constant Flow of DI Water through Bentomat GCL at 0.2 mL/hr. Data points were recorded electronically every 10 minutes.

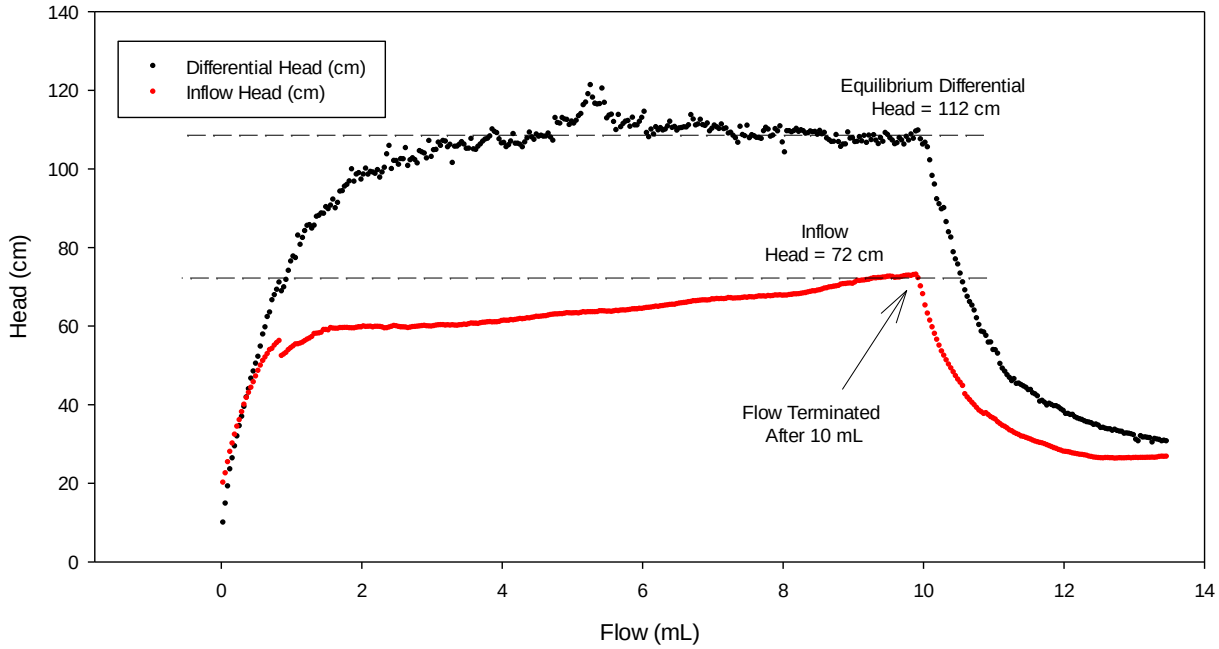

Figure 9.13: Differential and Inflow Head Results for 10 mL of Constant Flow of DI Water through Bentomat GCL at 0.2 mL/hr. Data points were recorded electronically every 10 minutes.

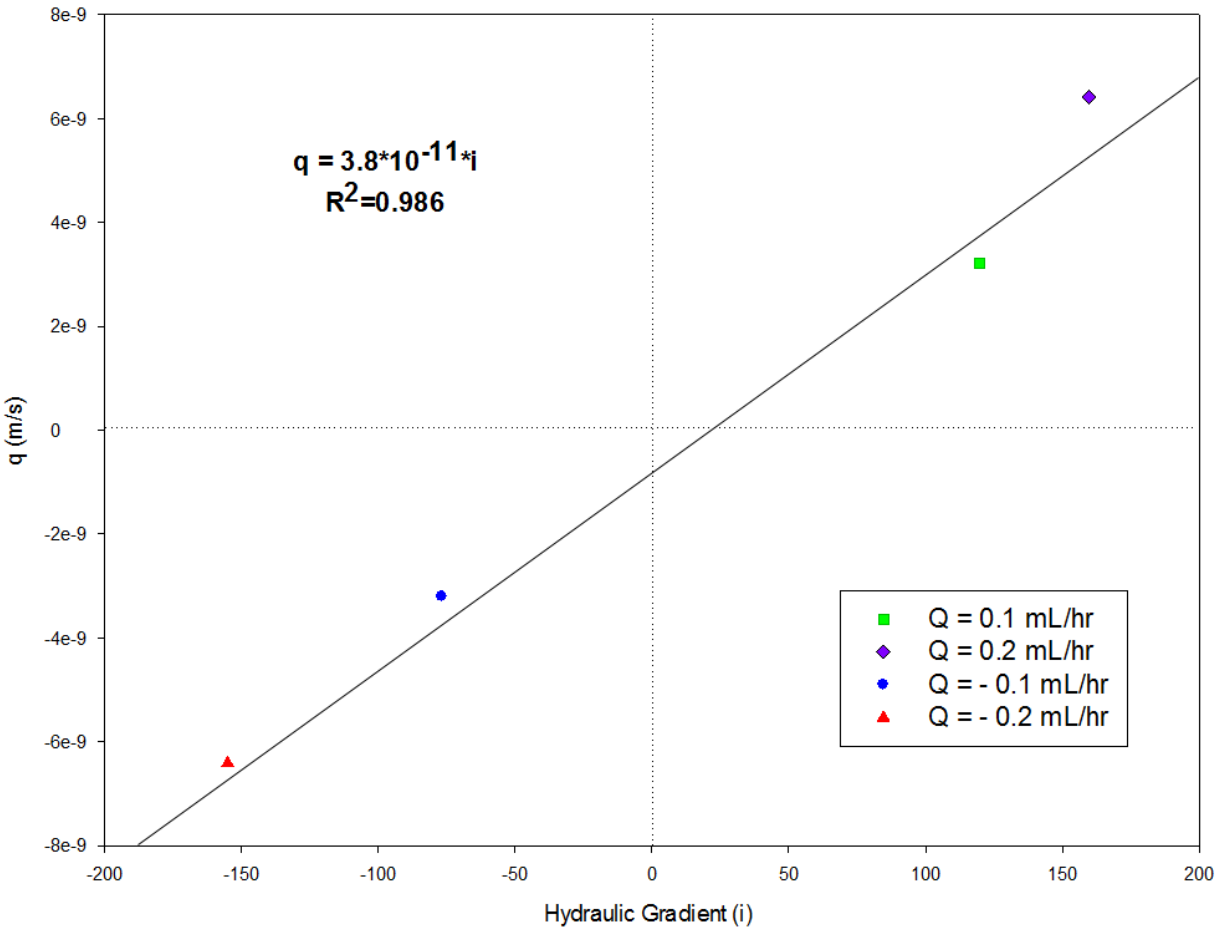

Figure 9.14: Bentomat GCL is permeated with DI water using a constant flow pump. Discharge per unit area (Q/A) is plotted versus the equilibrium hydraulic gradients achieved after 10 mL of flow. Darcy's Law gives a hydraulic conductivity of 3.8 * 10^{-11} m/s.

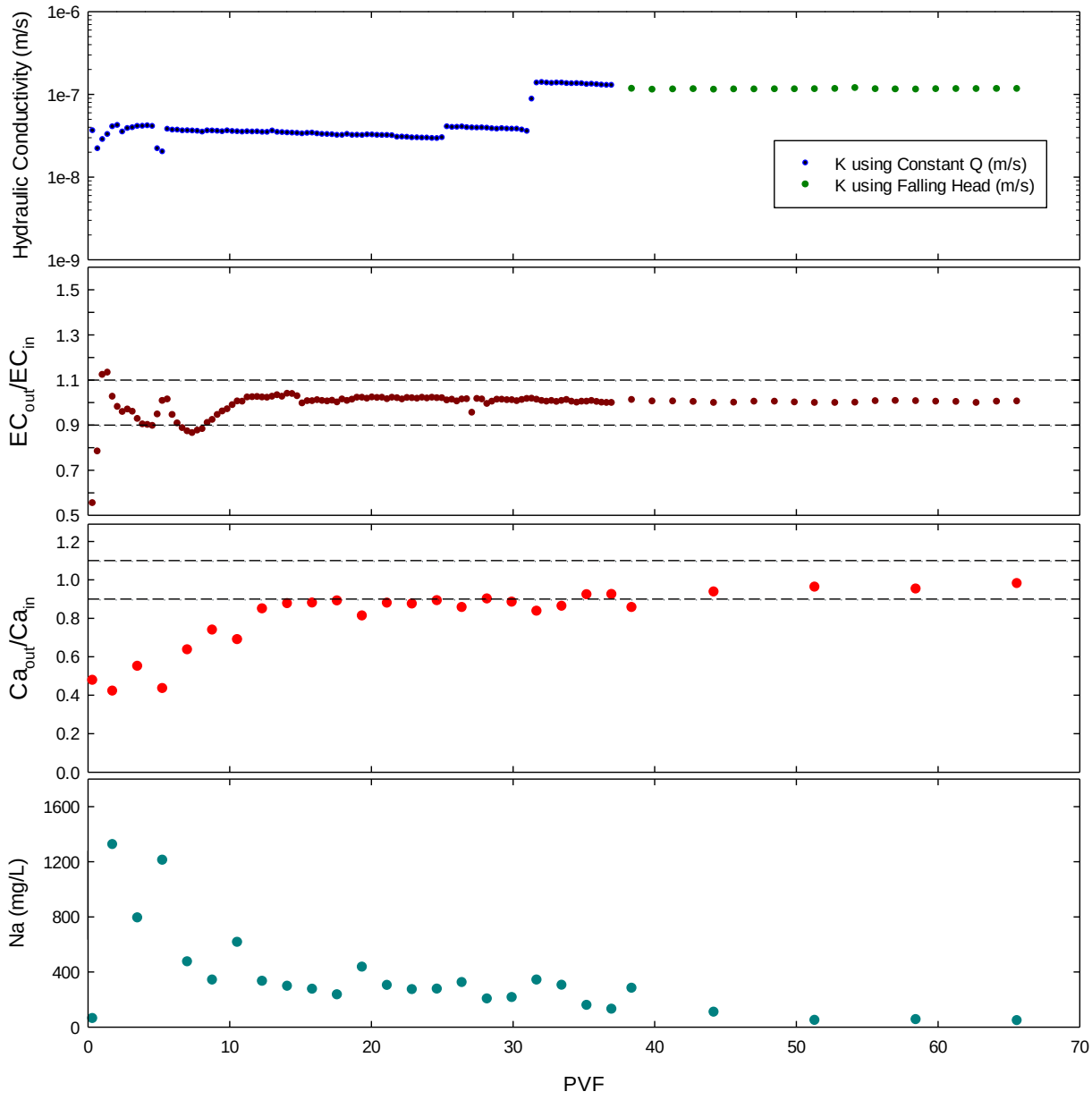

Figure 9.15: Hydraulic conductivity, EC_{out}/EC_{in} ratio, $Ca^{2+}_{out}/Ca^{2+}_{in}$ ratio, and Na^{+} concentrations plotted with PVF for constant flow of Bentomat GCL permeated with 50 mM $CaCl_2$.

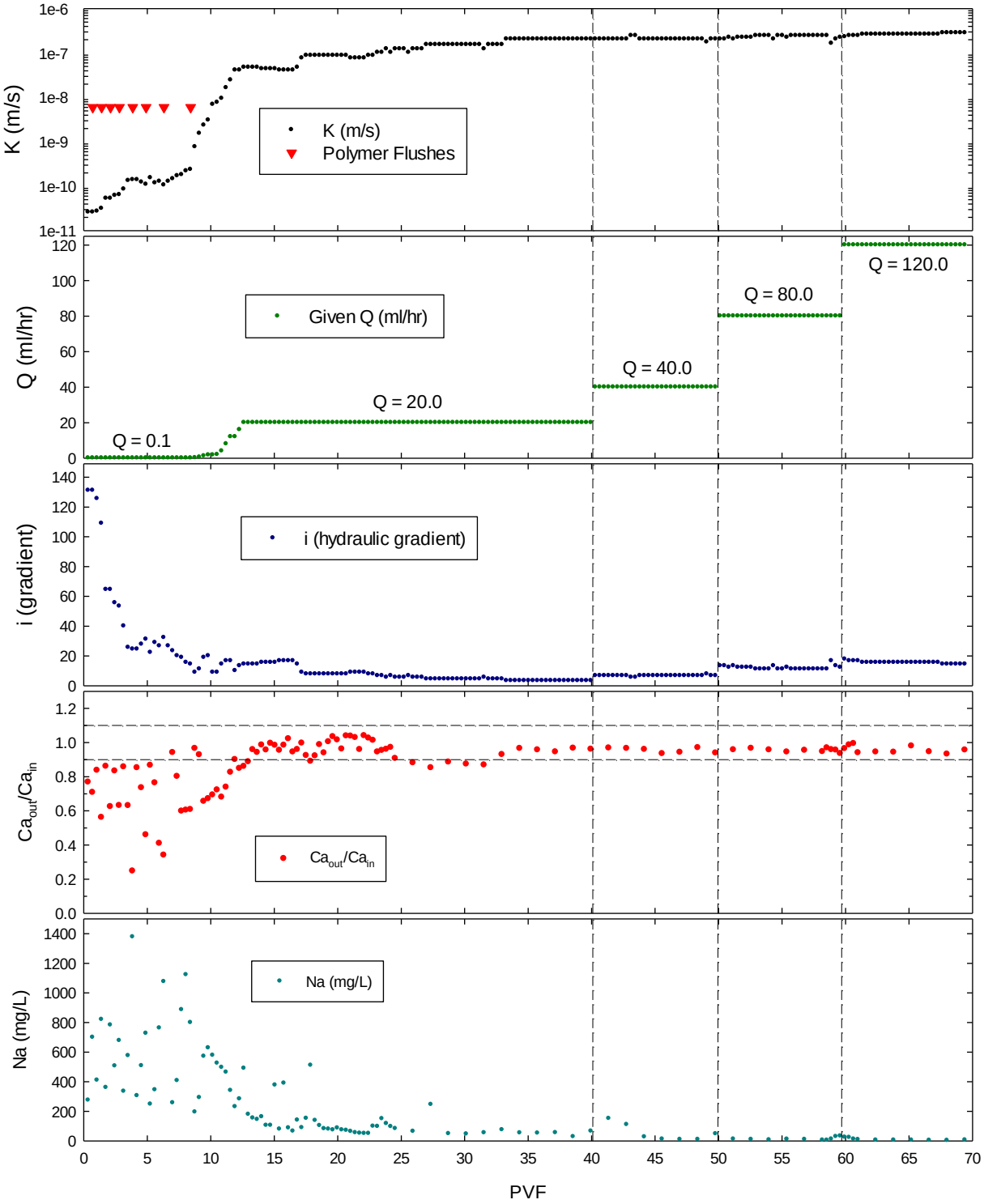

Figure 9.16: Hydraulic conductivity, polymer flushes, flow rate, hydraulic gradient, Ca^{2+out}/Ca^{2+in}, and Na^{+} concentrations plotted with PVF for constant flow testing of Resistex Plus GCL permeated with 50 mM $CaCl_2$.

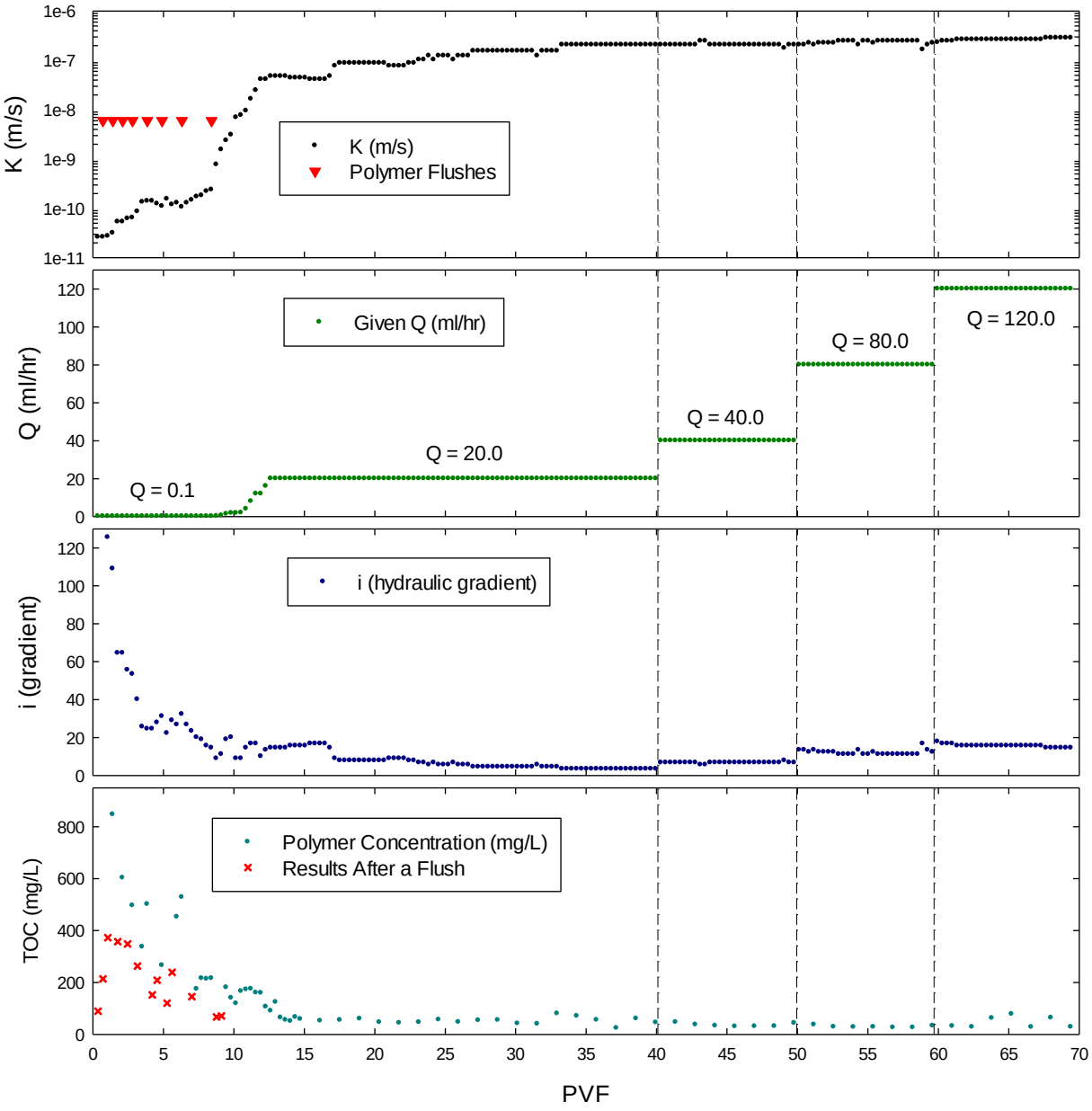

Figure 9.17: Hydraulic conductivity, flow rate, hydraulic gradient, and TOC plotted with PVF for constant flow testing of Resistex Plus GCL permeated with 50 mM CaCl2

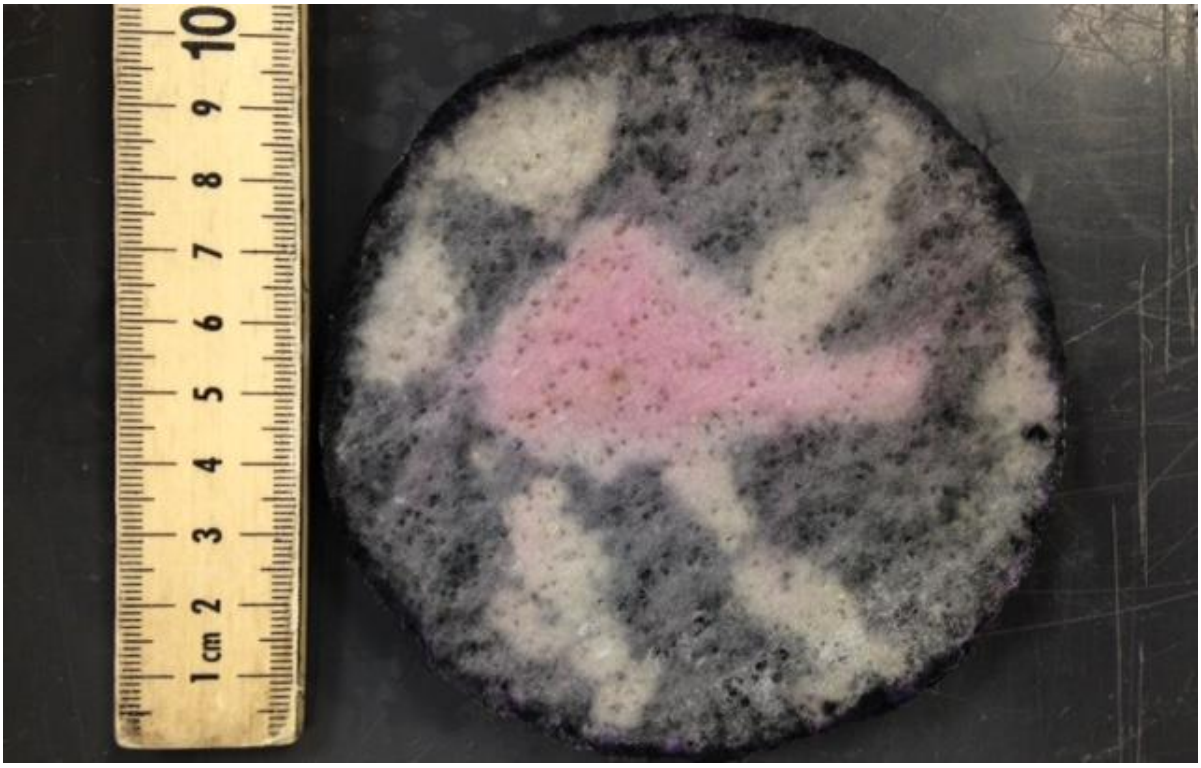

Figure 9.18 : Rhodamine dye tracer test for Resistex Plus GCL permeated with 50 mM $CaCl_2$. Pink areas indicate areas of concentrated flow.

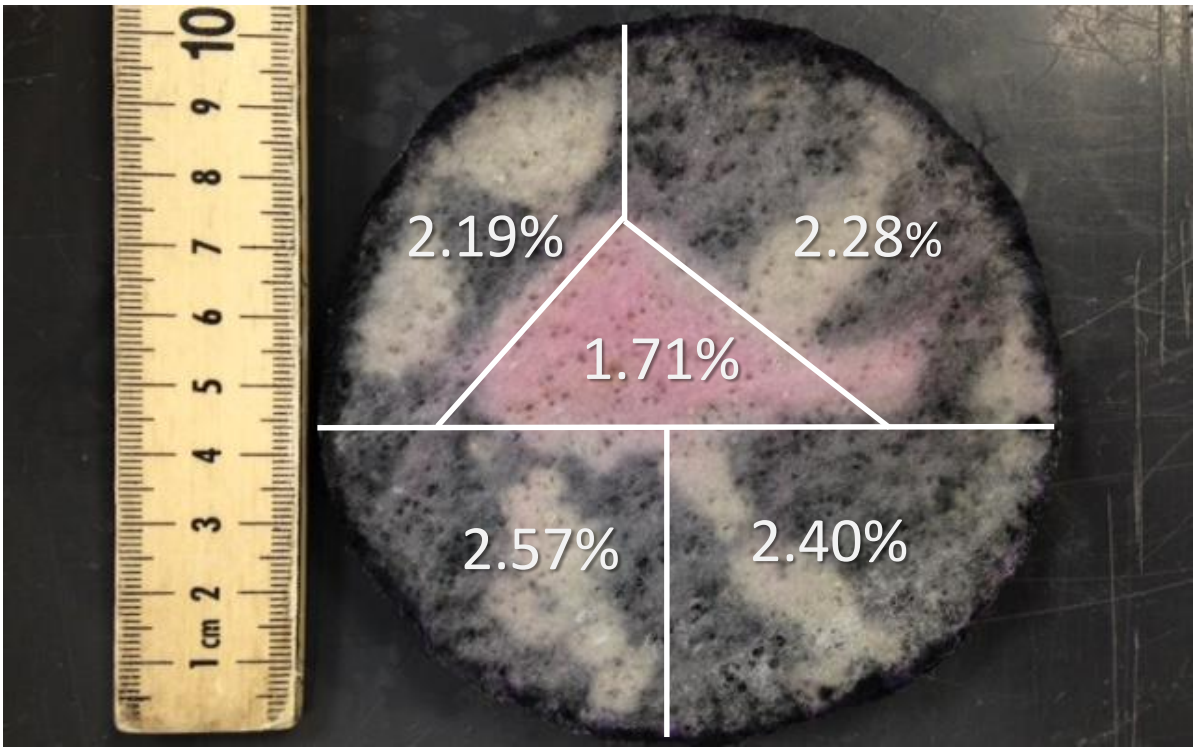

Figure 9.19: Polymer content distribution for Resistex Plus GCL permeated with 50 mM $CaCl_2$. Lowest polymer content exists in areas of concentrated flow.

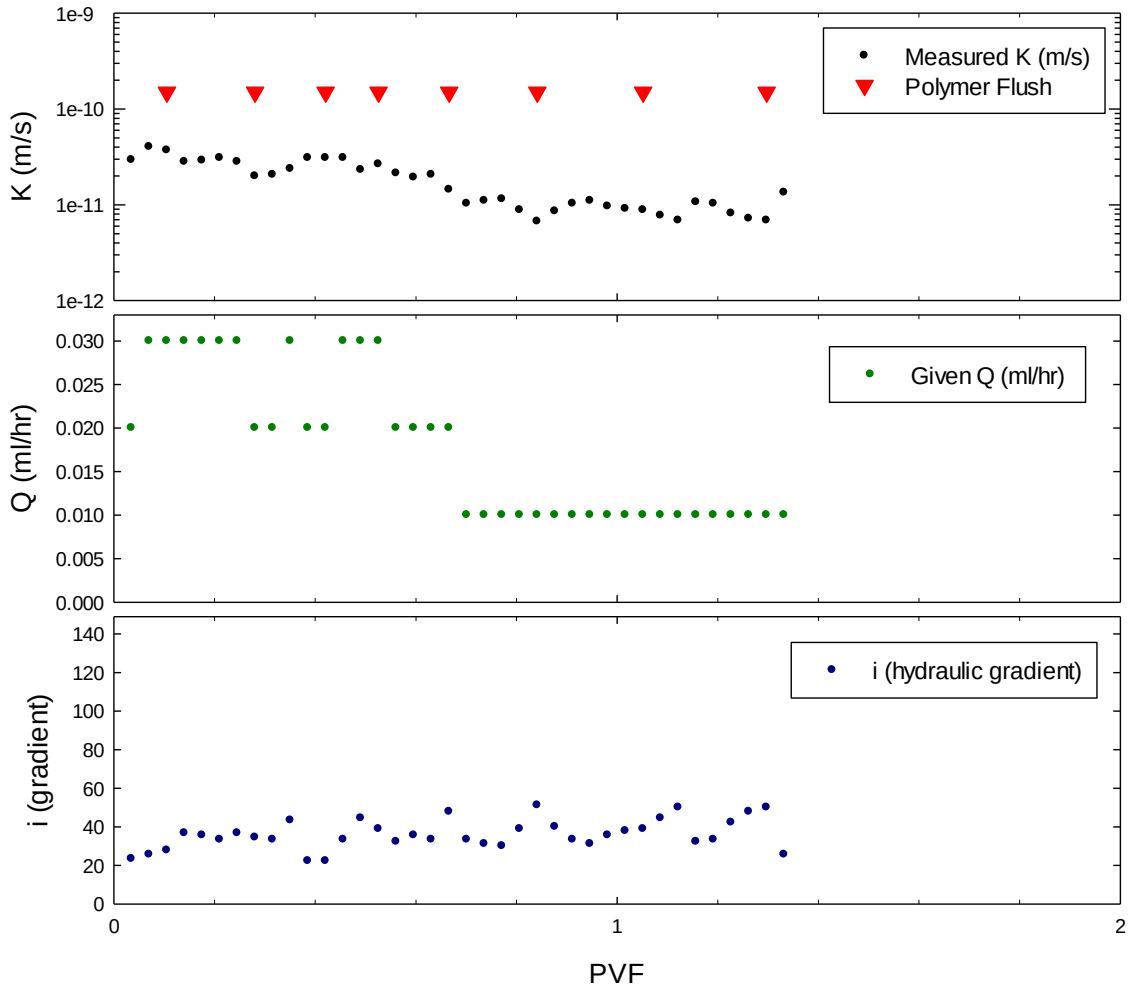

Figure 9.20 : Hydraulic conductivity, polymer flushes, flow rate, and hydraulic gradient plotted with PVF for replicate constant flow testing of Resistex Plus GCL permeated with 50 mM $CaCl_2$.

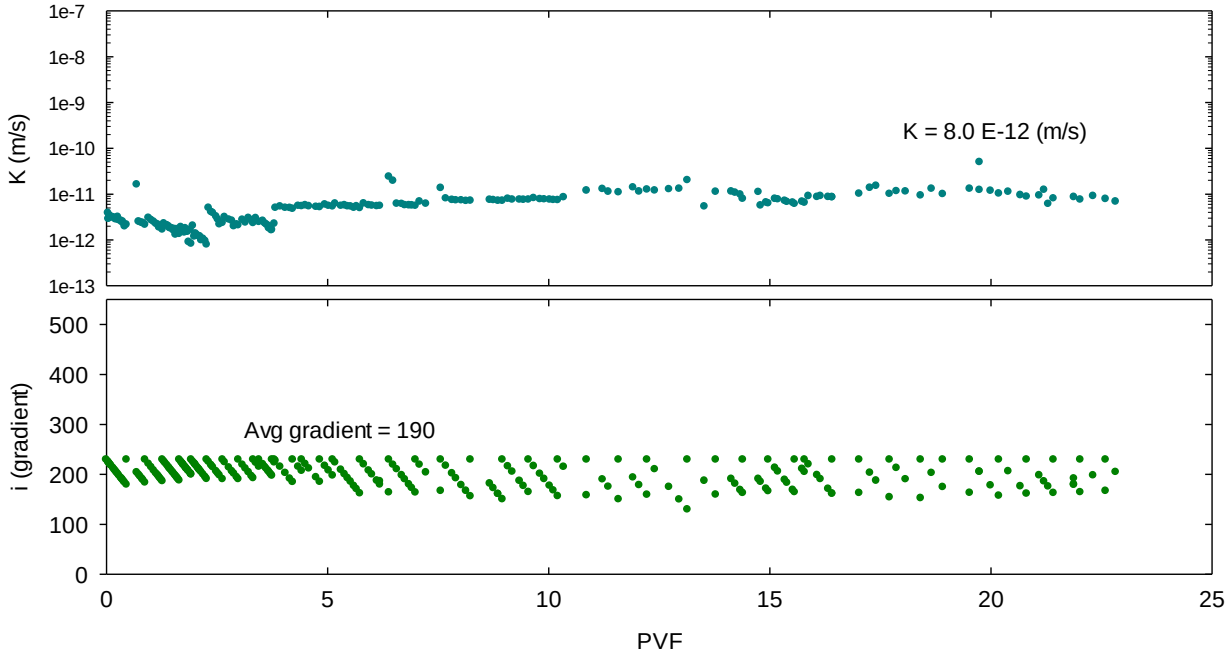

Figure 9.21 : Hydraulic conductivity and hydraulic gradient plotted with PVF for Resistex Plus GCL permeated with High Strength leachate for 992 days

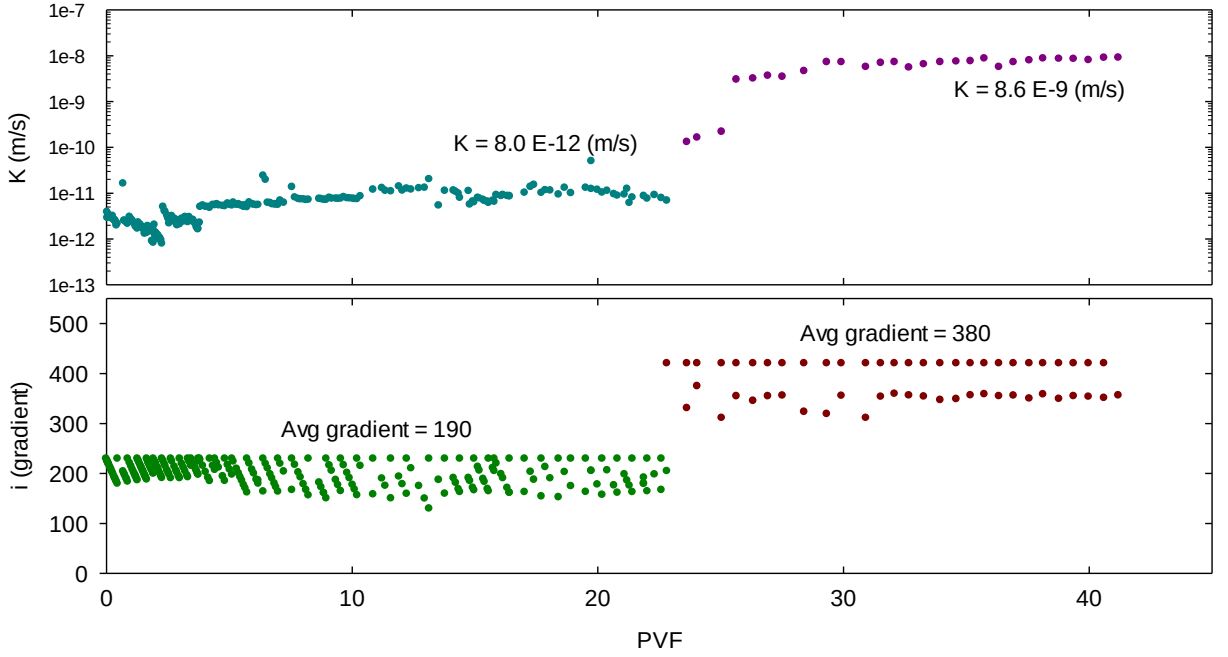

Figure 9.22 : Hydraulic conductivity and hydraulic gradient plotted with PVF for Resistex Plus GCL permeated with High Strength leachate before and after average gradient increase.

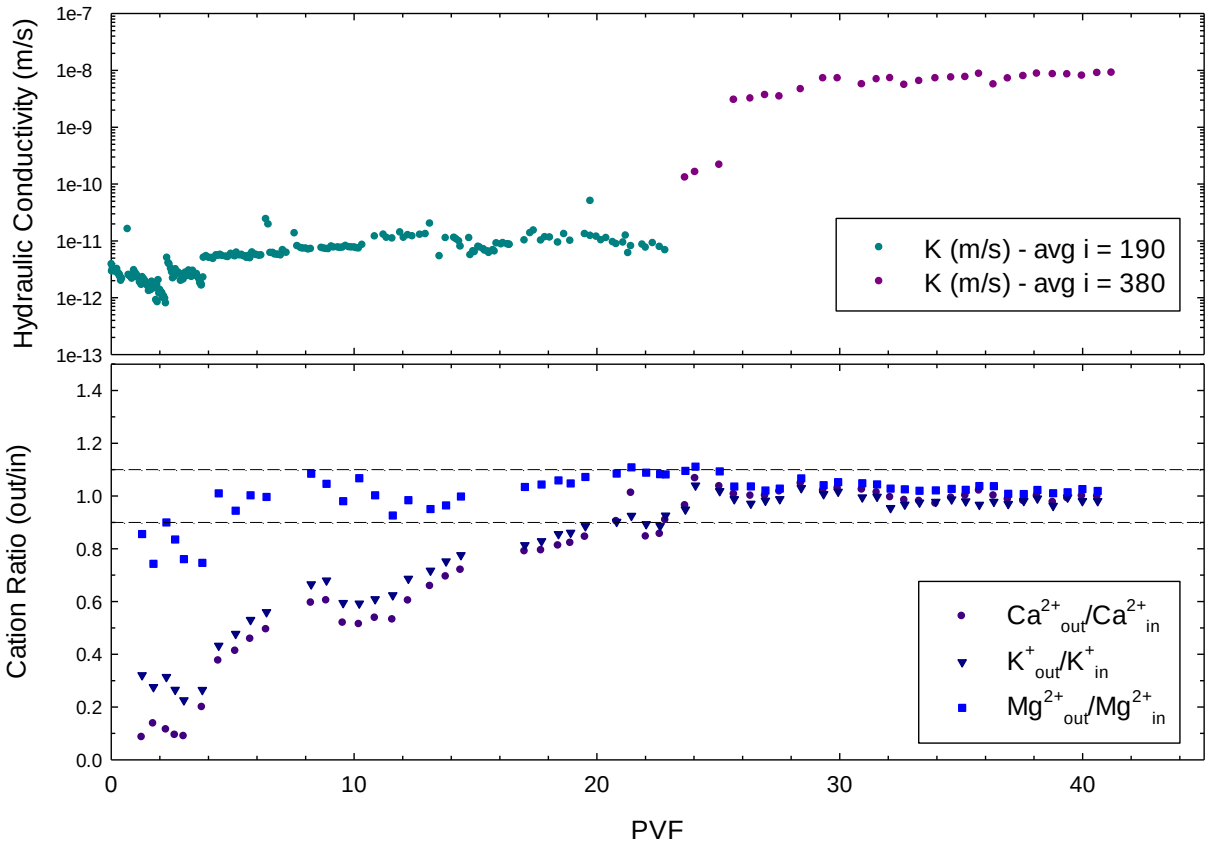

Figure 9.23 : Hydraulic conductivity and major cation concentration ratios plotted with PVF for Resistex Plus GCL permeated with High Strength leachate before and after average gradient increase.

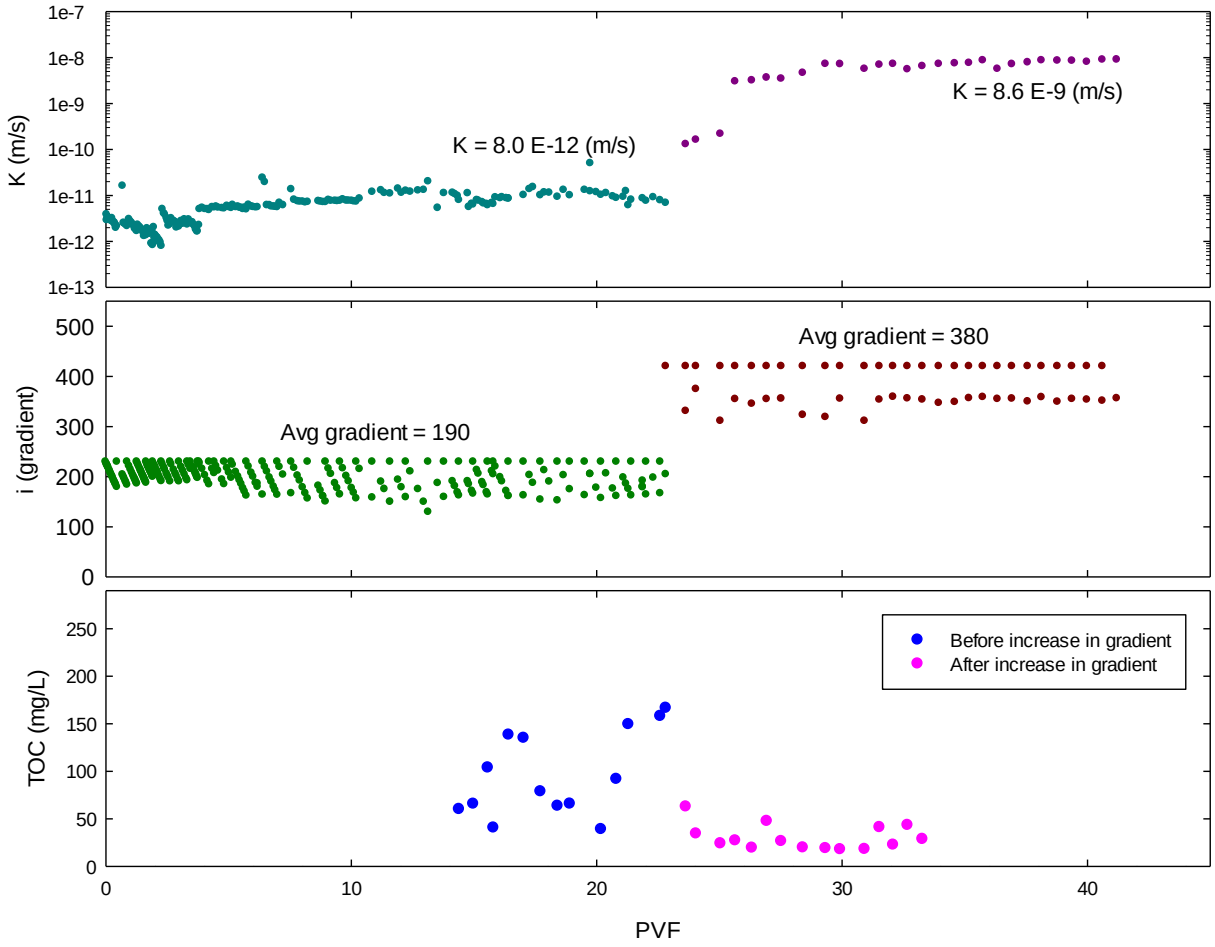

Figure 9.24 : Hydraulic conductivity, hydraulic gradient, and TOC plotted with PVF for Resistex Plus GCL permeated with High Strength leachate. A noticeable decrease in polymer content is observed after the increase in hydraulic gradient.

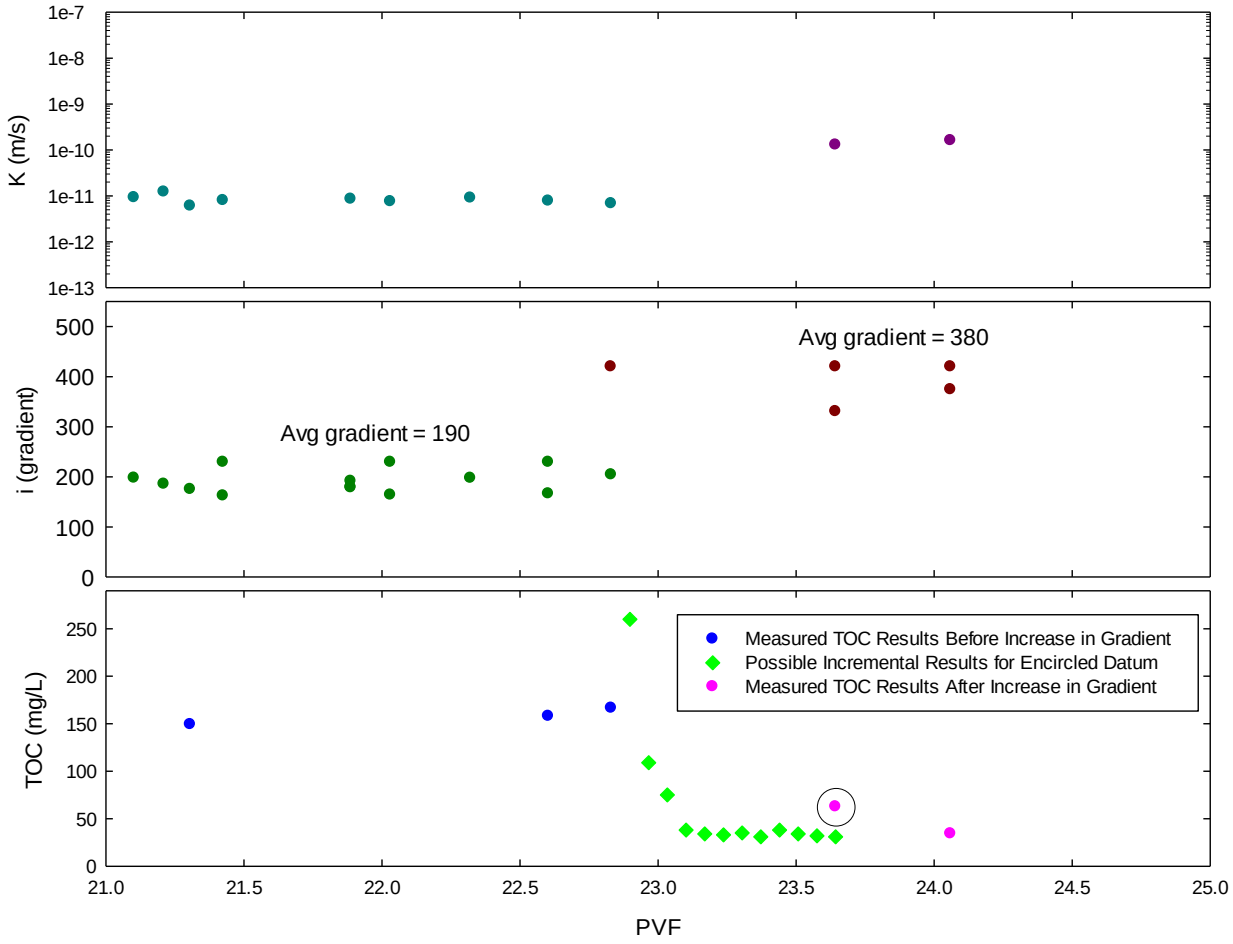

Figure 9.25: Measured hydraulic conductivity and hydraulic gradient results plotted with PVF of Resistex Plus GCL permeated with High Strength leachate, along with measured and possible TOC measurements. Possible incremental results give a potential explanation for the lack of measured TOC surge accompanying the increase in hydraulic conductivity.

Figure 9.26: Rhodamine dye tracer test for Resistex Plus GCL permeated with High Strength Leachate. Pink areas indicate areas of concentrated flow.

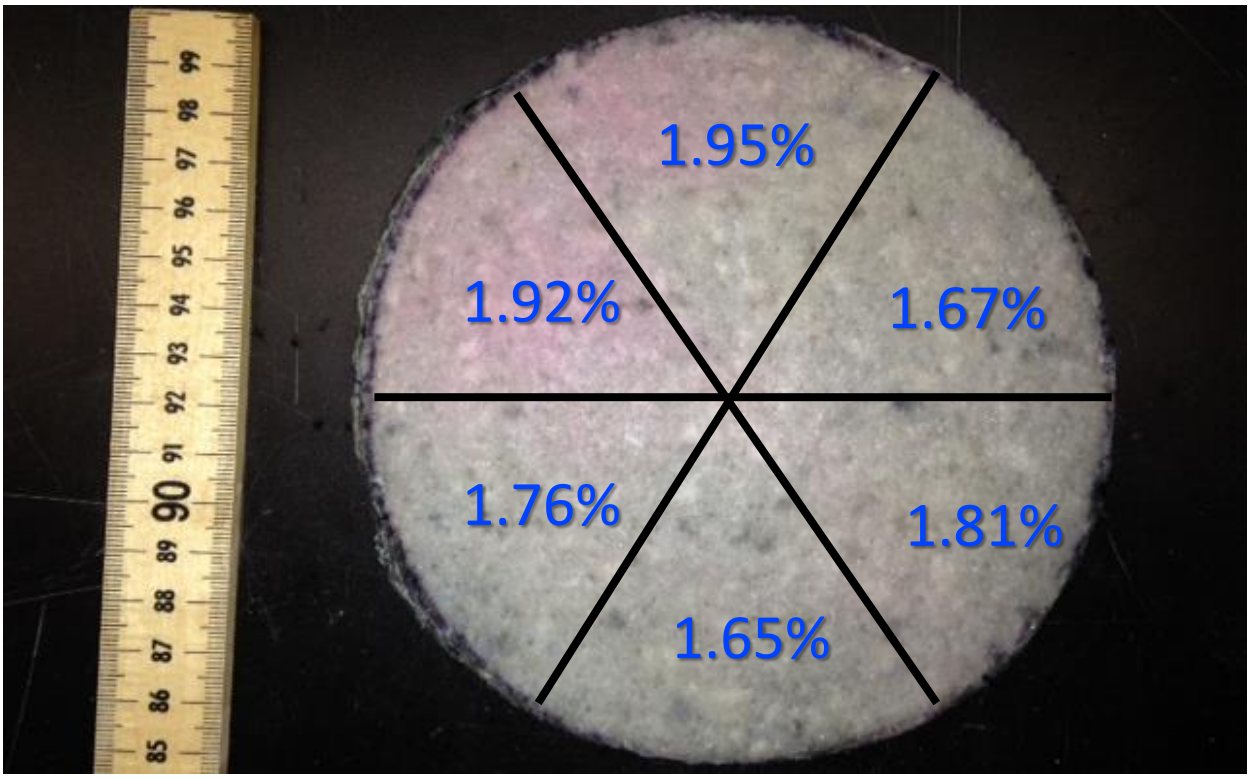

Figure 9.27: Polymer content distribution for Resistex Plus GCL: permeated with High Strength leachate. Polymer content is spatially homogeneous.

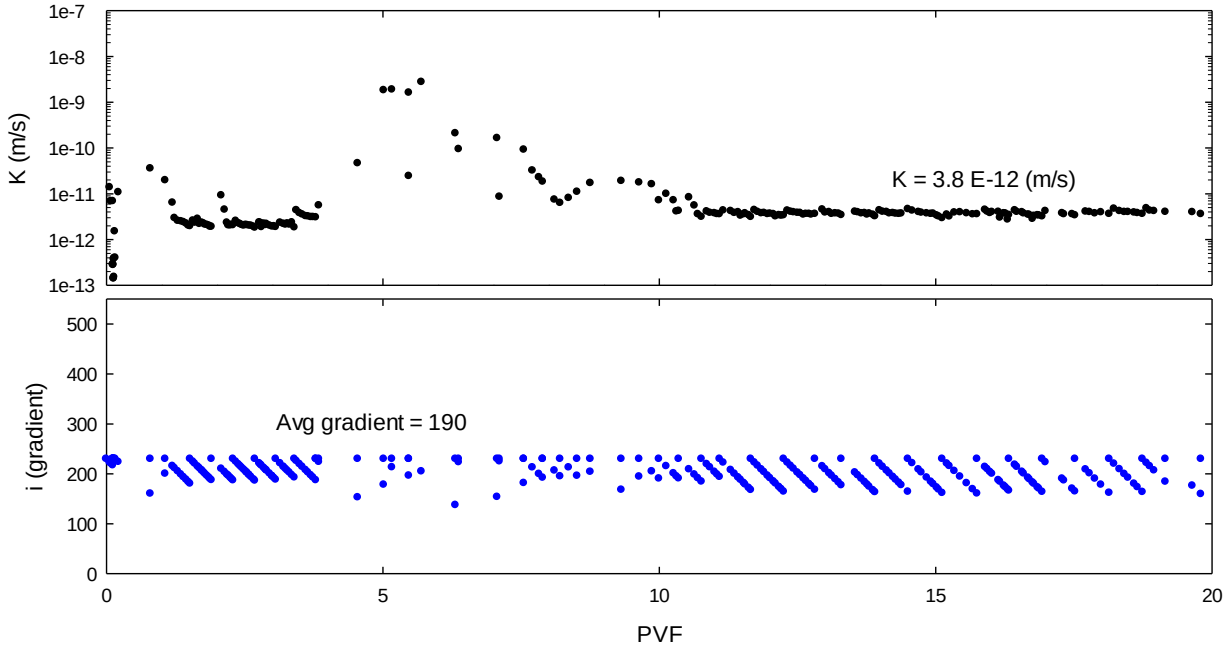

Figure 9.28: Hydraulic conductivity and hydraulic gradient plotted with PVF for Resistex Plus GCL permeated with Trona leachate for 997 days

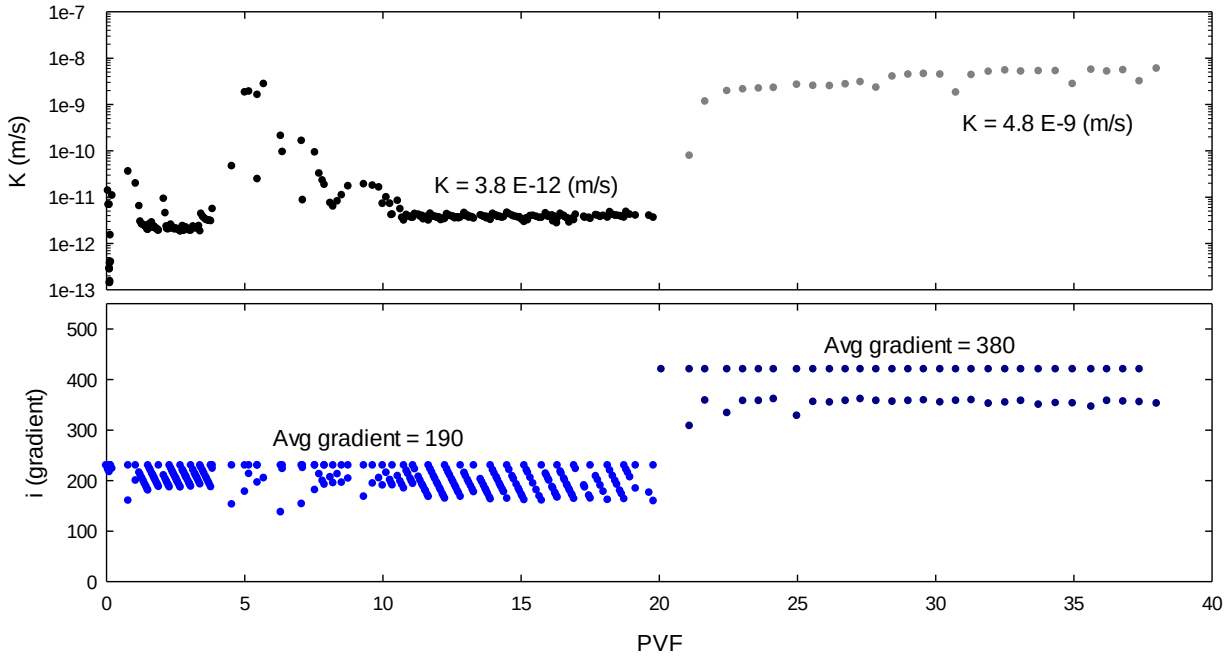

Figure 9.29: Hydraulic conductivity and hydraulic gradient plotted with PVF for Resistex Plus GCL permeated with Trona leachate before and after average gradient increase.

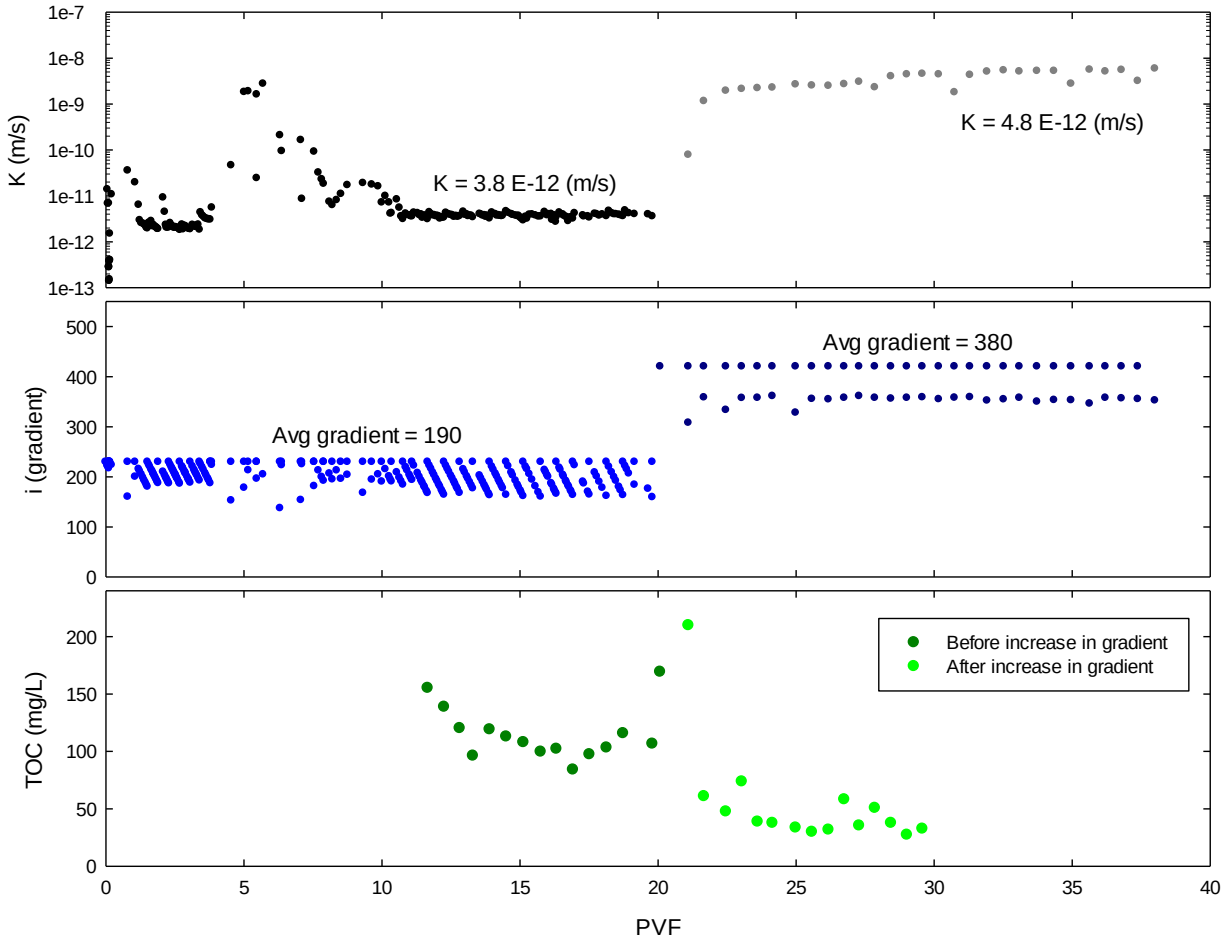

Figure 9.30: Hydraulic conductivity, hydraulic gradient, and TOC plotted with PVF before and after gradient increase of Resistex Plus GCL permeated with Trona leachate.

Figure 9.31: Rhodamine dye tracer test for Resistex Plus GCL permeated with Trona Leachate. Pink areas shows areas of concentrated flow.

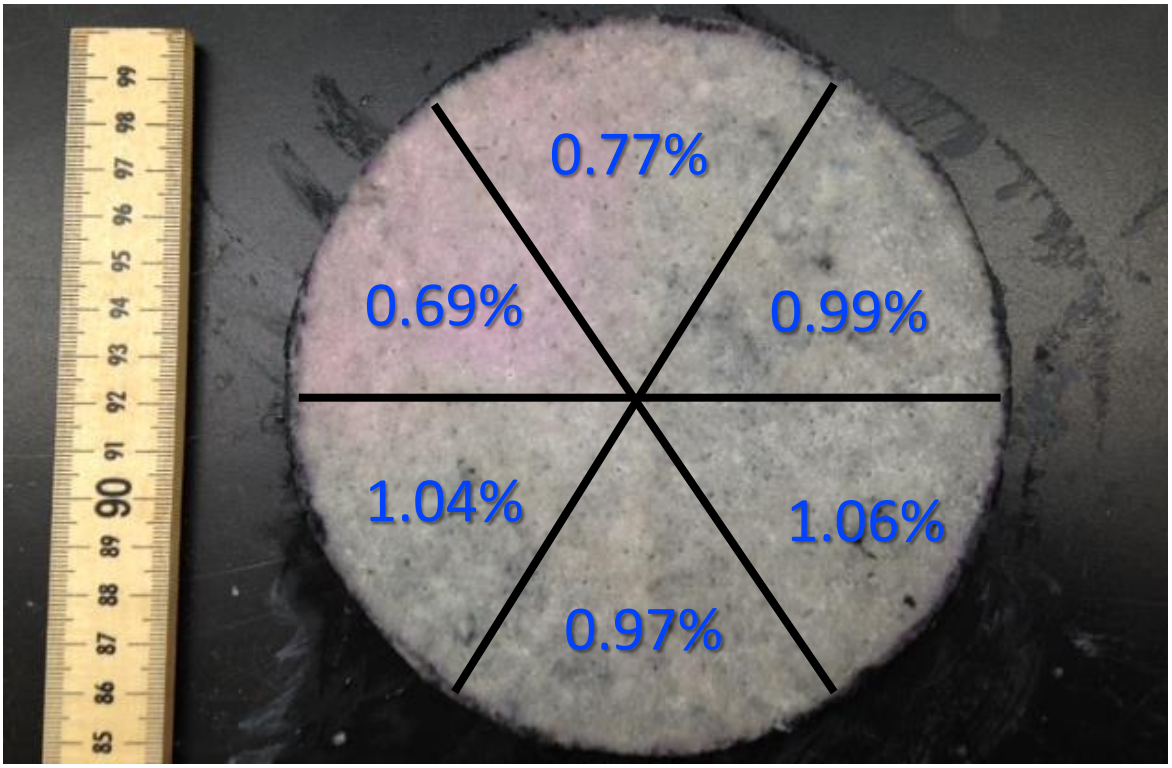

Figure 9.32: Polymer content distribution for Resistex Plus GCL permeated with Trona leachate. Polymer content is slightly lower in areas of concentrated flow.

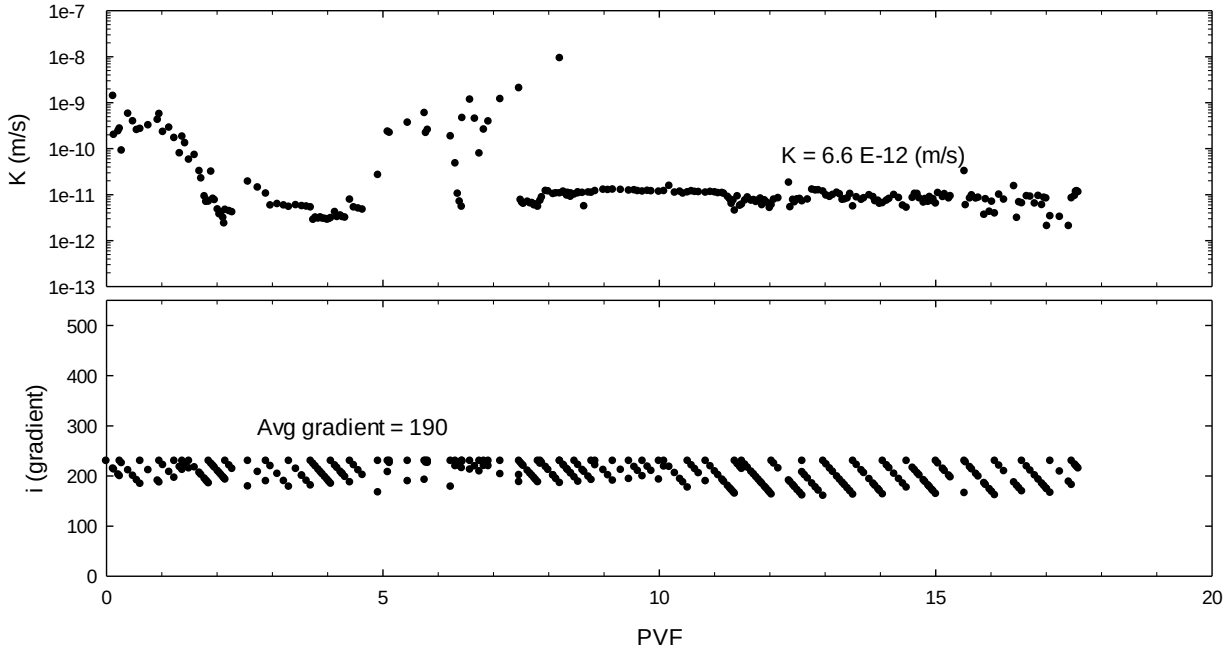

Figure 9.33: Hydraulic conductivity and hydraulic gradient plotted with PVF for Resistex GCL permeated with Trona leachate for 1016 days.

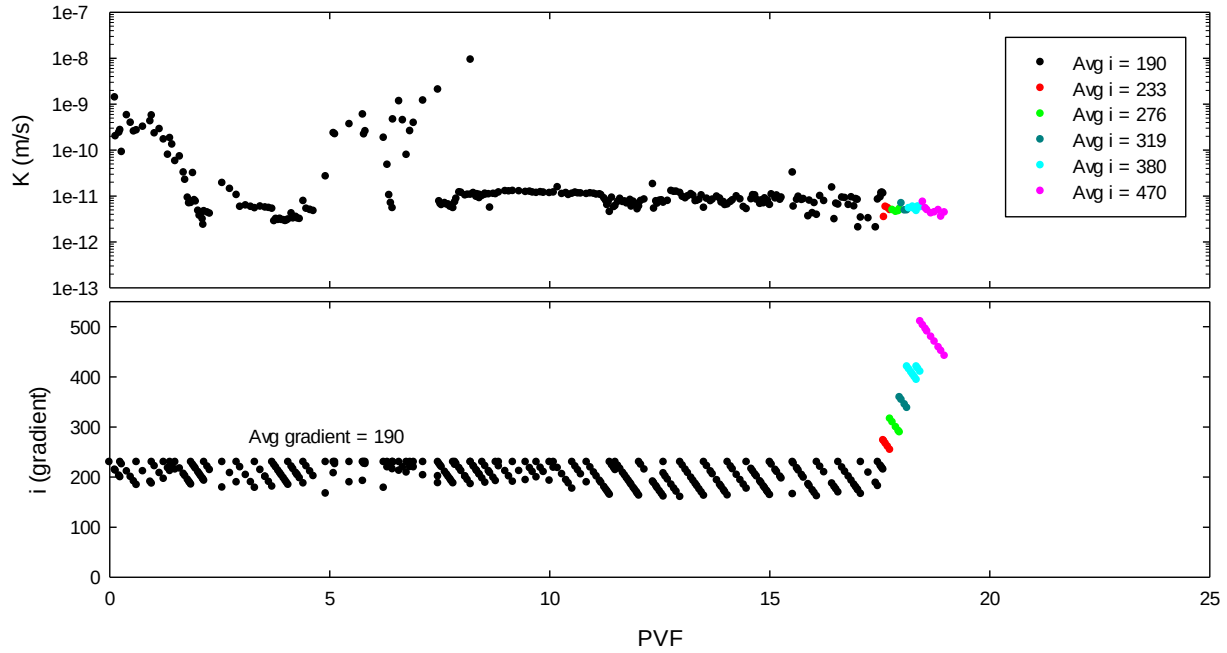

Figure 9.34: Hydraulic conductivity and hydraulic gradient plotted with PVF after incremental increases to hydraulic gradient for Resistex GCL permeated with Trona leachate.

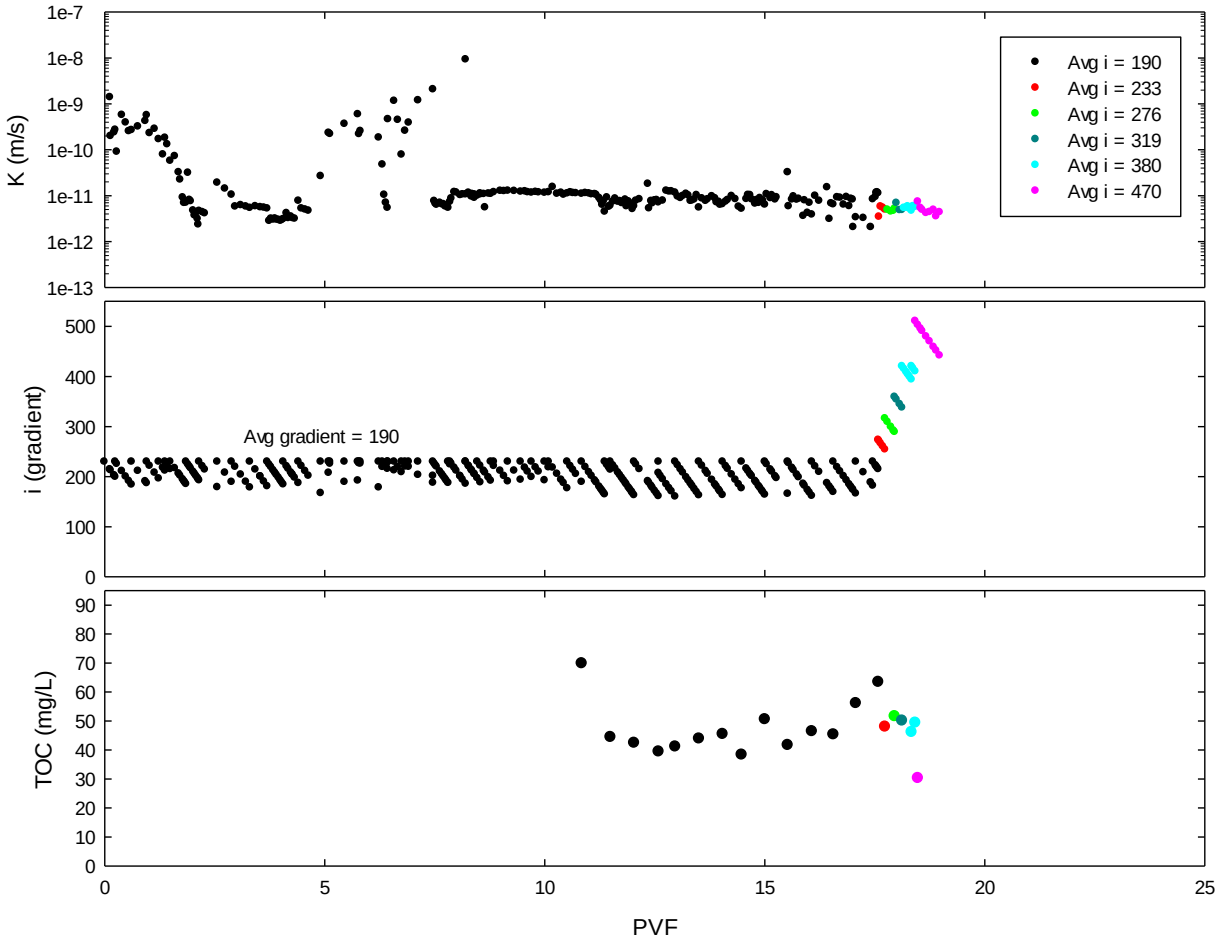

Figure 9.35: Hydraulic conductivity, hydraulic gradient, and TOC plotted with PVF of Resistex GCL permeated with Trona leachate.

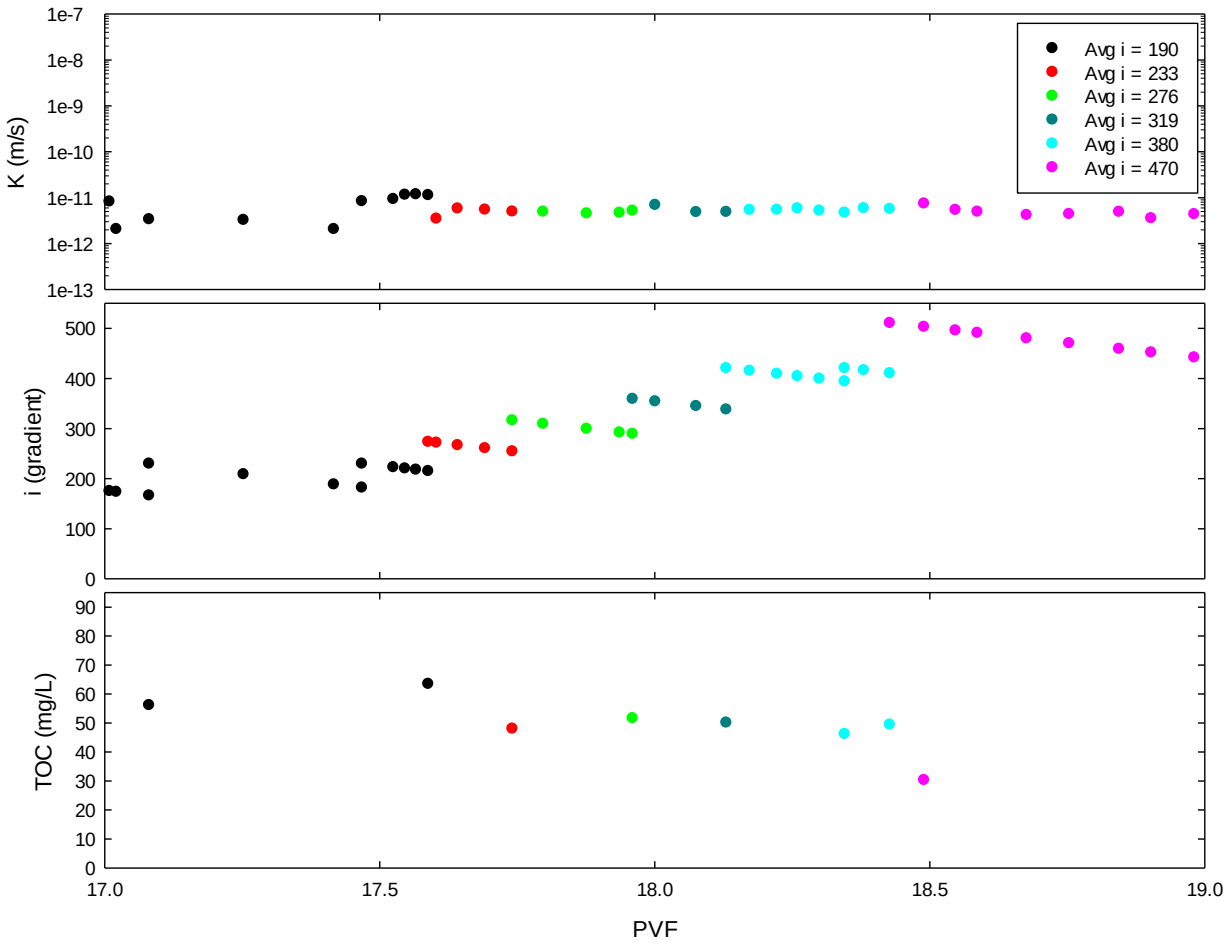

Figure 9.36: Hydraulic conductivity, hydraulic gradient, and TOC plotted with PVF of Resistex GCL permeated with Trona leachate.

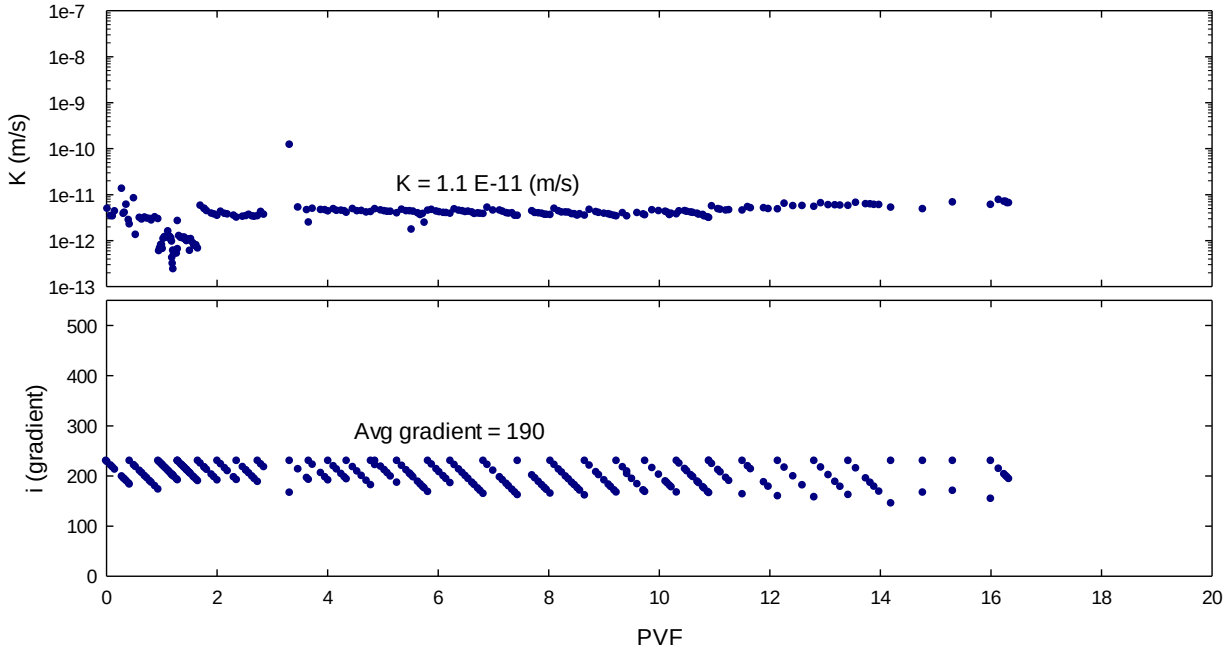

Figure 9.37: Hydraulic conductivity and hydraulic gradient plotted with PVF for Resistex Plus GCL permeated with Typical FGD leachate for 1016 days.

.

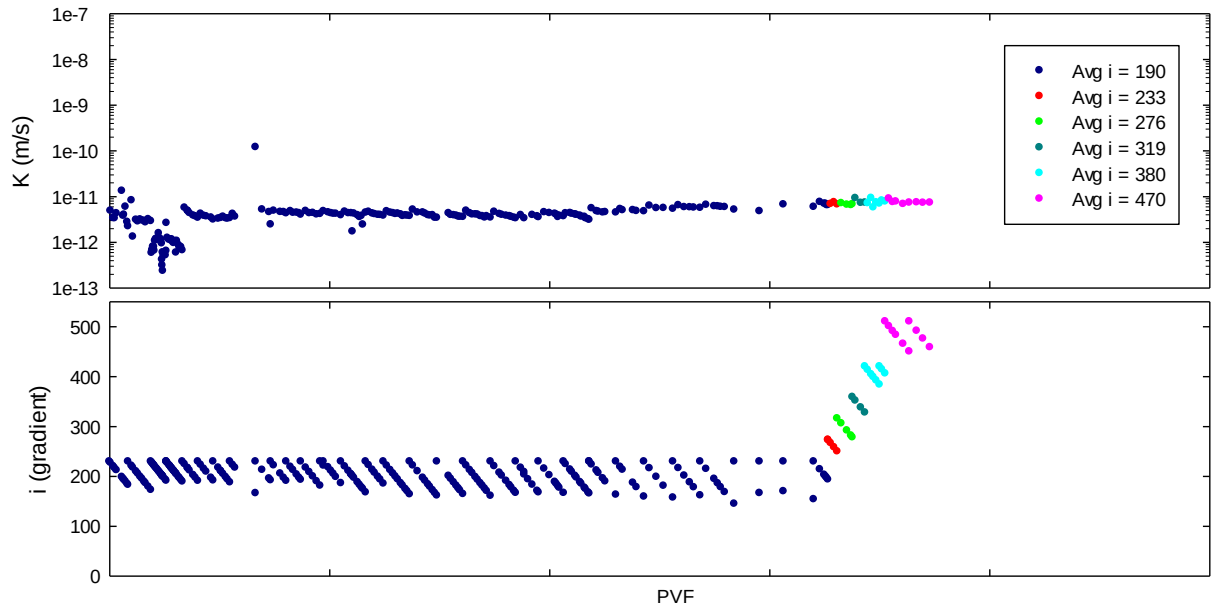

Figure 9.38: Hydraulic conductivity and hydraulic gradient plotted with PVF after incremental increases to hydraulic gradient for Resistex Plus GCL permeated with Typical FGD.

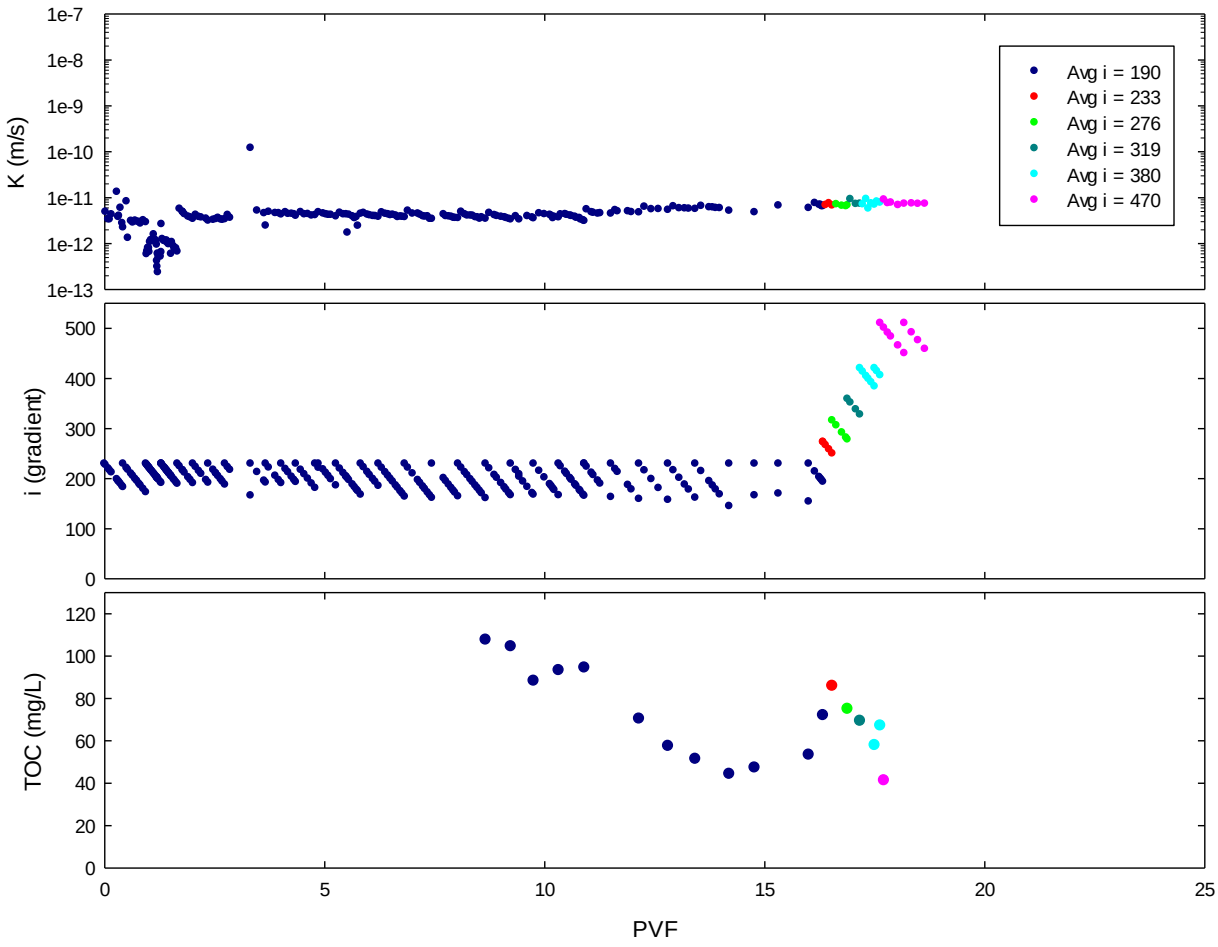

Figure 9.39: Hydraulic conductivity, hydraulic gradient, and TOC plotted with PVF of Resistex Plus GCL permeated with Typical FGD leachate.

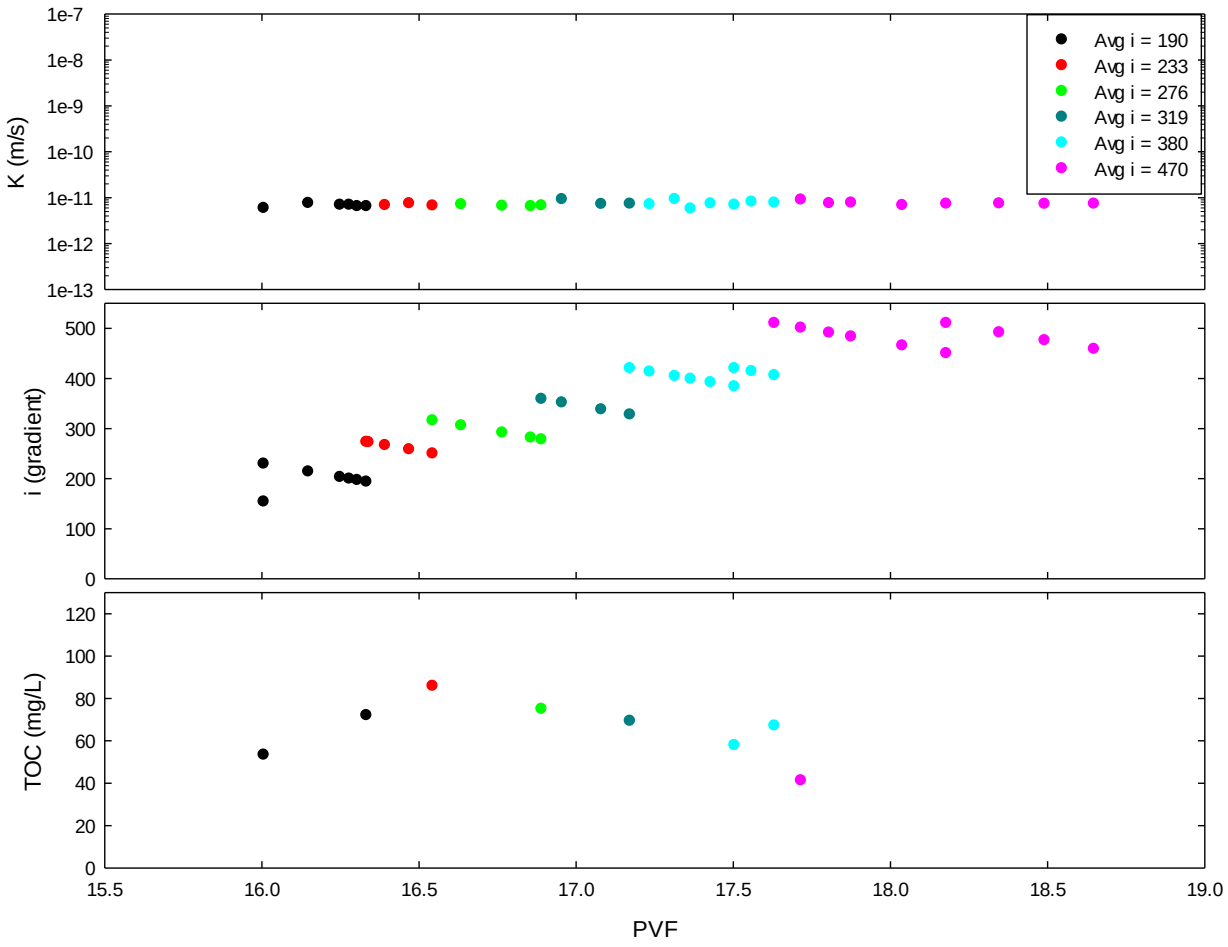

Figure 9.40: Hydraulic conductivity, hydraulic gradient, and TOC plotted with PVF of Resistex Plus GCL permeated with Typical FGD leachate.

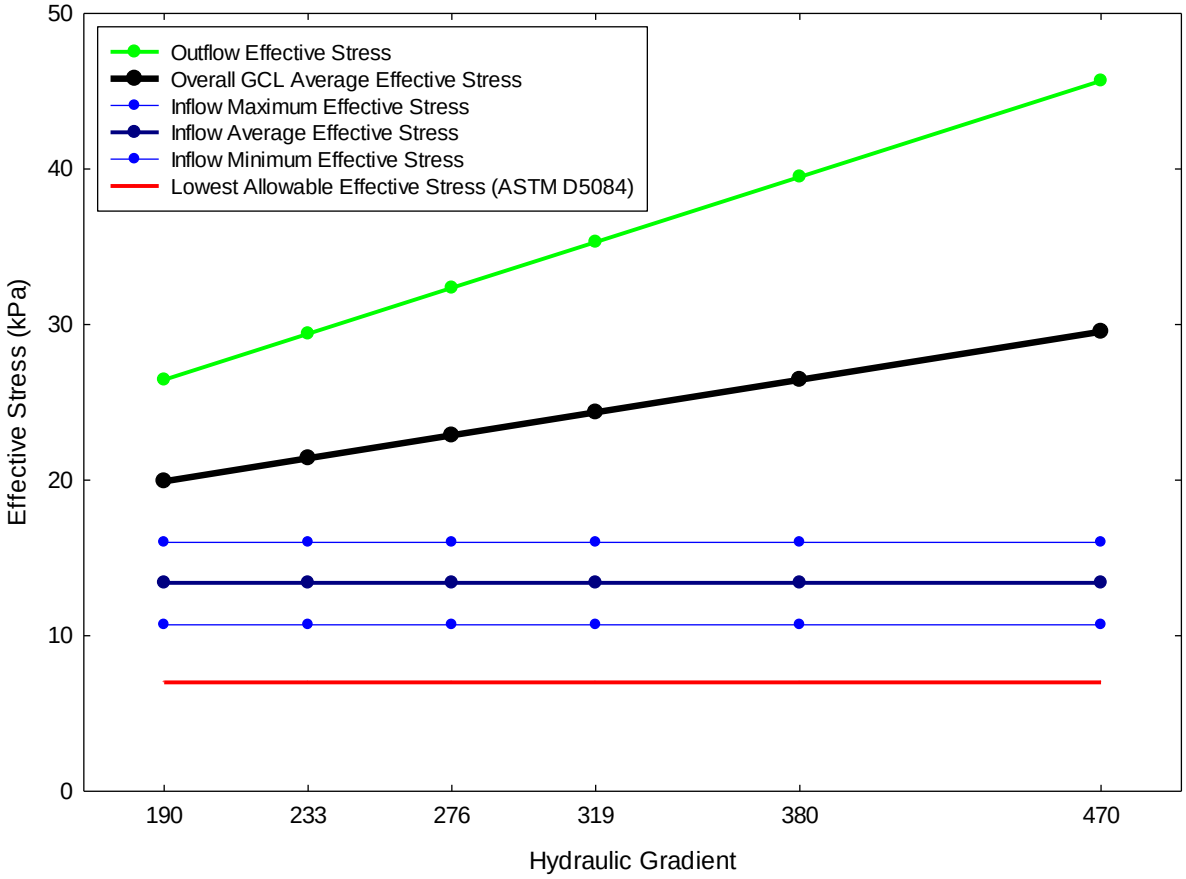

Figure 9.41: Outflow effective stress, overall GCL effective stress, maximum inflow effective stress, average inflow effective stress, minimum inflow effective stress, and lowest recommended effective stress (ASTM D5084) for hydraulic gradient increases in 4 falling head tests after changes in hydraulic gradients.

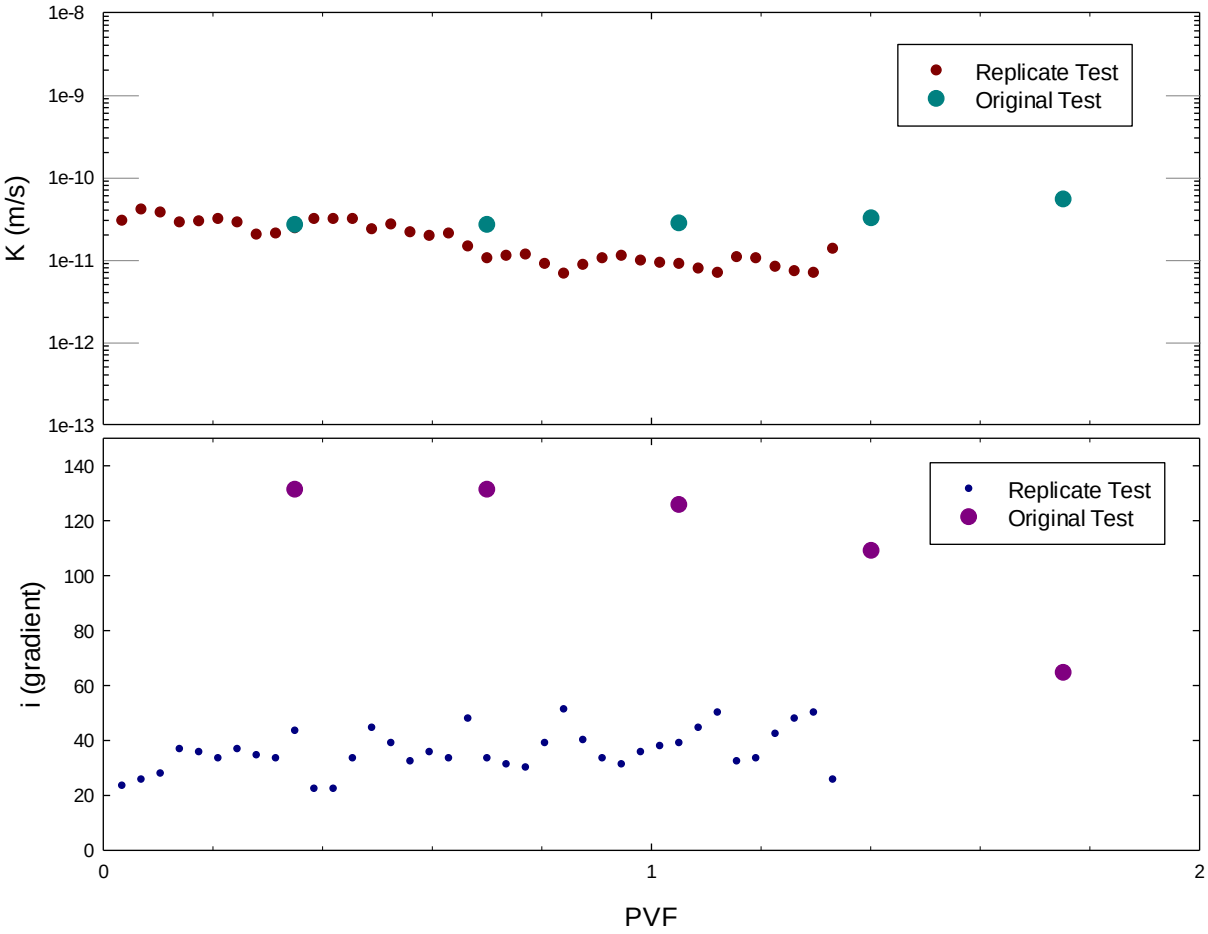

Figure 9.42: Hydraulic conductivity and hydraulic gradient plotted with PVF for both Resistex Plus GCLs permeated with 50 mM $CaCl_2$.

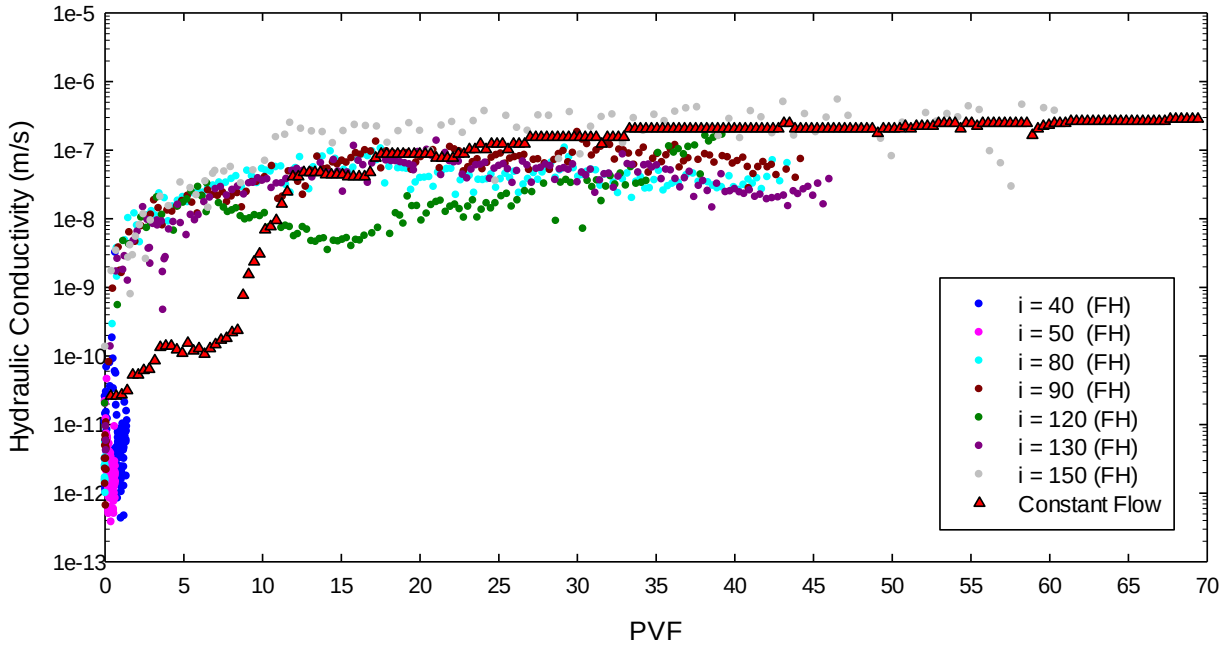

Figure 9.43: Hydraulic conductivity values plotted with PVF for constant flow method and falling head methods of varying average hydraulic gradients for Resistex Plus GCLs permeated with 50 mM $CaCl_2$.

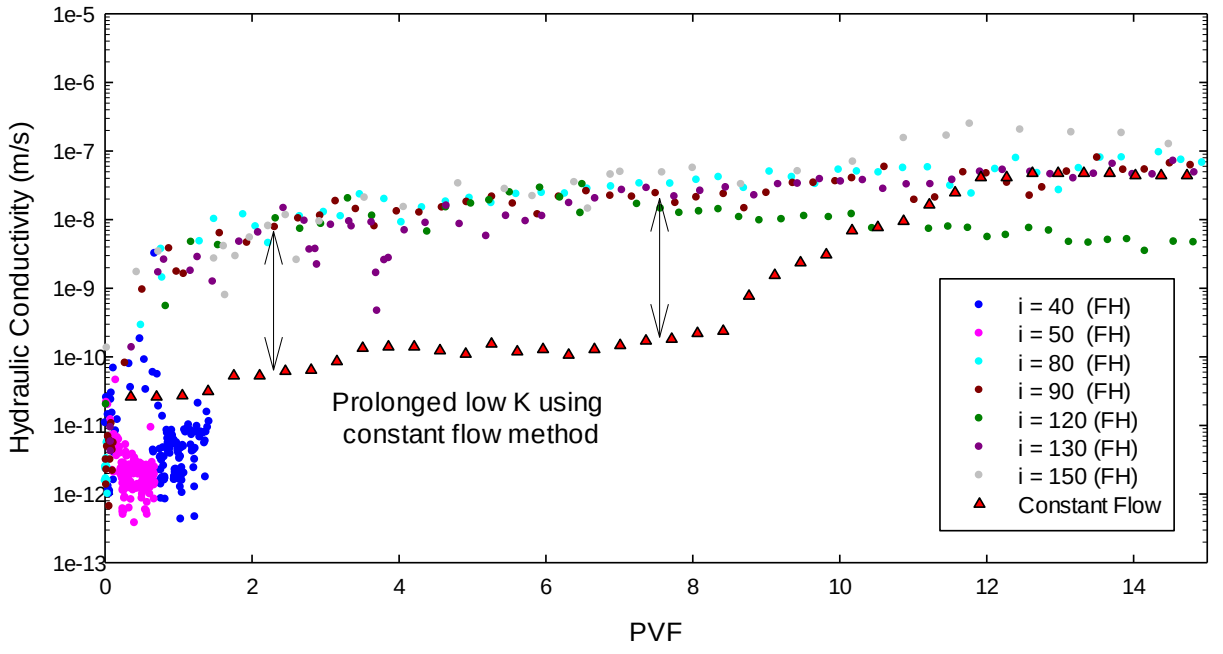

Figure 9.44: Hydraulic conductivity values plotted with PVF for constant flow method and falling head methods of varying average hydraulic gradients for 0-15 PVF for Resistex Plus GCLs permeated with 50 mM $CaCl_2$.

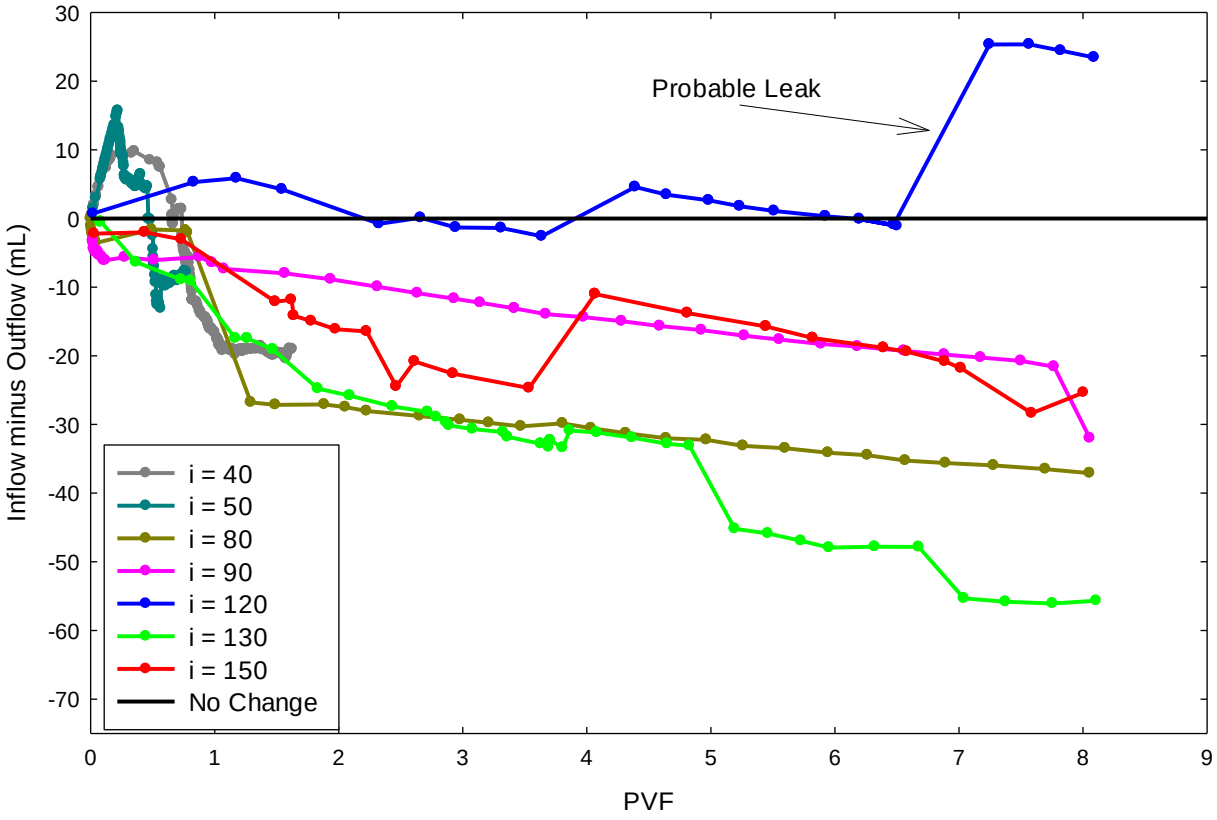

Figure 9.45: Cumulative inflow minus cumulative outflow plotted with PVF for falling head tests for Resistex Plus GCLs permeated with 50 mM $CaCl_2$ provided by Geng (2017). Only the first 8 PVF are plotted, because this is the range where the large difference in hydraulic conductivity values is seen. All of these results show a decrease in pore space volume ranging from 15 mL to 60 mL, excluding the permeameter where hydraulic gradient equals 120. This was likely due to a leak in the inflow plate. The 'no change' line represents the constant flow test method, where inflow is equal to the outflow.

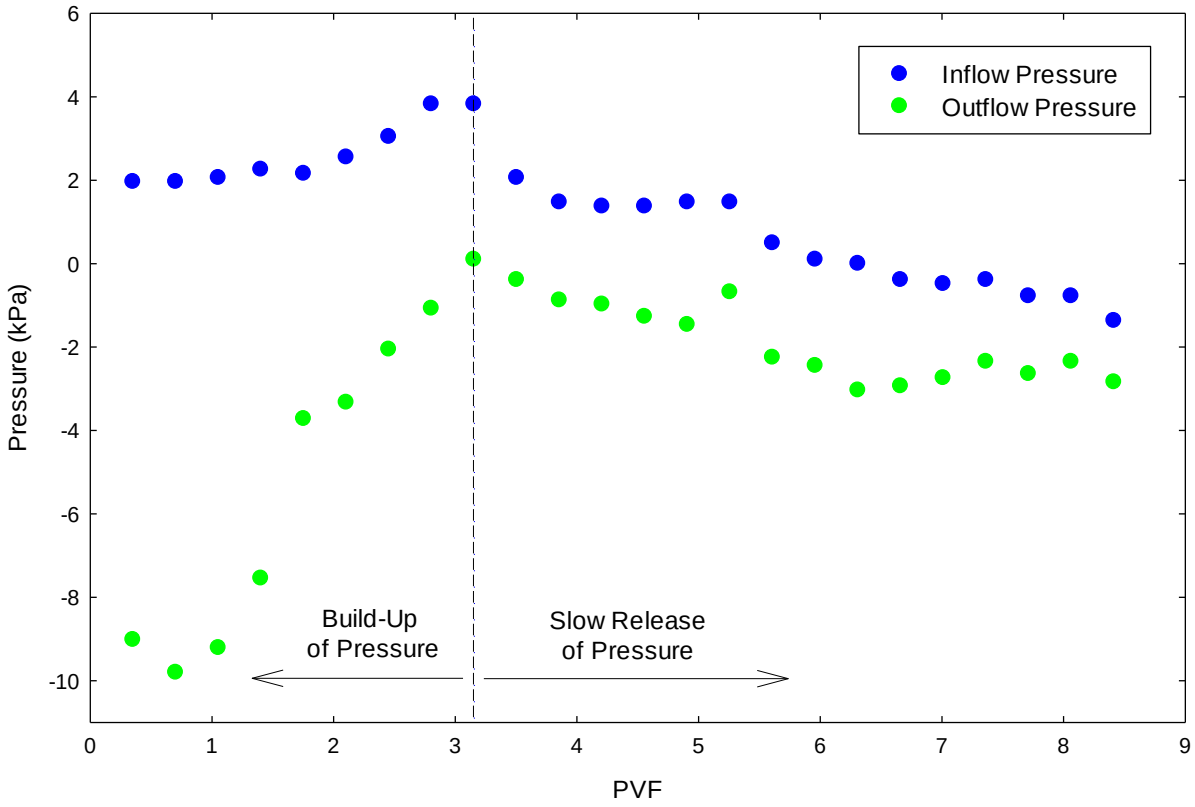

Figure 9.46: The inflow and outflow pressures measured using the constant flow method for Resistex Plus GCL permeated with 50 mM $CaCl_2$ from 0 – 8.5 PVF. Both the inflow and outflow pressures show a build-up of pressure from 0 – 3 PVF, followed by a slow decrease of pressure from 3 – 8.5 PVF.

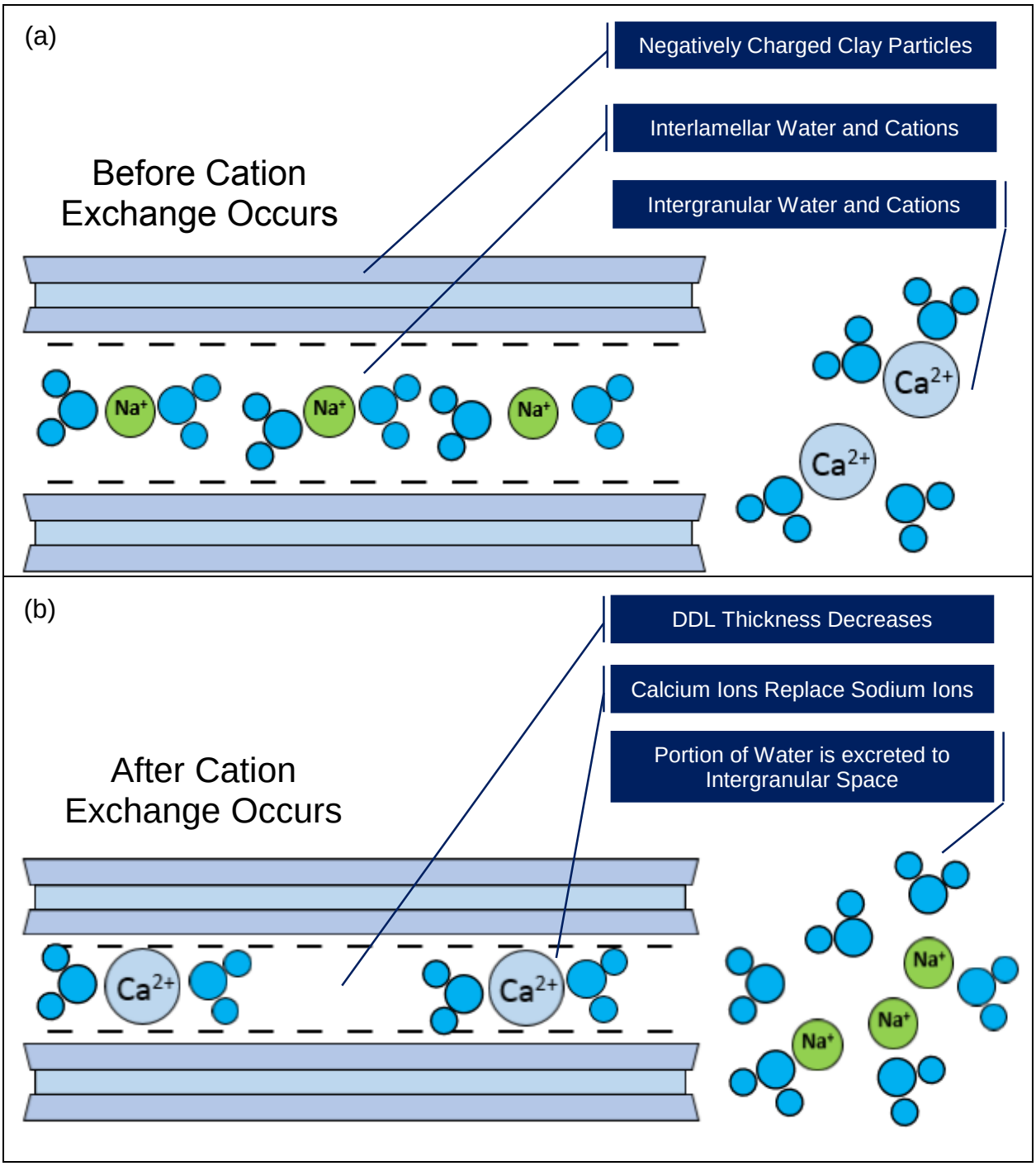

Figure 9.47: (a) Before cation exchange occurs, the Na-Bentonite will have negatively charged montmorillonite particles, with water and sodium ions occupying the interlamellar space giving it a large DDL thickness. Calcium ions and water will be occupying the intergranular pore space. (b) After cation exchange occurs, calcium ions will be occupying the interlamellar space. The stronger charges of the calcium ions will have a stronger pull on the negatively charge montmorillonite particles, which will cause the DDL thickness to decrease and cause a higher portion of water molecules to enter the intergranular space.

10 REFERENCES

Bouazza, A., & Bowders, J. (2010). *Geosynthetic Clay Liners for Waste Containment Facilities.* Leiden, The Netherlands: CRC Press/Balkema.

Bouzza, A. (2002). Geosynthetic clay liners. *Geotextiles and Geomembranes*, 20, 3-17.

Bradshaw, S. L., & Benson, C. H. (2014). Effect of Municipal Solid Waste Leachate on Hydraulic Conductivity and Exchange Complex of Geosynthetic Clay Liners. *Journal of Geotechnical and Geoenvironmental Engineering*, 140(4), 30-38.

Bradshaw, S. L., Benson, C. H., & Scalia IV, J. (2013). Hydration and Cation Exchange during Subgrade Hydration and Effect on Hydraulic Conductivity of Geosynthetic Clay Liners. *Journal of Geotechnical and Geoenvironmental Engineering*, 139(4), 526-538.

Breen, C. (1999). The characterisation and use of polycation-exchanged bentonites. *Applied Clay Science*, 15, 187-219.

Caulfield, M. J., Qiao, G. G., & Solomon, D. H. (2002). Some Aspects of the Properties and Degradation of Polyacrylamides. *American Chemical Society*, 3067-3083.

Chen, J. (2015). *Compatibility of Geosynthetic Clay Liners with Leachate From CCP Management Facilities.* (Doctor of Philosophy) University of Wisconsin-Madison.

Daniel, D. E., Bowders, J. J., & Gilbert, R. B. (1997). Laboratory Hydraulic Conductivity Testing of GCLs in Flexible-Wall Permeameters. *Testing and Acceptance Criteria for Geosynthetic Clay Liners, ASTM International*, 208-229.

Deng, Y., B., D. J., White, N. G., Loeppert, R. H., & Juo, A. S. (2006). Bonding between polyacrylamide and smectite. *Colloids and Surfaces A: Physicochemical and Engineering Aspects*, 82-91.

Dunn, J. R., & Mitchell, J. K. (1984). Fluid Conductivity Testing of Fine-Grained Soils. *Journal of Geotechnical Engineering*, 110(11), 1648-1665.

EPA. (2001). Geosynthetic Clay Liners Used in Municipal Solid Waste Landfills. *United States Environmental Protection Agency*.

Estornell, P., & Daniel, D. E. (1992). Hydraulic Conductivity of Three Geosynthetic Clay Liners. *Journal of Geotechnical Engineering*, 118(10), 1592-1606.

Fernandez, F., & Quigley, R. (1991). Controlling the destructive effects of clay-organic liquid interactions by applications of effective stresses. *Canadiant Geotechnical Journal*, 8(3), 388-398.

Fox, P. J. (1996). Analysis of Hydraulic Gradient Effects for Laboratory Hydraulic Conductivity Testing. *American Society for Testing and Materials*, 181-190.

Frankenberger, W. (1979). Bacterial Effects on Hydraulic Conductivity of Soils. *Soil Science Society of America*, 333-338.

Geng, W. (2017, January 25). Falling Head Hydraulic Conductivity Testing with Resistex Plus GCLs Permeated with 50 mM CaCl2 and Properties of CETCO's Proprietary Polymers. (W. Reybrock, Interviewer)

Gordon, M. E., Huebner, P. M., & Mitchell, G. R. (1990). Regulation, Construction and Performance of Clay-Lined Landfills in Wisconsin. *Waste Containment Systems: Construction, Regulation, and Performance*, 14-29.

Grim, R., & Guven, N. (1978). *Bentonites: geology, mineralogy, and uses.* New York City, NY: Elsevier.

Gunger, N., & Karaoglan, S. (2001). Interactions of polyacrylamide polymer with bentonite in aqueous systems. *Materials Letters*, 48(3-4), 168-175.

Jo, H. Y., Benson, C. H., Shackelford, C. D., Lee, J.-M., & Edil, T. B. (2005). Long-Term Hydraulic Conductivity of a Geosynthetic Clay Liner Permeated with Inorganic Salt Solutions. *Journal of Geotechnical and Geoenvironmental Engineering*, 131(4), 405-417.

Jo, H. Y., Katsumi, T., Benson, C. H., & Edil, T. B. (2001). Hydraulic Conductivity and Swelling of Nonprehydrated GCLs Permeated with Single-Species Salt Solutions. *Journal of Geotechnical and Geoenvironmental Engineering*, 127(7), 557-567.

Katsumi, T., Ishimori, H., Ogawa, A., Yoshikawa, K., Hanamoto, K., & Fukagawa, R. (2007). Hydraulic Conductivity of Nonprehydrated Geosynthetic Clay Liners Permeated with Inorganic Solutions and Waste Leachates. *The Japanese Geotechnical Society*, 47(1), 79-96.

Kmet, P., Quinn, K., & Slavik, C. (1981). Analysis of design parameters affecting the collection efficiency of clay-lined landfills. *Proceedings of the Fourth Annual Madison Waste Conference of Applied Research and Practice on Municipal and Industrial Waste*, (pp. 204-227).

Kolstad, D. C. (2000). *Compatibility of Geosynthetic Clay Liners (GCLs) with Multi-Species Inorganic Solutions.* (Master of Science) University of Wisconsin-Madison.

Kolstad, D. C., Benson, C. H., & Edil, T. B. (2004). Hydraulic Conductivity and Swell of Nonprehydrated Geosynthetic Clay Liners Permeated with Multispecies Inorganic Solutions. *Journal of Geotechnical and Geoenvironmental Engineering*, 130(12), 1236-1249.

Lagaly, G., Ogawa, M., & Dekany, I. (2006). Chapter 7.3 Clay Mineral Organic Interactions. In *Developments in Clay Science* (pp. 348-356). Elsevier.

Liu, P. (2007). Polymer modified clay minerals: A review. *Applied Clay Science*, 38(1), 64-76.

McRory, J. A., & Ashmawy, A. K. (2005). Polymer Treatment of Bentonite Clay for Contaminant Resistant Barriers. *Waste Containment and Remediation*, 1-11.

Mitchell, J. K., & Soga, K. (2005). *Fundamental of Soil Behavior, Third Edition.* Hoboken, New Jersey: John Wiley & Sons, Inc.

Norrish, K. (1954). The swelling of montmorillonite. *Discussions of the Faraday Society*, 18, 353-359.

Odom, I. E. (1984). Smectite clay Minerals: Properties and Uses. *Philosophical Transactions of the Royal Society of London A: Mathematical, Physical and Engineering Sciences*, 311(1517), 391-409.

Petrov, R. (1995). *Swelling and Compatibility Characterisitics of a Geosynthetic Clay Liner.* (Master of Science) The University of Western Ontario.

Petrov, R. J., & Rowe, R. K. (1997). Geosynthetic clay liner (GCL) - chemical compatibility by hydraulic conductivity testing and factors impacting its performance. *Canadian Geotechnical Journal*, 34, 863-885.

Petrov, R. J., Rowe, K. R., & Quigley, R. M. (1997). Selected Factors Influencing GCL Hydraulic Conductivity. *Journal of Geotechnical and Geoenvironmental Engineering*, 123(8), 683-695.

Petrov, R. J., Rowe, R. K., & Quigley, R. M. (1997). Comparison of Laboratory-Measured GCL Hydraulic Conductivity Based on Three Permeameter Types. *Geotechnical Testing Journal*, 120(1), 49-62.

Rad, N., Jacobson, B., & Bachus, R. (1994). Compatibility of Geosynthetic Clay Liners with Organic and Inorganic Permeants. *Fifth International Conference on Geotextiles, Geomembranes, and Related Products*, 1165-1168.

Salihoglu, H. (2015). *Behavior of Polymer-Modified Bentonites with Aggressive Leachates.* (Master of Science) University of Wisconsin-Madison.

Scalia IV, J. (2012). *Bentonite-Polymer Composites for Containment Applications.* (Doctor of Philosophy) University of Wisconsin-Madison.

Scalia IV, J., Benson, C. H., Bohnhoff, G. L., Edil, T. B., & Shackelford, C. D. (2014). Long-Term Hydraulic Conductivity of a Bentonite-Polymer Composite Permeated

with Aggressive Inorganic Solutions. *Journal of Geotechnical and Geoenvironmental Engineering*, 140(3), 04013025.

Schenning, J. A. (2004). *Hydraulic performance of polymer modified bentonite.* Tampa, FL: (Graduate Theses and Dissertations) University of South Florida Scholar Commons.

Shackelford, C. D., Benson, C. H., Katsum, T., Edil, T. B., & Lin, L. (2000). Evaluating the hydraulic conductivity of GCLs permeated with non-standard liquids. *Geotextiles and Geomembranes*, 18, 133-161.

Shackelford, C. D., Sevick, G. W., & Eykholt, G. R. (2010). Hydraulic conductivity of geosynthetic clay liners to tailings impoudment solutions. *Geotextiles and Geomembranes*, 28(2), 149-162.

Shan, H.-Y., & Lai, Y.-J. (2002). Effect of hydrating liquid on the hydraulic properties of geosynthetic clay liners. *Geotextiles and Geomembranes*, 20, 19-38.

Theng, B. (1982). Clay-Polymer Interactions: Summary and Perspectives. *Clays and Clay Minerals*, 30(1), 1-10.

Theng, B. (2012). *Formation and properties of clay-polymer complexes.* Elsevier.

Tian, K. (2015). *Long-Term Performance of Geosynthetic Liner Materials in Low-Level Radioactive Waste Disposal Facilities.* (Doctor of Philosophy) University of Wisconsin-Madison.

Tian, K., Likos, W. J., & Benson, C. H. (2016). Pore-Scale Imaging of Polymer-Modified Bentonite in Saline Solutions. In *Geo-Chicago 2016* (pp. 468-477). Chicago, IL.

Trauger, R., & Darlington, J. (2000). Next-generation geosynthetic clay liners for improved durability and performance. (pp. 2-14). Arlington Heights, IL: Colloid Environmental Technologies Company.

Wang, X., & Benson, C. H. (1999). Hydraulic Conductivity Testing of Geosynthetic Clay Liners (GCLs) Using the Constant Volume Method. *Geotechnical Testing Journal*, 22(4), 277-283.

Wong, J. (1977). The design of a system for collecting leachate from a lined landfill site. *Water Resources Research*, 13(2), 404-410.